

MODELLING WATERBORNE DISEASES

OBIORA C. COLLINS



Modelling Waterborne Diseases

OBIORA C. COLLINS

This dissertation is submitted in fulfilment of the academic requirements for the degree of Doctor of Philosophy in Applied Mathematics to the School of Mathematics, Statistics and Computer Science, College of Agriculture, Engineering and Science, University of KwaZulu-Natal, Durban.

November 2013

As the candidate's supervisor, I have approved this dissertation for submission.

Professor K S Govinder

November 2013

Abstract

Waterborne diseases are among the major health problems threatening the life of individuals globally. This thesis investigates the dynamics of waterborne disease under different conditions and consequently determines possible intervention strategies to minimize the spread of the disease. The following problems are addressed:

The effects of seasonal variations on the dynamics of waterborne disease together with the possible benefits of control intervention strategies such as vaccination, treatment and provision of clean water under the assumption of a homogeneous population are investigated. Specifically, we determine the optimal use of the intervention strategies to mitigate the spread of the disease.

The dynamics of waterborne disease in a multiple socioeconomic class community is explored. Particularly, we investigate the effects of migration of individuals due to socioeconomic reasons on the dynamics of waterborne disease under the assumption of heterogeneous mixing population.

We examine the effects of multiple contaminated water sources on the dynamics of waterborne disease under the assumption of homogeneous population. We also consider the problem of minimizing cost and determine the optimal use of vaccination to reduce the spread of infections.

The effects of heterogeneity on the transmission dynamics of waterborne disease is explored. Furthermore, we scrutinize use of the control intervention strategies to mitigate the spread of the infections under a heterogeneous population setting.

Declaration

I declare that the contents of this dissertation are original except where due reference has been made. It has not been submitted before for any degree to any other institution.

Obiora C. Collins

A small, square, light blue stamp containing a handwritten signature in dark ink. The signature appears to be 'O.C. Collins'.

November 2013

Declaration 1 - Plagiarism

I, Obiora C. Collins, declare that

1. The research reported in this thesis, except where otherwise indicated, is my original research.
2. This thesis has not been submitted for any degree or examination at any other university.
3. This thesis does not contain other persons data, pictures, graphs or other information, unless specifically acknowledged as being sourced from other persons.
4. This thesis does not contain other persons' writing, unless specifically acknowledged as being sourced from other researchers. Where other written sources have been quoted, then:
 - a. Their words have been re-written but the general information attributed to them has been referenced
 - b. Where their exact words have been used, then their writing has been placed in italics and inside quotation marks, and referenced.
5. This thesis does not contain text, graphics or tables copied and pasted from the Internet, unless specifically acknowledged, and the source being detailed in the thesis and in the references sections.

Signed:



Declaration of Publications

Details of contribution to publications presented in this thesis:

Chapter 2

O.C. Collins and K.S. Govinder. Analysis and control intervention strategies of a waterborne disease model. *Commun. Nonlinear Sci. Numer. Simul.* (2013), Submitted.

Chapter 3

O.C. Collins, S. L. Robertson and K.S. Govinder. Analysis of a waterborne disease model with socioeconomic classes. *Preprint: University of KwaZulu-Natal*, (2013).

Chapter 4

O.C. Collins and K.S. Govinder. On the mathematical analysis and application of a waterborne disease model with multiple water sources. *Nonlinear Anal. Real World Appl.* (2013), Submitted.

Chapter 5

O.C. Collins and K.S. Govinder. Heterogeneity and control intervention strategies of an n -patch waterborne disease model. *J. Theor. Biol.* (2013), Submitted.

Acknowledgements

May the GOD ALMIGHTY receive ALL THE GLORY.

My sincere gratitude goes to my supervisor Prof Kesh Govinder for his encouragement, support and quick response to all my questions/needs throughout the period of this project.

I am very grateful to Dr. Suzanne Robertson, Virginia Commonwealth University for her helpful suggestions.

I thank Dr. J. Tien, The Ohio State University and his research group for providing us with data on cholera outbreak in Haiti.

My invaluable gratitude goes to the African Institute for Mathematical Sciences and the College of Agriculture, Engineering and Science, University of KwaZulu-Natal for financial support.

I am especially grateful to the University of Nigeria, Nsukka for their financial support through the ETF for AST & D intervention scheme.

I am very grateful to the Members of Staff of University of Nigeria especially Prof. J.C. Amazigo, Prof. M.O. Oyesanya, Prof. F.I. Ochor, Prof. M.O Osilike, Prof. G.C.E Mbah, Prof. Asuzu, Mrs Nnebedum and Mike for their endless support throughout the years.

Finally, I thank Ebenezar Okechukwu and the members of CMFI Durban for their prayers and words of encouragement.

Dedication

To the HOLY SPIRIT of GOD.

To my loving wife Justina and my son Chukwubuikem.

To my parents, my parent-in-law and my siblings.

Contents

Abstract	ii
1 Introduction	1
1.1 Motivation	1
1.2 Literature review	2
1.3 Factors affecting the spread of waterborne diseases	5
1.3.1 Socioeconomic classes	6
1.3.2 Migration	6
1.3.3 Pathogen concentration	6
1.3.4 Multiple contaminated water sources	6
1.3.5 Heterogeneity in disease transmission	7
1.3.6 Seasonal variations	7
1.3.7 Control intervention strategies	7
1.3.8 Limited resources	7
1.4 Definition of terms	8
1.4.1 Dynamical system	8
1.4.2 Stability of equilibrium point of dynamical systems	9
1.4.3 Lyapunov stability theory	10

1.4.4	Invariant sets	13
1.4.5	Spectral radius of a matrix	14
1.4.6	Pontryagin's maximum principle	14
1.5	Outline of thesis	15
2	Analysis and control intervention strategies of a basic waterborne disease model	17
2.1	Introduction	18
2.2	Control free model formulation	19
2.3	Analysis of the control-free model	20
2.3.1	Basic reproduction number	20
2.3.2	Stability analysis of the DFE	21
2.3.3	Outbreak growth rate	22
2.3.4	Final outbreak size	23
2.3.5	Stability analysis of the endemic equilibrium	23
2.3.6	Effects of seasonal variation	24
2.4	Vaccination model	25
2.4.1	Analysis of the vaccination model	26
2.5	Treatment model	28
2.5.1	Analysis of the treatment model	29
2.6	Water purification model	31
2.6.1	Analysis of the water purification model	31
2.7	Multiple control intervention strategy model	33
2.7.1	Analysis of the multiple control intervention strategy model	33
2.7.2	Multiple control strategy vs. single control strategy	34

2.7.3	Sensitivity analysis of the multiple control strategy model	38
2.7.4	Optimal control problem	39
2.8	Discussion	44
3	Analysis of a waterborne disease model with socioeconomic classes	47
3.1	Introduction	47
3.2	Model formulation	49
3.3	SIWR model with two socioeconomic classes	53
3.3.1	The basic reproduction number	54
3.3.2	The dominant SEC	55
3.3.3	Homogeneous version of model (3.6)	56
3.3.4	Relationship between \mathcal{R}_1 , \mathcal{R}_2 and \mathcal{R}_0	57
3.3.5	Stability analysis	58
3.3.6	Outbreak growth rate	60
3.3.7	Model simulations	63
3.3.8	Sensitivity analysis	67
3.4	The n -socioeconomic class model	71
3.4.1	Disease free equilibrium for the n -SEC model	71
3.4.2	The basic reproduction number for the n -SEC model	72
3.4.3	Outbreak growth rate for the n -SEC model	74
3.5	Discussion	75
3.6	Appendix to Chapter 3	77
3.6.1	Stability of the endemic equilibrium	80

4 On the mathematical analysis and application of a waterborne disease model

with multiple water sources	82
4.1 Introduction	83
4.2 Model formulation	84
4.3 Model analysis	86
4.3.1 Existence of solutions	86
4.3.2 The basic reproduction number	87
4.3.3 Stability of the disease free equilibrium	90
4.3.4 Outbreak growth rate	91
4.3.5 Final outbreak size	92
4.3.6 Stability of the endemic equilibrium	94
4.3.7 Bifurcation diagram	95
4.4 A case study: the Haiti cholera outbreak	95
4.5 Vaccination model	98
4.5.1 Analysis of the vaccination model	100
4.5.2 Sensitivity analysis	102
4.5.3 Optimal control problem	105
4.6 Discussion	110
5 Heterogeneity and control intervention strategies of an n-patch waterborne disease model	114
5.1 Introduction	114
5.2 Model formulation	115
5.3 Model analysis	119
5.3.1 Quantifying heterogeneity	120
5.3.2 Homogeneous version of model (5.3)	122

5.3.3	The basic reproduction number	124
5.3.4	Type reproduction numbers	127
5.3.5	Final outbreak size	129
5.3.6	The general n -patch model with shared multiple water sources	132
5.4	Application of model (5.1) to cholera outbreak in Haiti	135
5.5	The multiple control strategy model	140
5.5.1	Analysis of the multiple control strategy model	140
5.6	The single control intervention strategy	142
5.6.1	Effects of vaccination	142
5.6.2	Effects of treatment	143
5.6.3	Effects of water purification	144
5.7	Discussion	145
6	Summary	147
	Bibliography	150

Chapter 1

Introduction

In this chapter we discuss the motivation for the thesis, review some literature, present the definitions of terms and theorems used throughout the thesis and give a brief outline of the thesis.

1.1 Motivation

Even though waterborne diseases have been in existence for ages, there is still some ambiguity as to what constitutes the diseases [6, 84]. For the purposes of this thesis, we consider a definition by Tien and Earn [84] which says that a waterborne disease is any disease for which transmission through water is a concern. Some examples of waterborne diseases include Cholera, Hepatitis A and E, Giardia, Cryptosporidium and Rotavirus. The primary means of transmission of these diseases is through environment-to-human contact [19, 80, 64, 65, 36, 101, 73]. However, a secondary, less important route exists, in the form of human-to-human transmission [84, 62]. The most important and common routes of waterborne disease transmission are water and food (especially seafood) contaminated with the bacterium [36, 80, 24]. This explains why these diseases are predominant in water environments such as fresh water, lakes, seas and rivers. Therefore, we consider only environment-to-human transmission in this thesis.

Poor sanitation and limited access to clean water are the major causes of waterborne diseases. More work needs to be done to remedy the situation in many parts of the world. Statistics

from the World Health Organization (WHO) [92] reveals that approximately 1.1 billion people globally do not have access to improved water supply sources whereas around 700,000 children die every year from diarrhoea caused by unsafe water and poor sanitation [89]. In addition to this, about 768 million people still relied on unimproved drinking water sources while 2.5 billion people still lacked access to improved sanitation facilities in 2011 [94]. All these contribute greatly to the current statistics of waterborne diseases globally.

The tremendous outbreaks of waterborne diseases remain a great challenge as the number of cases reported worldwide continues to rise. For instance, cholera outbreak was confirmed in Haiti on October 21, 2010, and according to Ministry of Public Health and Population (MSPP) of Haiti, a total of 669,396 cases and 8,217 deaths had been reported by August 4, 2013 [15]. Many more cases of cholera were confirmed in countries like Zimbabwe (2008-2009), India (2007), Congo (2008), Iraq (2008), Nigeria (2010) and Northern Viet Nam (2009)[83]. The cholera outbreak of Zimbabwe lasted for about one year and by July 2009, more than 98,000 cases and 4,000 deaths had been reported [62]. According to the WHO, cholera affects 3–5 million people worldwide, and causes 100,000–130,000 deaths yearly as of 2010 [83].

Limited resources is one of the major problems facing most developing countries where waterborne diseases are endemic. It is stated that developing countries need to spend up to US\$58 billion more each year to meet the Millennium Development Goal (MDG) targets on water and sanitation [95]. Achieving this universal access to safe water and sanitation would save about 2.5 million lives every year [95]. Therefore, there is a need to determine the optimal control intervention strategies that minimize cost.

1.2 Literature review

Mathematical models can provide key insights into the cause of an outbreak and help the management in allocating health care resources by investigating the impact of alternative interventions [74]. A number of different mathematical models have been used to study the dynamics of waterborne diseases and we give a brief overview of some approaches.

The earliest mathematical waterborne disease model was proposed by Capasso and Paveri-

Fontana [12] to study the 1973 cholera epidemic in the Mediterranean region. The model is made up of two components, the population of the infected individuals and the concentration of the pathogens in water reservoir. They assumed that transmission is only through interaction with contaminated water. In 2001 Codeco [19] extended the work of Capasso and Pavari-Fontana [12] by including an additional compartment (the susceptible population) into the model. She used her model to study the role of the aquatic reservoir in cholera dynamics as well as to investigate the long-term dynamics of the disease. She assumed a non-linear (in this case, a logistic function) incidence. Similar to the work of Capasso and Pavari-Fontana [12], Codeco's model assumed that ingestion of contaminated water is the only transmission route. Merrell and Butler [58] published a finding that freshly shed cholera bacteria from human intestines are 700 times more infectious than bacteria shed only hours previously. Based on this finding, Hartley et al. [36] formulated a model which is an extension of Codeco's model but took into account the role of a hyper-infective stage of *V. cholerae* (i.e., freshly shed vibrios) introduced into the water reservoir by the infected people in the population. This model explained the explosive nature of the disease as based on the laboratory measurements that freshly shed *V. cholerae* from human intestines outcompeted other *V. cholerae* by as much as 700-fold for the first few hours in the environment [83, 3]. The model also used a similar non-linear incidence as Codeco's model and assumed that ingestion of contaminated water is the only transmission route.

Tien and Earn [84] in 2010 developed a waterborne disease model which includes dual transmission pathways, with bilinear incidence rates employed for both the environment-to-human and human-to-human infection routes. They used the model to investigate the distinction between the different transmission routes in the dynamics of waterborne diseases. In 2011, Mukandavire et al. [62] proposed a model to estimate the basic reproduction number for the 2008-2009 cholera outbreak in Zimbabwe. Their model also included both environment-to-human and human-to-human transmission pathways. However, the incidence consists of two parts: one is due to the environment-to-human transmission which is again similar to the non-linear incidence in Codeco's model; the other which represents the human-to-human interaction is modelled by a linear function. Eisenberg et al. [28] considered the Tien and Earn [84] model to examine

whether parameters of waterborne disease transmission dynamics can be identified, both in the ideal setting of noise-free data (structural identifiability) and in the more realistic setting in the presence of noise (practical identifiability). Robertson et al. [76] extended the Tien and Earn [84] model to an n -patch waterborne disease model in networks with a common water source to investigate the effect of heterogeneity in dual transmission pathways on the spread of the disease. Miller Neilan et al. [59] formulated a mathematical model that includes essential components such as a hyperinfectious, short-lived bacterial state, a separate class for mild human infections, and waning disease immunity. Using the model, they investigated optimal control of three strategies for slowing the spread of the disease for two endemic populations. Mwasa and Tchuente [65] formulated a cholera model with public health interventions to study the impact of public health educational campaigns, vaccination and treatment as control strategies in curtailing the disease. Alexanderian et al. [4] formulated an age-structured model for the spread of epidemic cholera by using a system of hyperbolic (first-order) partial differential equations in combination with ordinary differential equations. Sanches et al. [80] proposed a mathematical model for cholera epidemics which comprises seasonality, loss of host immunity, and control mechanisms acting to reduce cholera transmission. Hove-Musekwa et al. [39] developed a deterministic model for cholera in a community and applied it to determine the effects of malnutrition in the spread of the disease.

Tian and Wang [83] in 2011 used three different techniques: the methods of monotone dynamical systems, geometric approach and Lyapunov functions to investigate the global asymptotic stability of the endemic equilibria for several deterministic cholera models. Wang and Liao [91] presented a unified deterministic model for cholera that incorporates a general incidence rate and a general formulation of the pathogen concentration in water reservoir. The model enabled them to study the complex epidemic and endemic behaviour of the disease. Rinaldo et al. [74] proposed a model for Haitian epidemic cholera and applied it to the year-long dataset of reported cases. Their model allowed them to make predictions on longer-term epidemic cholera in Haiti. Other studies on the dynamics of waterborne diseases include [72, 33, 42, 29, 52, 64, 88]. Although the results presented here focus on cholera, the theoretical results for the models are more broadly applicable to other waterborne diseases, such as *Giardia*, *Cryptosporid-*

ium, Campylobacter, hepatitis A and E, norovirus, rotavirus, and Escherichia coli O157:H7 [6, 78, 28].

There is no doubt that the above studies have contributed immensely towards understanding the dynamics of waterborne diseases. However, theoretical studies for waterborne diseases are not complete. The objectives of this thesis are as follows: to develop mathematical models in order to improve the understanding of the transmission dynamics of water borne disease in a community, to investigate the optimal use of control intervention strategies to reduce the spread of the disease with minimum cost and to use these models to inform healthcare practitioners of the likely impact of the different intervention strategies and their optimal use with minimum cost. Rinaldo et al. [74] says that, despite differences in methods that can be tested through model-guided field validation, mathematical modelling of large-scale outbreaks emerges as an essential component of future cholera epidemic control. To make sure that our result is an improvement of the existing results in the literature, we critically studied the factors affecting the dynamics of waterborne diseases and take them into consideration while developing our models.

1.3 Factors affecting the spread of waterborne diseases

The dynamics of a waterborne disease is as a result of interaction between human and pathogen. Some of the several different factors that must be considered in attempting to understand the dynamics of waterborne diseases include: sanitation, different transmission pathways, water treatment efforts, pathogen ecology outside of human hosts, climatological factors or rainfall [7, 25, 6, 27, 40, 84, 31, 77, 69]. Understanding how these factors interact to determine the dynamics of waterborne diseases is challenging. In addition to the above mention factors, any good mathematical model that can explain the dynamics must also incorporate the factors explained below.

1.3.1 Socioeconomic classes

Socioeconomic classes influence the dynamics of most infectious diseases including waterborne disease [79]. Moreover, waterborne diseases have been associated with poverty and malnutrition [39]. Most individuals that are suffering from poverty and malnutrition belong to a low socioeconomic class in the society. Therefore, it is necessary to consider individuals socioeconomic status in formulating waterborne disease models.

1.3.2 Migration

Migration of individuals is one of the means whereby infections are spread across a population, meta-population or communities or even countries. So, it is necessary to consider migration of individuals in studying the dynamics of waterborne diseases.

1.3.3 Pathogen concentration

Contamination of drinking water source can lead to waterborne disease outbreaks. To estimate a potential risk for waterborne disease caused by drinking contamination water source, knowledge of the pathogen concentrations in the water source is required. We also know that pathogen concentration is not constant but varies with time within and across the environment. To address this, we will define a measure of pathogen concentration which can be used to estimate the pathogen in water source at an point in time. For variability in pathogen concentration across the environment, we consider a multiple contaminated water sources and define a measure of pathogen concentration for each water source.

1.3.4 Multiple contaminated water sources

Some of the communities where waterborne diseases are endemic are exposed to multiple contaminated water sources such as lakes, ponds, wells, rivers, etc., with different levels of pathogen concentration. Therefore, considering multiple contaminated water sources is reasonable in

studying the dynamics of waterborne disease for a community where individuals have access to multiple contaminated water sources.

1.3.5 Heterogeneity in disease transmission

Many waterborne disease models assume homogeneity in disease transmission, but in reality most factors influencing the spread of the disease (such as contact rates, shedding rates, susceptibility or infectivity) vary both within and across populations even in the absence of external influences such as seasonality [76]. Therefore, incorporating heterogeneity will make the model more realistic even though the mathematics might be more difficult to handle [10, 76].

1.3.6 Seasonal variations

Waterborne diseases such as cholera are characterised by repeated seasonal outbreaks which occur mainly during the rainy season [79, 80]. Hence, it is necessary to consider seasonal variation to study the dynamics of waterborne diseases.

1.3.7 Control intervention strategies

Whenever a waterborne disease outbreak occurs in a community, most infected individuals will start taking some treatment while the susceptible individuals are prompted to get vaccinated. Thus, we need to take this into account in order to get a better understanding of the dynamics of waterborne disease as well as determine the impact of the control interventions.

1.3.8 Limited resources

One of the reasons why individuals in poor rural areas are mostly the victims of waterborne disease is due to limited resources. Waterborne diseases have been associated with poverty and malnutrition [39]. Even when an effective control is available, most of the victims of the disease cannot afford it. Therefore, it is necessary to take this into consideration while studying the

dynamics of waterborne disease.

Incorporating all these into a single waterborne disease model will improve the understanding of the dynamics of waterborne disease in a community. However, a single model incorporating all these factors will be too complex and difficult to analyze. In this thesis, we shall develop mathematical models for waterborne disease that include some of these factors.

1.4 Definition of terms

In this section, we present some definitions that will aid our explanation in subsequent chapters. The definitions and theorems in this section are standard in the literatures and can be found in most text on dynamical systems and ordinary differential equations [48, 47, 53, 46, 26].

1.4.1 Dynamical system

A dynamical system may be regarded as a process which is changing (or evolving) in time [46]. Examples include but are not limited to the mathematical models that describe the spread of an epidemic, population growth and decline, variations in the stock market, chemical reactions etc. From a mathematical viewpoint, a dynamical system can be seen as a system that has a **state vector** which describes the state of the system at a given time and a **function** which maps the state at one instant of time to the state at a later time. A more precise definition of a dynamical system is given as follows:

Definition 1.4.1. [46] Let X represent some state space and let $T \subseteq \mathbb{R}$. A function $\psi : X \times T \rightarrow X$ that has the two properties

$$(i) \quad \psi(x_0, 0) = x_0$$

$$(ii) \quad \psi(\psi(x_0, t), s) = \psi(x_0, t + s)$$

is called a **dynamical system** on X . If $T = \mathbb{R}^+$ (the set of non-negative real numbers), we have a continuous dynamical system (CDS) or flow.

Mathematical models of evolutionary processes often take the form of differential equations such as

$$\begin{cases} \dot{x}(t) = F(x(t)); & x(t) \in \mathbb{R}^n \\ x(t_0) = x_0 \end{cases} \quad (1.1)$$

where F is a given vector-valued function. For existence and uniqueness of solutions, we require that F is Lipschitz continuous. Note that F does not depend explicitly on t , so equation (1.1) is an autonomous differential equation and such differential equations lead to continuous time dynamical systems. In most cases, the exact solutions of the models which will help in determining the long-term behaviour of the models are difficult to obtain. In what follows, we will describing the techniques that can be used to obtain information on the long-term behaviour of solutions to the models even when we do not know what these solutions are.

1.4.2 Stability of equilibrium point of dynamical systems

Definition 1.4.2. Consider the initial value problem (IVP) (1.1). A point $x^* \in \mathbb{R}^n$ is said to be a steady state, stationary point, critical point or equilibrium point of the IVP (1.1) if

$$F(x^*) = 0. \quad (1.2)$$

Definition 1.4.3. [53, 26]

An equilibrium point $x^* \in \mathbb{R}^n$ of (1.1) is said to be:

- (i) **stable** if for every $\epsilon > 0$ there exists a $\delta > 0$ (which depends on ϵ) such that

$$\|x_0 - x^*\| < \delta \implies \|\psi(x_0, t) - x^*\| < \epsilon \quad \forall t \geq 0, \quad (1.3)$$

for any solution $\psi(x_0, t)$ of the IVP (1.1),

- (ii) **unstable** if it is not stable,

- (iii) **locally asymptotically stable** if it is stable and in addition, there exists an $r > 0$ such that

$$\|x_0 - x^*\| < r \implies \|\psi(x_0, t) - x^*\| \longrightarrow 0 \quad \text{as } t \longrightarrow \infty \quad (1.4)$$

for any solution $\psi(x_0, t)$ of the IVP (1.1),

(iv) **globally asymptotically stable** if (iii) holds for all $r > 0$.

In other words, x^* is **stable** if all solutions starting near x^* stay nearby; if, in addition, nearby solutions converge to x^* as $t \rightarrow \infty$, we say that x^* is **locally asymptotically stable**. When there is no restriction on the size of r , we say that x^* is **globally asymptotically stable** [46].

1.4.3 Lyapunov stability theory

Here, we seek sufficient conditions that ensure the stability of system (1.1) based on the above definitions and these conditions will be presented as the Lyapunov stability theorem. It should be noted that a large part of the theory that follows in this study will focus on the theorems, rather than the above definitions of stability. Hence, it is necessary that we state them.

Remark 1.4.4. Without loss of generality, we will assume that equilibrium point $x^* = 0$ to simplify the notation. However, by performing a transformation of the form $x^*(t) \rightarrow x^*(t) + y(t)$, the theory can be applied to any solution $y(t)$ of (1.1) [26]. We will present the theorem for different forms of F .

Firstly, when F is linear autonomous i.e. $F = Ax$. Consider the linear autonomous system

$$\dot{x} = Ax, \tag{1.5}$$

where $x \in \mathbb{R}^n$ and A is an $n \times n$ matrix.

Theorem 1.4.5. [53, 46, 26]

Let λ_i be the eigenvalues of A and $\mathbb{R}_e(\lambda_i)$ be the real part of the eigenvalues of A . The

- equilibrium point $x^* = 0$ of system (1.5) is said to be stable if and only if $\mathbb{R}_e(\lambda_i) \leq 0$ for all λ_i ,
- equilibrium point $x^* = 0$ of system (1.5) is globally asymptotically stable if and only if $\mathbb{R}_e(\lambda_i) < 0$ for all λ_i .

Secondly, when F is a non-linear autonomous system. We will discuss two methods of investigating the stability of the equilibrium point $x^* = 0$ of system (1.1):

Lyapunov's Indirect Method

Theorem 1.4.6. [53, 46, 26]

Suppose $F : D \rightarrow \mathbb{R}^n$ is continuously differentiable where D is the domain of F . Let

$$A = \frac{\partial F}{\partial x}(0). \quad (1.6)$$

Then:

- the equilibrium point $x^* = 0$ of system (1.1) is said to be locally asymptotically stable if and only if $\Re_e(\lambda_i) < 0$ for all eigenvalues λ_i of A ,
- equilibrium point $x^* = 0$ of system (1.1) is unstable if $\Re_e(\lambda_i) > 0$ for some eigenvalues λ_i of A .

Lyapunov's Direct Method

This Direct Method has to do with analysis of stability of equilibrium point using Lyapunov function.

Theorem 1.4.7. (Lyapunov Stability [53, 26])

Let $x^* = 0$ be the equilibrium point of system (1.1) and $S \subset D$ be a domain containing $x^* = 0$. Assume there exists continuous function $V : S \rightarrow \mathbb{R}$ for some open region $S \subseteq \mathbb{R}^n$ containing the origin such that V satisfies the following:

- $V(0) = 0$,
- $V(x) \geq 0, \forall x \in S$,
- $\dot{V}(x) \leq 0, \forall x \in S$.

Then $x^* = 0$ is stable.

\dot{V} denotes the derivative of V along the solution trajectory of (1.1). This V is sometimes referred as a Lyapunov function.

Theorem 1.4.8. (*Lyapunov Asymptotic Stability [53, 26]*)

Assume there exists a differential function $V : S \rightarrow \mathbb{R}$ defined on some open region $S \subseteq \mathbb{R}^n$ containing the origin such that V satisfies the following:

- $V(0) = 0$,
- $V(x) > 0$, $\forall x \in S$ with $x \neq 0$,
- $\dot{V}(x) < 0$, $\forall x \in S$ with $x \neq 0$.

Then $x^* = 0$ is locally asymptotically stable. If in addition $\|V\| \rightarrow \infty$ as $\|x\| \rightarrow \infty$, then $x^* = 0$ is globally asymptotically stable.

Another stability theorem which we will consider in this thesis is the global stability result by Castillo-Chavez et al. [13] which is stated in Theorem 1.4.9 below.

Theorem 1.4.9. *Consider a model system written in the form [13]*

$$\begin{aligned} \frac{dX_1}{dt} &= F(X_1, X_2), \\ \frac{dX_2}{dt} &= G(X_1, X_2), \quad G(X_1, 0) = 0, \end{aligned} \tag{1.7}$$

where $X_1 \in \mathbb{R}^m$ denotes the number of uninfected individuals and $X_2 \in \mathbb{R}^n$ denotes the number of infected individuals including latent, infectious, etc. $X_0 = (X_1^*, 0)$ denotes the disease-free equilibrium (DFE) of the system. Assume that

(H1) For $\frac{dX_1}{dt} = F(X_1, 0)$, X_1^* is globally asymptotically stable;

(H2) $G(X_1, X_2) = AX_2 - \hat{G}(X_1, X_2)$, $\hat{G}(X_1, X_2) \geq 0$ for $(X_1, X_2) \in \Omega$, where the Jacobian $A = \frac{\partial G}{\partial X_2}(X_1, 0)$ is an M -matrix (the off diagonal elements of A are non-negative) and Ω is the region where the model makes biological sense.

Then the DFE X_0 is globally asymptotically stable provided that $\mathcal{R}_0 < 1$.

1.4.4 Invariant sets

Definition 1.4.10. [48, 53]

A set $S \subseteq \mathbb{R}^n$ is said to be **invariant** of (1.1) if for every $x_0 \in S$ and for all $t \in \mathbb{R}$, $x \in S$. Equilibria are special class of invariant sets.

Definition 1.4.11. A set $S \subseteq \mathbb{R}^n$ is said to be **positively invariant** of (1.1) if for every $x_0 \in S$ and for all $t \geq 0$, $x \in S$.

Definition 1.4.12. A set $S \subseteq \mathbb{R}^n$ is said to be **negatively invariant** of (1.1) if for every $x_0 \in S$ and for all $t \leq 0$, $x \in S$.

Theorem 1.4.13. (LaSalle's Invariance Principle [47, 53])

Let $S \subseteq \mathbb{R}^n$ be compact (i.e., closed and bounded). Assume there exists a differential function $V : S \rightarrow \mathbb{R}$ such that

$$\dot{V}(x) \leq 0, \quad \forall x \in S. \quad (1.8)$$

Let M be the largest invariant set contained in $\{x \in S : \dot{V}(x) = 0\}$. Then all trajectories starting from S approaches M as $t \rightarrow \infty$. In particular, if $\{x \in S : \dot{V}(x) = 0\}$ contains no trajectory other than the equilibrium $x^* = 0$, then all trajectories starting from S converge to $x^* = 0$ as $t \rightarrow \infty$ (i.e., $x^* = 0$ is asymptotically stable).

Theorem 1.4.14. (Local invariant set theorem [11])

Suppose there exists a continuously differential function $V(x)$ such that the level set $\Omega = \{x : V(x) \leq V_0\}$ is bounded for some V_0 and $\dot{V}(x) \leq 0$ whenever $x \in \Omega$, then:

(i) Ω is an invariant set.

(ii) $x(0) \in \Omega \implies \dot{V}(x) \rightarrow 0$ as $t \rightarrow \infty$.

(iii) $x(t) \rightarrow M =$ largest invariant set contained in $\{x : \dot{V}(x) = 0\}$.

Theorem 1.4.15. (Global invariant set theorem [11])

Suppose there exists a continuously differential function $V(x)$ such that $V(x)$ is positive definite, $V(x) \leq V_0$, $V(x) \rightarrow \infty$ as $\|x\| \rightarrow \infty$, then:

(i) $\dot{V}(x) \rightarrow 0$ as $t \rightarrow \infty$.

(ii) $x(t) \rightarrow M = \text{largest invariant set contained in } \{x : \dot{V}(x) = 0\}$.

1.4.5 Spectral radius of a matrix

Definition 1.4.16. Let A be an $n \times n$ matrix and $\lambda_i (1 \leq i \leq n)$ be the eigenvalues of A . The spectral radius of the matrix A is the eigenvalue with the largest absolute value given by

$$\rho(A) = \max \{|\lambda_i| : 1 \leq i \leq n\}. \quad (1.9)$$

1.4.6 Pontryagin's maximum principle

Pontryagin's Maximum Principle is a classical result in the optimal control theory that provides a necessary condition an optimal solution must satisfy [35, 71]. There are different versions of the Pontryagin's maximum principle depending on the problem statements. We present here a version that is most suitable for the problems discussed in this thesis (see [8, 32] for more general versions). Before presenting the Principle, we first review some terminology.

Let $[t_0, t_f] \subset \mathbb{R}$, U be a bounded subset of \mathbb{R}^m and $u : [t_0, t_f] \rightarrow U$ be a measurable function. The function $u(t)$ is called the control applied at time t and $x : [t_0, t_f] \rightarrow \mathbb{R}^n$ is the system trajectory corresponding to control u and initial condition x_0 .

Definition 1.4.17. Let $T_0, T_f \subset \mathbb{R}$ denote the sets of possible values for the initial time t_0 and the final time t_f , respectively. Let $X_0, X_f \subset \mathbb{R}^n$ denote the sets of possible values for the initial state x_0 and final state x_f , respectively. Then the set of allowable boundary values for a trajectory is defined by $B = \{(t_0, x_0, t_f, x_f) : t_0 \in T_0, x_0 \in X_0, t_f \in T_f \text{ and } x_f \in X_f\}$ [35].

We assume that there exist functions $\Psi_0, \Psi_f \in C_1(\mathbb{R}^n, \mathbb{R})$ such that $X_0 = \Psi_0^{-1}$ and $X_f = \Psi_f^{-1}$ and $D\Psi_0(z)$ and $D\Psi_f(y)$ are surjective for all $z \in X_0$ and $y \in X_f$, where $D\Psi_i(z)$ denotes the Jacobian of Ψ_i [35].

Given a continuous function $\Upsilon : \mathbb{R}^n \rightarrow \mathbb{R}$ and a function $f^0 : \mathbb{R}^n \times U \rightarrow \mathbb{R}$ that is continuous

on U and continuously differentiable on \mathbb{R}^n , define the cost function

$$J(x, u) = \int_{t_0}^{t_f} (f^0(x(t), u(t)))dt + \Upsilon(x(t_f)). \quad (1.10)$$

The aim is to find a control $u : [t_0, t_f] \rightarrow U$ and corresponding trajectory $x : [t_0, t_f] \rightarrow \mathbb{R}^n$ such that J is minimized.

Problem statement

Assume U is a bounded set in \mathbb{R}^m , f is continuous in U and continuously differentiable in \mathbb{R}^{n+1} . Let \mathcal{A} be non-empty denote the set of all admissible pairs (x, u) . Find an admissible pair $(x^*, u^*) \in \mathcal{A}$ such that $J(x^*, u^*) \leq J(x, u)$ for every $(x, u) \in \mathcal{A}$ [35].

Theorem 1.4.18. (*Pontryagin's maximum principle*)[35, 71]

If (x^*, u^*) is a solution to the above problem statement then there exists an absolutely continuous function $\lambda : [t_0, t_f] \rightarrow \mathbb{R}^{n+1}$ such that

- (i) $\dot{\lambda}(t) = \frac{\partial H(\lambda, x, u)}{\partial x}$, a.e on $[t_0, t_f]$, where H is the Hamiltonian,
- (ii) $\lambda(t) \neq 0$, for all $t \in [t_0, t_f]$,
- (iii) $\lambda_0 \in \{0, -1\}$,
- (iv) $H(\lambda(t), x^*(t), u^*(t)) = \sup_{u \in U} H(\lambda(t), x^*(t), u(t))$, a.e on $[t_0, t_f]$,
- (v) there exists $c \in \mathbb{R}$ such that $H(\lambda(t), x^*(t), u(t)) = c$, a.e on $[t_0, t_f]$,
- (vi) if the end time t_f is free then c can be taken to be zero, and
- (vii) $\lambda(t_0)$ is orthogonal to $\ker(D\Psi_0(x^*(t_0)))$ and $\lambda(t_f)$ is orthogonal to $\ker(D\Psi_1(x^*(t_f)))$.

1.5 Outline of thesis

A brief outline of this thesis is given below.

- In Chapter 2, we formulate a basic SIWR waterborne disease mathematical epidemiological model. We start by using the model to study the dynamics of waterborne disease under the assumption of a homogeneous population setting. We also use the model to investigate the effects of seasonal variation in the dynamics of waterborne disease. Next, we extend the model by introducing three different control intervention strategies such as vaccination, treatment and provision of clean water. The analyses of these control models enable us to determine the benefits of these control interventions. Finally, we use optimal control theory to determine the best control intervention that can reduce the spread of waterborne disease with minimum cost.
- In Chapter 3, we propose an n -patch waterborne disease model by extending the basic SIWR model to account for different socioeconomic classes in a population. This socioeconomic class model allows us to investigate the effects of socioeconomic status in the dynamics of the disease.
- In Chapter 4, we develop another model by extending the basic SIWR model to account for a situation where individuals are exposed to multiple contaminated water sources. We explore the effect of considering multiple contaminated water sources. Next, we consider this model to study the recent cholera outbreak in Haiti. Furthermore, we include vaccination as a control intervention strategy in our multiple contaminated water source model to assess the optimal use of vaccine to reduce the spread of the disease with minimum cost.
- In Chapter 5, we formulate a more general n -patch waterborne disease model which is an extension of all the previous models. We consider this model to investigate the effects of heterogeneity in the dynamics of waterborne disease. Furthermore, we use the model to study the dynamics of cholera outbreak in each of the Departments in Haiti as well as for the total population. Since heterogeneity is more realistic, we examine the benefits of control intervention strategies in a heterogeneous population setting using simple extensions of this model.
- Finally, in Chapter 6, we summarise our results and conclude the thesis.

Chapter 2

Analysis and control intervention strategies of a basic waterborne disease model

We formulate a simple mathematical model that captures the essential dynamics of waterborne disease transmission in a homogeneous mixing population setting. The important mathematical features of the model are determined and analysed accordingly. We extend the model by introducing control intervention strategies such as vaccination, treatment and water purification. The mathematical analyses of the vaccination, treatment, water purification and the multiple control strategy models are carried out to determine the possible benefits of these control intervention strategies. Sensitivity analysis is performed to determine the relative importance of each of the control parameters to disease transmission. An appropriate optimal control problem is analysed to determine the optimal use of the multiple control strategy to mitigate the spread of the disease with minimum cost. Numerical simulations are carried out using published data to support the analytical results. The contents of this chapter have been submitted for publication [20].

2.1 Introduction

Waterborne diseases which include Cholera, Hepatitis A and E, Giardia, Cryptosporidium and Rotavirus are some of the serious health problems threatening the life of individuals globally. This is especially so in developing countries where there is limited access to clean water. Unsafe water supply, poor sanitation and poor hygiene are major causes of waterborne diseases [93]. According to WHO [92], approximately 1.1 billion people globally do not have access to improved water supply sources. In addition, around 700,000 children die every year from diarrhoea caused by unsafe water and poor sanitation [89]. The prevalence of waterborne diseases could be controlled especially in developing countries through access to safe water supply, provision of adequate sanitation facilities and better hygiene practices [93]. Control intervention strategies such as water purification, vaccination and effective treatment of infected individuals are among the most important ways of reducing the spread of the disease [59, 65, 80]. Even though these control strategies are available, affordability has remain the greatest obstacle for most communities where the disease is endemic. This is due to the fact that the spread of waterborne diseases has been associated with poverty, limited resources and low socioeconomic status [21]. Optimal control theory can give insight into the best strategy to control the spread of the disease with minimum cost [49, 59].

Some of the essential factors that must be taken into consideration in attempting to understand the dynamics of waterborne diseases include: sanitation, transmission pathways, water treatment efforts, pathogen ecology outside of human hosts, climatological factors or rainfall [77, 69, 25, 27, 40, 6, 7, 31, 84]. Understanding how these factors interact to determine the dynamics of waterborne diseases is challenging. As a result, a variety of approaches has been used for modelling the dynamics of waterborne diseases [12, 72, 19, 29, 33, 36, 42, 84, 62]. To the best of our knowledge, none of those studies has considered a situation where secondary infections are generated only through linear interactions between humans and pathogens in water reservoir. Our purpose is to fill this gap in the analysis.

The remaining part of this chapter is organized as follows. We present a control-free model in Section 2.2 and analyse it in Section 2.3. The analyses of the vaccination, treatment and water

purification models are presented in Sections 2.4, 2.5 and 2.6 respectively. The multiple control model (with all controls imposed simultaneously) is presented and analysed in Section 2.7. We conclude the chapter by discussing our results in Section 2.8.

2.2 Control free model formulation

We consider an extension of the standard SIR model under the assumption of constant human population size $N(t)$ by adding a compartment $W(t)$ that measures pathogen concentration in the water reservoir [5, 84]. As usual, we assume that the total human population $N(t)$ is partitioned into susceptible $S(t)$, infected $I(t)$ and recovered individuals $R(t)$ such that $N(t) = S(t) + I(t) + R(t)$. Individuals enter the susceptible class $S(t)$ through birth at a rate μ . Susceptible individuals $S(t)$ become infected with the waterborne disease through contact with contaminated water reservoir at rate β . We do not consider direct person-to-person transmission because water-to-person transmission has been shown to be the most important and common route of waterborne disease transmission [24, 36, 80]. Infected individuals $I(t)$ shed pathogens into water reservoir at rate ν and recover naturally at rate γ . Pathogens are generated naturally in the water reservoir at rate α and decay at rate ξ . Natural death occurs in all human compartments at rate μ . Putting these assumptions and formulations together, we obtain

$$\begin{aligned}
 \dot{S}(t) &= \mu N(t) - \beta S(t)W(t) - \mu S(t), \\
 \dot{I}(t) &= \beta S(t)W(t) - (\mu + \gamma)I(t), \\
 \dot{W}(t) &= \nu I(t) - \sigma W(t), \\
 \dot{R}(t) &= \gamma I(t) - \mu R(t),
 \end{aligned} \tag{2.1}$$

where $\sigma = \xi - \alpha > 0$, is the natural decay rate of pathogens in the water reservoir. Note that our model (2.1) is in the form of the model considered by Tien and Earn [84] to study the multiple transmission pathways for waterborne disease. The difference between the two models is that they considered infections to be generated through both direct person-to-person and indirect water-to-person contact but we consider infections to be generated only through indirect water-

to-person contact. Therefore, the analysis of our model will help us understand the dynamics of waterborne disease for the case of single transmission pathway as well as determine the optimal use of the multiple control strategy to reduce the spread of the infections with minimum cost thus complementing the work of Tien and Earn [84].

We assume that all the parameters are positive and the initial conditions are assumed as follows:

$$S(0) > 0, \quad I(0) \geq 0, \quad W(0) \geq 0, \quad R(0) \geq 0. \quad (2.2)$$

All the solutions of model (2.1) will enter the feasible region

$$\Phi = \{(S, I, W, R) \in \mathbb{R}_+^4 : S + I + R = N, \quad S, I \leq N, \quad R \leq \gamma N/\mu, \quad W \leq \nu N/\sigma\}. \quad (2.3)$$

By considering a continuously differentiable function $V(x) = (V_a, V_b) = (S + I + R, W)$ and applying the local invariant set theorem 1.4.14, we have that the region Φ is positively invariant. Thus model (2.1) is well posed mathematically and epidemiologically in Φ .

2.3 Analysis of the control-free model

The control-free model (2.1) represents dynamics of waterborne disease in a homogeneous population without any control intervention measures. The analysis of this model is necessary in understanding the effects of control intervention strategies in subsequent models. All the results below are consistently with [84] if we set their b_I to zero.

2.3.1 Basic reproduction number

The control-free model (2.1) has a unique disease-free equilibrium (DFE) given by

$$(S^0, I^0, W^0) = (N, 0, 0). \quad (2.4)$$

The basic reproduction number [90], defined as the expected number of secondary infections that result from introducing a single infected individual into an otherwise susceptible population, is determined to be

$$\mathcal{R}_0 = \frac{\nu\beta N}{\sigma(\gamma + \mu)}. \quad (2.5)$$

2.3.2 Stability analysis of the DFE

The stability at the DFE determines the short-term dynamics of a disease [52]. Therefore to determine the short-term dynamics of waterborne disease, it is necessary to investigate the stability of the DFE. From Theorem 2 of van den Driessche and Watmough [90], the following result holds.

Theorem 2.3.1. *The DFE of the control-free model (2.1) is locally asymptotically stable if $\mathcal{R}_0 < 1$ and unstable if $\mathcal{R}_0 > 1$.*

Theorem 2.3.1 implies that waterborne disease can be eliminated from the entire population (when $\mathcal{R}_0 < 1$) if the initial size of the infected population is in the basin of attraction of the DFE (2.4). On the other hand, the disease will be established in the population if $\mathcal{R}_0 > 1$. To ensure disease elimination is independent of the initial size of the infected individuals, it is necessary to show that the DFE is globally-asymptotically stable. This is established using a global stability result by Castillo-Chavez et al. [13].

Theorem 2.3.2. *The DFE of the control-free model (2.1) is globally asymptotically stable provided that $\mathcal{R}_0 < 1$.*

Proof. We only need to show that the conditions (H1) and (H2) of the global stability result by Castillo-Chavez et al. [13] stated in Theorem 1.4.9 hold when $\mathcal{R}_0 < 1$. In our model (2.1), we have $X_1 = S, X_2 = (I, W)$ and $X_1^* = N$. The system

$$\frac{dX_1}{dt} = F(X_1, 0) = \mu N - \mu S$$

is linear and its solution can be easily found as

$$S(t) = N - (N - S(0))e^{-\mu t}.$$

Clearly $S(t) \rightarrow N$ as $t \rightarrow \infty$, regardless of the value of $S(0)$. Thus X_1^* is globally asymptotically stable. Next, we have that

$$G(X_1, X_2) = \begin{pmatrix} \beta W S - (\gamma + \mu) I \\ \nu I - \sigma W \end{pmatrix}.$$

We obtain

$$A = \begin{pmatrix} -(\gamma + \mu) & \beta N \\ \nu & -\sigma \end{pmatrix}$$

which is clearly an M–matrix with non-negative off diagonal elements. Hence, we find

$$\hat{G}(X_1, X_2) = \begin{pmatrix} \beta W(N - S) \\ 0 \end{pmatrix}.$$

Since $0 \leq S \leq N$, it is obvious that $\hat{G}(X_1, X_2) \geq 0$. This completes the proof. \square

2.3.3 Outbreak growth rate

We have seen that introducing any number of infected individuals into a community cannot lead to an outbreak whenever $\mathcal{R}_0 < 1$. At this stage, the disease can be completely eradicated from the community since DFE is globally asymptotically stable. However, if $\mathcal{R}_0 > 1$, then the DFE (2.4) becomes unstable and a disease outbreak occurs in the community. The positive (dominant) eigenvalue of the Jacobian at the DFE is typically referred to as the initial outbreak growth rate [84]. The Jacobian matrix J^0 of model (2.1) evaluated at the DFE (2.4) is

$$J^0 = \begin{pmatrix} -\mu & 0 & -\beta N \\ 0 & -(\mu + \gamma) & \beta N \\ 0 & \nu & -\sigma \end{pmatrix}. \quad (2.6)$$

The Jacobian matrix J^0 has 3 distinct eigenvalues given by

$$\begin{aligned} \lambda_1 &= -\mu, \\ \lambda_2 &= \frac{1}{2} \left[-(\mu + \gamma + \sigma) - \sqrt{(\mu + \gamma - \sigma)^2 + 4\sigma(\mu + \gamma)\mathcal{R}_0} \right], \\ \lambda_3 &= \frac{1}{2} \left[-(\mu + \gamma + \sigma) + \sqrt{(\mu + \gamma - \sigma)^2 + 4\sigma(\mu + \gamma)\mathcal{R}_0} \right]. \end{aligned}$$

We can see that $\lambda_1, \lambda_2 < 0$. Thus, the positive (dominant) eigenvalue is given by

$$\lambda^+ = \lambda_3. \quad (2.7)$$

Graphically, the value of $\lambda^+ > 0$ represents the steepness of the ascending infection curve (with respect to time). Thus, a higher λ^+ implies a more severe disease outbreak. Note that if $\mathcal{R}_0 < 1$,

then all the three eigenvalues become negative confirming Theorem 2.3.1. The epidemiological implications of this is that when there is no control measure to reduce the spread of the infection such that $\mathcal{R}_0 > 1$, then an outbreak will occur in the entire community and will grow at a rate λ^+ . To obtain the expected magnitude of this outbreak, it is necessary to determine the final epidemic size relation of the model.

2.3.4 Final outbreak size

Our analyses have shown that when $\mathcal{R}_0 > 1$ a waterborne disease outbreak occurs and grows at the rate λ^+ . The likely magnitude of this outbreak is often called the expected final size of the outbreak [57]. The final outbreak size of the SIR epidemiological models and some similar models are given by the relation

$$Z = 1 - \exp(-\mathcal{R}_0 Z), \quad (2.8)$$

where Z denotes the proportion of the population who becomes infected at some point during the outbreak. This also applies to our model (2.1) [84]. This result implies that if there is no control intervention to reduce the spread of the disease such that $\mathcal{R}_0 > 1$ and an outbreak occurs, then the final outbreak size of the epidemic can be determined by the relation (2.8).

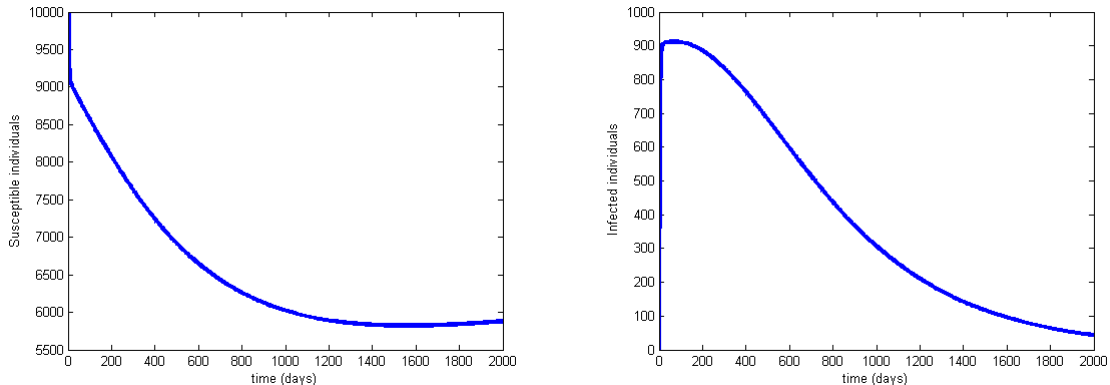
2.3.5 Stability analysis of the endemic equilibrium

The long-term dynamics of a disease is characterized by the stability at the endemic equilibrium [52]. In order to determine the long-term dynamics of the waterborne disease, we investigate the stability of model (2.1) at the endemic equilibrium (EE). When $\mathcal{R}_0 > 1$, a unique EE occurs in the model and is given by

$$(S^e, I^e, W^e) = (N/\mathcal{R}_0, \mu\sigma(\mathcal{R}_0 - 1)/(\nu\beta), \nu I^e/\sigma). \quad (2.9)$$

Obviously, I^e will vanish if $\mathcal{R}_0 \leq 1$. This confirms that the disease cannot be endemic when $\mathcal{R}_0 \leq 1$. The stability analyses of the EE (2.9) are summarized as follows [51, 43, 44, 84, 83]:

Theorem 2.3.3. *The unique EE (2.9) is locally asymptotically stable whenever $\mathcal{R}_0 > 1$.*



(a) Plot of $S(t)$ vs. time.

(b) Plot of $I(t)$ vs. time.

Figure 2.1: Numerical solution of the model (2.1) for $\mathcal{R}_0 = 1.1455$.

Theorem 2.3.4. *The unique EE (2.9) is globally asymptotically stable whenever $\mathcal{R}_0 > 1$.*

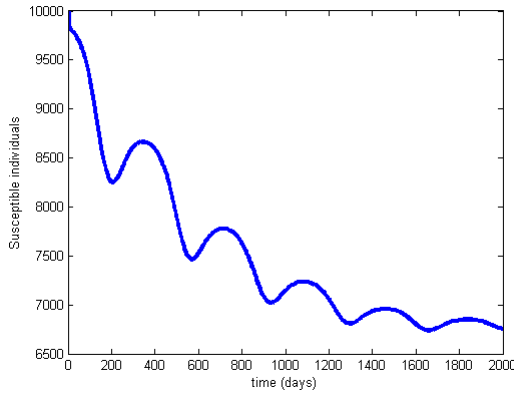
A simple illustration of the long-term dynamics of model (2.1) for $\mathcal{R}_0 > 1$ is presented in Figures 2.1(a) and 2.1(b). The Figures are obtained by solving model (2.1) numerically using parameter values from published data and a realistic range as shown in Table 2.1. This demonstrates the dynamics of model (2.1) in the absence of any control intervention strategy or external influences like seasonal variation over a long period of 2000 days.

2.3.6 Effects of seasonal variation

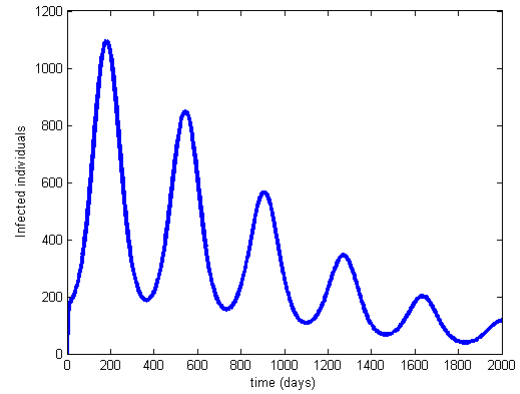
Waterborne disease outbreaks such as cholera have been associated with seasonal variations of weather, rainfall, humidity, water temperature, floods, drought and temperature [19, 65]. Here, we numerically investigate the effects of seasonal variations on the dynamics of our model. In the simulations, we consider a sine function with period of 365 days to model the seasonal oscillations. Using a similar approach in [19, 65, 80], we replace the contact rate β in model (2.1) by the sine function

$$\beta(t) = \beta(1 + \delta \sin(2\pi t/365)), \quad (2.10)$$

where β is the mean contact rate and δ describes the relative amplitude of seasonal variations. The numerical solutions of model (2.1) using the sine function are given in Figures 2.2(a) and



(a) Plot of $S(t)$ vs. time.



(b) Plot of $I(t)$ vs. time.

Figure 2.2: Numerical solution of the model (2.1) considering seasonal variation.

2.2(b). The figures describe the oscillations generated by our model due to seasonal variations. From the numerical solutions of model (2.1) in the presence and absence of seasonal variations, we observe some differences in their solutions. Particularly, in the absence of seasonal variations, we observe from the Figures 2.1(a) and 2.1(b) that there are no oscillations in the solutions of model (2.1). Thus seasonal variations have some influence on the dynamics of waterborne disease.

We have shown that in the absence of any control intervention strategy such that $\mathcal{R}_0 > 1$ an outbreak which grows at a rate λ^+ with the expected final size Z occurs in the population. This outbreak persists in the population whenever $\mathcal{R}_0 > 1$. To minimize the chances of such outbreak, we need the intervention of control strategies that can keep the basic reproduction number below unity.

2.4 Vaccination model

Vaccination is one of the control strategies for reducing the spread of waterborne diseases such as cholera. There are two types of effective oral cholera vaccines currently available and each can offer about 50-90% protection against the disease [99]. According to WHO [99], the vaccine (Dukoral) has been shown to provide short-term protection of 85-90% against *V. cholerae* O1

among all age groups at 4-6 months following immunization. The other vaccine (Shanchol) provides longer-term protection against *V. cholerae* O1 and O139 in children under five years of age. To determine the effects of vaccination in reducing the spread of waterborne diseases, we extend model (2.1) by assuming that susceptible individuals are vaccinated at rate ϕ with a vaccine whose efficacy is ε to obtain the model

$$\begin{aligned}
\dot{S}(t) &= \mu N(t) - \beta S(t)W(t) - (\mu + \phi)S(t), \\
\dot{V}(t) &= \phi S(t) - (1 - \varepsilon)\beta VW - \mu V, \\
\dot{I}(t) &= \beta S(t)W(t) + (1 - \varepsilon)\beta VW - (\mu + \gamma)I(t), \\
\dot{W}(t) &= \nu I(t) - \sigma W(t), \\
\dot{R}(t) &= \gamma I(t) - \mu R(t),
\end{aligned} \tag{2.11}$$

where $V(t)$ is vaccinated individuals at time t . The feasible region of model (2.11) is given by

$$\Phi_v = \{(S, V, I, W, R) \in \mathbb{R}_+^5 : S \leq S_v^0, V \leq V_v^0, I \leq N, R \leq \gamma N/\mu, W \leq \nu N/\sigma\}, \tag{2.12}$$

where $S_v^0 = \frac{\mu N}{\mu + \phi}$, $V_v^0 = \frac{\phi N}{\mu + \phi}$ and $N = S + V + I + R$. The region Φ_v is positively invariant, thus model (2.11) is mathematically and epidemiologically well posed in Φ_v .

2.4.1 Analysis of the vaccination model

The DFE of the vaccination model (2.11) is given by

$$(S_v^0, V_v^0, I_v^0, W_v^0) = \left(\frac{\mu N}{\mu + \phi}, \frac{\phi N}{\mu + \phi}, 0, 0 \right) \tag{2.13}$$

and the vaccination reproduction number is

$$\mathcal{R}_0^v = \frac{\mu + (1 - \varepsilon)\phi}{\mu + \phi} \mathcal{R}_0. \tag{2.14}$$

This threshold quantity \mathcal{R}_0^v represents the expected number of secondary infections that result from introducing a single infected individual into an otherwise susceptible population in the presence of vaccination [84, 85]. We can rewrite equation (2.14) as

$$\mathcal{R}_0^v = E_v \mathcal{R}_0, \quad E_v = \frac{\mu + (1 - \varepsilon)\phi}{\mu + \phi}. \tag{2.15}$$

The following equations

$$E_v < 1 \iff \mathcal{R}_0^v < \mathcal{R}_0, \quad \forall 0 < \varepsilon, \phi \leq 1, \quad (2.16)$$

$$E_v = 1 \iff \mathcal{R}_0^v = \mathcal{R}_0, \quad \text{for } \varepsilon = 0 \text{ or } \phi = 0, \quad (2.17)$$

hold. These equations can be verified by elementary algebraic manipulation. Equation (2.16) implies that vaccination decreases the number of secondary infected individuals by a factor E_v or alternatively, vaccination decreases \mathcal{R}_0 by a factor E_v [65]. The parameter $\varepsilon = 0$, means that vaccine has no effect or is useless [85] while $\phi = 0$, means that no susceptible individual is vaccinated. Therefore, the above discussion suggests that vaccination has some influence in reducing the number of secondary infections across the population provided $0 < \varepsilon, \phi \leq 1$.

The quantity E_v measures the effectiveness of vaccination as a control intervention strategy in reducing the spread of waterborne diseases. Since $\mathcal{R}_0 - \mathcal{R}_0^v = \mathcal{R}_0(1 - E_v)$ and $0 < E_v \leq 1$, then $E_v \rightarrow 1$ means that vaccination has no effect while $E_v \rightarrow 0$ means that vaccination has great effect. Therefore, the effectiveness of vaccination E_v can be express in percentages as

$$E_v^0 = (1 - E_v) \times 100. \quad (2.18)$$

This means that vaccination reduces the number of secondary infections by E_v^0 percent. To determine the short-term dynamics of waterborne diseases in the presence of vaccination, we investigate the stability of the vaccination model at DFE.

Theorem 2.4.1. *The DFE of the vaccination model (2.11) is both locally and globally asymptotically stable provided that $\mathcal{R}_0^v < 1$.*

Theorem 2.4.1 can be proved using a similar approach in the proof of Theorem 2.3.2 and a stability result from Theorem 2 of van den Driessche and Watmough [90]. The epidemiological implication of Theorem 2.4.1 is that waterborne disease will be eradicated from the entire population using vaccination, provided $\mathcal{R}_0^v < 1$. We have shown that infections can be eradicated in the absence of control measures provided $\mathcal{R}_0 < 1$. Since $\mathcal{R}_0^v < \mathcal{R}_0 < 1$, we can deduce from the above that introducing vaccination will lead to faster eradication of the outbreak. On the other hand, if vaccination is not strong enough such that $\mathcal{R}_0^v > 1$, then a waterborne disease

outbreak occurs in the population. The vaccination-induced outbreak growth rate is given by

$$\lambda_v^+ = \frac{1}{2} \left[-(\mu + \gamma + \sigma) + \sqrt{(\mu + \gamma - \sigma)^2 + 4\sigma(\mu + \gamma)\mathcal{R}_0^v} \right]. \quad (2.19)$$

Since $\mathcal{R}_0^v \leq \mathcal{R}_0$, we obtain

$$\lambda_v^+ \leq \lambda^+. \quad (2.20)$$

This shows that vaccination reduces the outbreak growth rate. Epidemiologically, this result demonstrates that even when vaccination is not strong enough such that an outbreak occurs in the population, the outbreak will be less severe compared to when no control was introduced. Equation (2.19) can be rewritten as

$$\lambda_v^+ = \frac{1}{2} \left[-(\mu + \gamma + \sigma) + \sqrt{(\mu + \gamma + \sigma)^2 - 4\sigma(\mu + \gamma)(1 - \mathcal{R}_0^v)} \right].$$

From this, it is easy to see that when $\mathcal{R}_0^v = 1$, the outbreak growth rate vanishes. Therefore, to have any chance of outbreak in the community, the vaccination reproduction number must be greater than unity.

2.5 Treatment model

Effective treatment of waterborne disease is very important in reducing the spread of the disease. Some waterborne diseases like cholera can kill within hours of contacting the disease if there is no proper treatment. If people infected with cholera are treated quickly and properly, the mortality rate is less than 1% but if they are left untreated, the mortality rate rises to 50 - 60% [78, 87]. Hence, it is necessary to investigate how to reduce the spread of waterborne disease using treatment as a control intervention strategy. We introduce treatment in the control-free model (2.1) by assuming that infected individuals are treated at rate τ (where $0 \leq \tau \leq 1$) and treated individuals $T(t)$ recover due to treatment at rate γ_τ to obtain the treatment model

given by

$$\begin{aligned}
\dot{S}(t) &= \mu N(t) - \beta S(t)W(t) - \mu S(t), \\
\dot{I}(t) &= \beta S(t)W(t) - (\mu + \gamma + \tau)I(t), \\
\dot{T}(t) &= \tau I(t) - (\mu + \gamma_\tau)T, \\
\dot{W}(t) &= \nu I(t) - \sigma W(t), \\
\dot{R}(t) &= \gamma I(t) + \gamma_\tau T(t) - \mu R(t).
\end{aligned} \tag{2.21}$$

The solutions of model (2.21) enter the feasible region

$$\Phi_\tau = \{(S, I, T, W, R) \in \mathbb{R}_+^5 : S \leq N, I \leq N, T \leq T^\circ, R \leq R^\circ, W \leq \nu N/\sigma\}, \tag{2.22}$$

where $T^\circ = \tau N/(\mu + \gamma_\tau)$, $R^\circ = \gamma N/\mu + \tau N/(\mu(\mu + \gamma_\tau))$ and $N = S + I + T + R$. The region Φ_τ is positively invariant, thus model (2.21) is mathematically and epidemiologically well posed in Φ_τ .

2.5.1 Analysis of the treatment model

The DFE of the treatment model (2.21) is given by

$$(S_\tau^0, I_\tau^0, T_\tau^0, W_\tau^0) = (N, 0, 0, 0) \tag{2.23}$$

and the treatment reproduction number is

$$\mathcal{R}_0^\tau = \mathcal{R}_0 E_\tau, \tag{2.24}$$

where

$$E_\tau = \frac{\mu + \gamma}{\mu + \gamma + \tau}. \tag{2.25}$$

The threshold quantity \mathcal{R}_0^τ represents the expected number of secondary infections that results from introducing a single infected individual into an otherwise susceptible population in the presence of treatment. Clearly, the following equations

$$E_\tau < 1 \iff \mathcal{R}_0^\tau < \mathcal{R}_0 \quad \forall \tau \neq 0, \tag{2.26}$$

$$E_i^\tau = 1 \iff \mathcal{R}_0^\tau = \mathcal{R}_0, \quad \text{for } \tau = 0, \tag{2.27}$$

hold. Epidemiologically, this suggests that treatment of infected individual has some influence in reducing the number of secondary infections in the population provided that $0 < \tau \leq 1$. To determine the short-term dynamics of waterborne diseases in the presence of treatment, we investigate the stability of the treatment model at DFE.

Theorem 2.5.1. *The DFE of the treatment model (2.21) is both locally and globally asymptotically stable, provided $\mathcal{R}_0^\tau < 1$.*

Biologically speaking, Theorem 2.5.1 implies that waterborne disease can be eradicated from the population through treatment of infected individuals whenever $\mathcal{R}_0^\tau < 1$. However, if infected individuals are not properly treated such that $\mathcal{R}_0^\tau > 1$, then an outbreak occurs in the population. The treatment-induced outbreak growth rate is given by

$$\lambda_\tau^+ = \frac{1}{2} \left[-(\mu + \gamma + \tau + \sigma) + \sqrt{(\mu + \gamma + \tau - \sigma)^2 + 4\sigma(\mu + \gamma + \tau)\mathcal{R}_0^\tau} \right]. \quad (2.28)$$

To determine the strength of this outbreak, we compare it with the outbreak growth rate in the absence of control intervention.

Theorem 2.5.2. *Suppose that $\tau \geq 0$, then $\lambda_\tau^+ \leq \lambda^+$. Furthermore, $\lambda_\tau^+ = \lambda^+$ if and only if $\tau = 0$.*

Proof. Given that

$$\lambda^+ = \frac{1}{2} \left[-(\mu + \gamma + \sigma) + \sqrt{(\mu + \gamma - \sigma)^2 + 4\sigma(\mu + \gamma)\mathcal{R}_0} \right]. \quad (2.29)$$

Let $M = \gamma + \mu + \sigma$, $P = \gamma + \mu - \sigma$, then $M - P = 2\sigma > 0$. We rewrite equation (2.29) as

$$(2\lambda^+ + M)^2 = P^2 + 4\sigma(\mu + \gamma)\mathcal{R}_0 \quad (2.30)$$

and equation (2.28) as

$$(2\lambda_\tau^+ + M + \tau)^2 = (P + \tau)^2 + 4\sigma(\mu + \gamma + \tau)\mathcal{R}_0^\tau. \quad (2.31)$$

Subtracting equation (2.31) from (2.30) and simplifying gives

$$(2\lambda^+ + M)^2 - (2\lambda_\tau^+ + M)^2 = 2\tau(M - P) + 4\tau\lambda_\tau^+ \geq 0.$$

Hence, $\lambda_\tau^+ \leq \lambda^+$ if $\tau \geq 0$. □

The above result can be summarized as follows:

Theorem 2.5.3. *When $\mathcal{R}_0^r > 1$, the DFE of the treatment model (2.21) is unstable with a lower outbreak growth rate than that of the control-free model (2.1).*

This illustrates that treatment of infected individuals reduces outbreak growth rate.

2.6 Water purification model

According to the World Health Organization [93], unsafe water supply, poor sanitation and poor hygiene are the major causes of waterborne diseases. A significant number of cases of the disease could be reduced through access to clean water supply, provision of adequate sanitation facilities and better hygiene practices. To determine the effects of water purification as a control intervention strategy, we extend model (2.1) by assuming that water purification reduces pathogen concentration at a rate d to obtain

$$\begin{aligned}\dot{S}(t) &= \mu N(t) - \beta S(t)W(t) - \mu S(t), \\ \dot{I}(t) &= \beta S(t)W(t) - (\mu + \gamma)I(t), \\ \dot{W}(t) &= \nu I(t) - (d + \sigma)W(t), \\ \dot{R}(t) &= \gamma I(t) - \mu R(t),\end{aligned}\tag{2.32}$$

where $0 \leq d \leq 1$. The solutions of model (2.32) enter the feasible region

$$\Phi_w = \{(S, I, W, R) \in \mathbb{R}_+^4 : S \leq N, I \leq N, R \leq \gamma N/\mu, W \leq \nu N/(\sigma + d)\},\tag{2.33}$$

where $N = S + I + R$. The region Φ_w is positively invariant, thus model (2.32) is mathematically and epidemiologically well posed in it.

2.6.1 Analysis of the water purification model

The DFE of the water purification model (2.32) is given by

$$(S_w^0, I_w^0, W_w^0) = (N, 0, 0)\tag{2.34}$$

and the water purification reproduction number is

$$\mathcal{R}_0^w = \mathcal{R}_0 E_w, \quad (2.35)$$

where

$$E_w = \frac{\sigma}{\sigma + d}. \quad (2.36)$$

The threshold quantity \mathcal{R}_0^w represents the expected number of secondary infections that results from introducing a single infected individual into an otherwise susceptible population in the presence of water purification. Similarly, we obtain that

$$E_w < 1 \iff \mathcal{R}_0^w < \mathcal{R}_0, \quad \forall d \neq 0, \quad (2.37)$$

$$E_w = 1 \iff \mathcal{R}_0^w = \mathcal{R}_0, \quad \text{if } d = 0. \quad (2.38)$$

This suggests that water purification has some influence in reducing the number of secondary infections in the population provided that $0 < d \leq 1$. To determine the short-term dynamics of waterborne in the presence of water purification, it is necessary to investigate the stability of the water purification model at the DFE.

Theorem 2.6.1. *The DFE of the water purification model (2.32) is both locally and globally asymptotically stable, whenever $\mathcal{R}_0^w < 1$.*

Epidemiologically, Theorem 2.6.1 means that waterborne disease can be eliminated from the entire population through water purification whenever $\mathcal{R}_0^w < 1$. On the contrary, if water purification is not effective enough such that $\mathcal{R}_0^w > 1$, then a waterborne disease outbreak occurs in the population. The water purification-induced outbreak growth rate is given by

$$\lambda_w^+ = \frac{1}{2} \left[-(\mu + \gamma + d + \sigma) + \sqrt{(\mu + \gamma - d - \sigma)^2 + 4(\sigma + d)(\mu + \gamma)\mathcal{R}_0^w} \right]. \quad (2.39)$$

Using the same approach in the proof of Theorem 2.5.2, we can show that if $d \geq 0$, then

$$\lambda_w^+ \leq \lambda^+. \quad (2.40)$$

This shows that water purification also reduces the outbreak growth rate.

2.7 Multiple control intervention strategy model

We have seen that each of the single control intervention strategy have some influence in reducing the number of secondary infections in the population. Furthermore, we discovered that even when the single control is not effective enough and an outbreak occurs, the outbreak growth rate of each of the single control is lower than that of the control-free model. In this section, we consider the multiple control intervention strategy, a situation whereby all the three control intervention strategies are introduced into the model (2.1) simultaneously to obtain

$$\begin{aligned}
\dot{S}(t) &= \mu N(t) - \beta S(t)W(t) - (\mu + \phi)S(t), \\
\dot{V}(t) &= \phi S(t) - (1 - \varepsilon)\beta VW - \mu V, \\
\dot{I}(t) &= \beta S(t)W(t) + (1 - \varepsilon)\beta VW - (\mu + \gamma + \tau)I(t), \\
\dot{T}(t) &= \tau I(t) - (\mu + \gamma_\tau)T, \\
\dot{W}(t) &= \nu I(t) - (d + \sigma)W(t), \\
\dot{R}(t) &= \gamma I(t) + \gamma_\tau T(t) - \mu R(t).
\end{aligned} \tag{2.41}$$

All the solutions of model (2.41) enter the feasible region

$$\Phi_c = \{(S, V, I, T, W, R) \in \mathbb{R}_+^6 : S \leq S_v^0, V \leq V_v^0, I \leq N, T \leq T_c^o, R \leq R_c^o, W \leq W_c^o\}, \tag{2.42}$$

where $N = S + V + I + T + R$, $T_c^o = \tau N / (\mu + \gamma_\tau)$, $R_c^o = \gamma N / \mu + \tau N / (\mu(\mu + \gamma_\tau))$ and $W_c^o = \nu N / (\sigma + d)$. The region Φ_c is positively invariant, thus it is sufficient to consider the solutions of model (2.41) in Φ_c .

2.7.1 Analysis of the multiple control intervention strategy model

The multiple control intervention strategy model (2.41) has DFE given by

$$(S_c^0, V_c^0, I_c^0, T_c^0, W_c^0) = \left(\frac{\mu N}{\mu + \phi}, \frac{\phi N}{\mu + \phi}, 0, 0, 0 \right), \tag{2.43}$$

and a basic reproduction number given by

$$\mathcal{R}_0^c = \mathcal{R}_0 E_c, \tag{2.44}$$

where

$$E_c = \frac{\sigma(\gamma + \mu)(\mu + (1 - \varepsilon)\phi)}{(d + \sigma)(\gamma + \mu + \tau)(\mu + \phi)} = E_w E_\tau E_v. \quad (2.45)$$

The threshold quantity \mathcal{R}_0^c represents the expected number of secondary infections that results from introducing a single infected individual into an otherwise susceptible population in the presence of vaccination, treatment and clean water. From equations (2.45) and (2.44), we have that

$$E_c < 1 \iff \mathcal{R}_0^c < \mathcal{R}_0. \quad (2.46)$$

This implies that the multiple control intervention strategy reduces the number of secondary infections by a factor E_c . Equations (2.16), (2.26), (2.37) and (2.46) can be written in compact form as

$$\mathcal{R}_0^c, \mathcal{R}_0^v, \mathcal{R}_0^w, \mathcal{R}_0^\tau < \mathcal{R}_0. \quad (2.47)$$

To determine the short-term dynamics of waterborne in the presence of the multiple control intervention strategy, we investigate the stability of the multiple control intervention strategy model at the DFE.

Theorem 2.7.1. *If $\mathcal{R}_0^c < 1$, the DFE (2.43) of model (2.41) is globally asymptotically stable and unstable if $\mathcal{R}_0^c > 1$.*

The epidemiological implication of this is that waterborne diseases will be eradicated from the entire population using the multiple control intervention strategy whenever $\mathcal{R}_0^c < 1$.

2.7.2 Multiple control strategy vs. single control strategy

Whenever an outbreak occurs in an unprepared population, the population will consider the most available and accessible control intervention strategy (First Aid/ First Control) at that point in time while making plans for other controls if they are not satisfied with the first control. Here, we consider a situation where the multiple control intervention strategy is being introduced to facilitate reducing the spread of waterborne disease across a population in the presence

of the single control intervention strategy. To understand the effects of the multiple control intervention in the presence of one of the single control intervention strategies, it is desirable to determine the relationship between their various reproduction numbers. For vaccination, we rewrite equation (2.44) as

$$\mathcal{R}_0^c = \mathcal{R}_0^v K_v, \quad K_v = \frac{\sigma(\gamma + \mu)}{(d + \sigma)(\gamma + \mu + \tau)},$$

and have that

$$K_v < 1 \iff \mathcal{R}_0^c < \mathcal{R}_0^v. \quad (2.48)$$

Equation (2.48) means that the multiple control strategy reduces the number of secondary infections in the presence of vaccination by a factor K_v . Similarly, for the treatment model we have

$$\mathcal{R}_0^c = \mathcal{R}_0^\tau K_\tau, \quad K_\tau = \frac{\sigma(\mu + (1 - \varepsilon)\phi)}{(d + \sigma)(\mu + \phi)}.$$

It is easy to observe that

$$K_\tau < 1 \iff \mathcal{R}_0^c < \mathcal{R}_0^\tau. \quad (2.49)$$

Equation (2.49) implies that the multiple control intervention strategy reduces the number of secondary infections in the presence of treatment by a factor K_τ . Finally, for water purification we have

$$\mathcal{R}_0^c = \mathcal{R}_0^w K_w, \quad K_w = \frac{(\gamma + \mu)(\mu + (1 - \varepsilon)\phi)}{(\gamma + \mu + \tau)(\mu + \phi)}.$$

Obviously,

$$K_w < 1 \iff \mathcal{R}_0^c < \mathcal{R}_0^w. \quad (2.50)$$

This implies that the multiple control intervention strategy reduces the number of secondary infections in the presence of water purification by a factor K_w . Combining equations (2.47), (2.48), (2.49) and (2.50) we obtain

$$\mathcal{R}_0^c \leq \mathcal{R}_0^w, \mathcal{R}_0^\tau, \mathcal{R}_0^v \leq \mathcal{R}_0, \quad (2.51)$$

which is equivalent to

$$E_0^c \leq E_0^w, E_0^\tau, E_0^v \leq 1. \quad (2.52)$$

This also reveals the importance of the multiple control intervention strategy. Consequently, this scenario for an endemic community settings will imply that they should focus more on exploring the multiple control intervention strategy as it has the greatest positive impact on reducing the spread of waterborne disease than each of the single control intervention strategy.

Suppose that the multiple control strategy is not effective enough such that $\mathcal{R}_0^c > 1$. Then the DFE (2.43) becomes unstable and a disease outbreak occurs. The outbreak growth rate of the multiple control strategy model is given by

$$\lambda_c^+ = \frac{1}{2} \left[-(\mu + \gamma + \tau + \sigma + d) + \sqrt{(\mu + \gamma + \tau - \sigma - d)^2 + 4(\sigma + d)(\mu + \gamma + \tau)\mathcal{R}_0^c} \right]. \quad (2.53)$$

Similar to each of the single control strategy, we can show that the multiple control reduces the outbreak growth rate.

Theorem 2.7.2. *Suppose that $d \geq 0$, $\phi \geq 0$, $\tau \geq 0$ and $\varepsilon \geq 0$, then $\lambda_c^+ \leq \lambda^+$. Furthermore, $\lambda_c^+ = \lambda^+$ if and only if $d = \phi = \tau = \varepsilon = 0$.*

The proof can be established by the same approach used in the proof of Theorem 2.5.2. We have shown that each of the single control intervention strategy and the multiple control intervention strategy reduces the outbreak growth rate. Next, we show that the multiple control intervention strategy reduces the outbreak growth rate more than each of the single control intervention strategy. The details are given in Theorem (2.7.3) below.

Theorem 2.7.3. *Suppose that $d \geq 0$, $\phi \geq 0$, $\tau \geq 0$ and $\varepsilon \geq 0$, then*

$$\lambda_c^+ \leq \lambda_v^+, \quad \lambda_c^+ \leq \lambda_\tau^+, \quad \lambda_c^+ \leq \lambda_w^+. \quad (2.54)$$

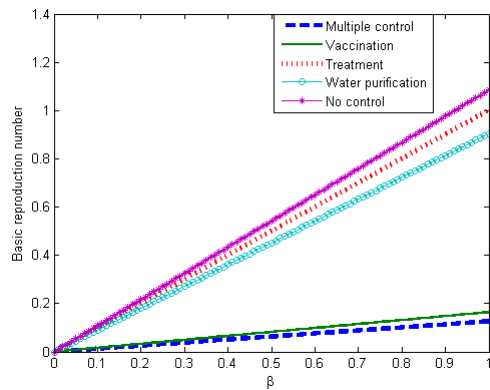
Furthermore,

$$\lambda_c^+ = \lambda_v^+ = \lambda_\tau^+ = \lambda_w^+ \iff d = \phi = \tau = \varepsilon = 0. \quad (2.55)$$

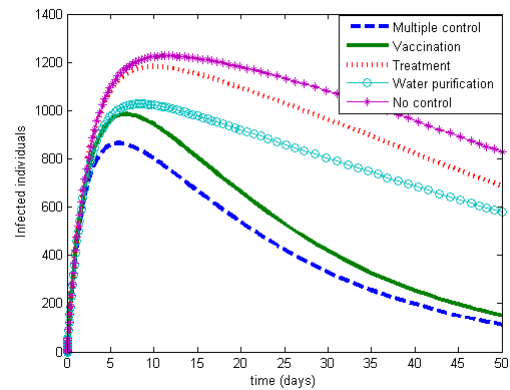
The procedure for the proof is the same as in Theorem 2.5.2.

Table 2.1: Parameter values for numerical simulations with reference

Parameter	Symbol	Value	Reference
Contact rate	β	0.214 day ⁻¹	[19, 36]
Shedding rate	ν	0.50 day ⁻¹	[50, 41]
Birth/death rate	μ	0.0001 day ⁻¹	[19]
Natural recovery rate	γ	0.0592 day ⁻¹	[42]
Recovery rate due to treatment	γ_τ	0.1184 day ⁻¹	[70]
Net decay rate of pathogen in water	σ	0.333 day ⁻¹	[19]
Efficacy of vaccine	ε	0.85 day ⁻¹	[65]
Rate of reduction of W due to water purification	d	0.0667 day ⁻¹	assumed
Rate of vaccination	ϕ	0.07 day ⁻¹	[65]
Treatment rate	τ	0.005 day ⁻¹	[65]



(a) Plot of $\mathcal{R}_0, \mathcal{R}_0^v, \mathcal{R}_0^\tau, \mathcal{R}_0^w, \mathcal{R}_0^c$ vs. β .



(b) Plot of $I(t)$ vs. time for the various models.

Figure 2.3: Graphical representation of the basic reproduction numbers and infected individuals of the models.

2.7.3 Sensitivity analysis of the multiple control strategy model

We have seen that the multiple control intervention strategy is the best control strategy for reducing the spread of waterborne disease. In order to determine the impact of each of the control parameters in the presence of the multiple control intervention strategy, it is necessary to carry out sensitivity analysis. Sensitivity analysis is used to determine the relative importance of model parameters to disease transmission and prevalence [17, 39]. We perform the analysis by calculating the sensitivity index of the basic reproduction number \mathcal{R}_0^c (2.44) with respect to the control parameters d, ε, τ and ϕ using the normalized forward sensitivity approach defined below.

Definition[17]. The normalized forward sensitivity index of a variable u , that depends differentially on a parameter ρ , is defined as:

$$\Upsilon_{\rho}^u = \frac{\partial u}{\partial \rho} \times \frac{\rho}{u}. \quad (2.56)$$

Note that when $\Upsilon_{\rho}^u > 0$, we say that ρ increases the value of u as its value increases. On the other hand, if $\Upsilon_{\rho}^u < 0$ we say that ρ decreases the value of u as its value increases. Using this definition, we compute the sensitivity index of each of the control parameters as follows. The sensitivity index of \mathcal{R}_0^c with respect to d, ε, τ and ϕ denoted by $\Upsilon_d^{\mathcal{R}_0^c}, \Upsilon_{\varepsilon}^{\mathcal{R}_0^c}, \Upsilon_{\tau}^{\mathcal{R}_0^c}$ and $\Upsilon_{\phi}^{\mathcal{R}_0^c}$ respectively, are given by

$$\Upsilon_d^{\mathcal{R}_0^c} = \frac{-d}{d + \sigma}, \quad \Upsilon_{\varepsilon}^{\mathcal{R}_0^c} = \frac{-\phi\varepsilon}{\mu + (1 - \varepsilon)\phi}, \quad \Upsilon_{\tau}^{\mathcal{R}_0^c} = \frac{-\tau}{\gamma + \mu + \tau}, \quad \Upsilon_{\phi}^{\mathcal{R}_0^c} = \frac{-\phi\varepsilon\mu}{(\mu + (1 - \varepsilon)\phi)(\mu + \phi)}.$$

This shows that each of the control parameters decreases \mathcal{R}_0^c as the parameter increases. However, it is difficult to determine the exact magnitude of the sensitivity index since all the sensitivity indices are parameter dependent. Therefore, to estimate the magnitude of these indices, we resort to parameter values from published data as shown in Table 2.1. Using these parameter values, we calculate the estimate magnitude of the indices as

$$\Upsilon_d^{\mathcal{R}_0^c} = -0.1668, \quad \Upsilon_{\varepsilon}^{\mathcal{R}_0^c} = -5.6132, \quad \Upsilon_{\tau}^{\mathcal{R}_0^c} = -0.0778, \quad \Upsilon_{\phi}^{\mathcal{R}_0^c} = -0.0081.$$

The above results show that vaccine efficacy ε is the most sensitive control parameter with sensitivity index of -5.6132 followed by reduction in pathogen concentration d , then treatment

rate τ and vaccination rate ϕ . Therefore, decreasing (or increasing) vaccine efficacy by 10% increases (or decreases) the basic reproduction number by 56.132%. Note that these results are consistent with intuitive expectation.

We note that an alternative approach which has been used by some authors is to simply consider parameter values in the literature [59, 64, 65, 85]. By considering the values in Table 2.1, one can conclude that vaccination is the best single control intervention, followed by water purification and then treatment. Numerical illustrations of this can be found in Figures 2.3(a) and 2.3(b). From Figure 2.3(a), we can see that the inequality

$$\mathcal{R}_0^c \leq \mathcal{R}_0^v \leq \mathcal{R}_0^w \leq \mathcal{R}_0^\tau \leq \mathcal{R}_0 \quad (2.57)$$

holds. This is consistent with the results in [59, 65, 85] even though the models are not the same. Similarly, we can show that

$$\lambda_c^+ \leq \lambda_v^+ \leq \lambda_w^+ \leq \lambda_\tau^+ \leq \lambda^+. \quad (2.58)$$

2.7.4 Optimal control problem

Even though the multiple control intervention strategy has been shown to be the best control measure for reducing the spread of water borne disease, some communities where this disease is endemic cannot afford it due to limited resources. A successful multiple control intervention scheme is one which reduces disease related deaths with minimum cost [59]. To minimize the cost of implementing the multiple controls (vaccination, treatment and water purification), we assume that the control parameters ϕ , τ , d in the multiple control model (2.41) are measurable functions of time t and then formulate an appropriate optimal control functional that minimizes the cost of implementing the controls subject to the model. For simplicity, we let $\phi = u_1(t)$, $\tau = u_2(t)$, $d = u_3(t)$. Therefore, the multiple control scheme is said to be optimal if it minimizes the objective functional

$$J(u_1, u_2, u_3) = \int_0^{t_f} [A_1 S(t) + A_2 I(t) + A_3 W(t) + C_1 u_1^2(t) + C_2 u_2^2(t) + C_3 u_3^2(t)] dt \quad (2.59)$$

subject to the multiple control model (2.41), where t_f is the final time and the coefficients, $A_1, A_2, A_3, C_1, C_2, C_3$ are balancing cost coefficients. The performance specification involves

minimizing the number of susceptible, infected individuals and pathogens in water reservoir, as well as the costs for applying the controls. We consider quadratic functions for measuring the control cost [100, 2, 59, 85].

The existence of the optimal control triple $(u^*(t), u_2^*(t), u_3^*(t)) = u^*(t)$ that minimizes our objectives functional (2.59) subject to the state system which is the multiple control model (2.41) comes from Fleming and Rishel [32], i.e.,

$$J(u^*(t)) = \min \{J : u(t) \in U, t \in [0, t_f]\}, \quad (2.60)$$

where $u(t) = (u_1(t), u_2(t), u_3(t))$ and $U = \{u(t) : u(t) \text{ are measurable, } 0 \leq u(t) \leq 1\}$ is the control set. The Pontryagin's Maximum Principle [71] introduces adjoint functions that enable us to combine the state system (2.41) to the objective functional (2.59). This principle converts the problem of minimizing the objective functional subject to the state system into a problem of pointwise minimizing a Hamiltonian H , with respect to $u_1(t)$, $u_2(t)$ and $u_3(t)$. The Hamiltonian for the objective functional (2.59) and the state system is given by

$$\begin{aligned} H = & A_1 S(t) + A_2 I(t) + A_3 W(t) + C_1 u_1^2(t) + C_2 u_2^2(t) + C_3 u_3^2(t) \\ & + \lambda_S (\mu N(t) - \beta S(t)W(t) - (\mu + u_1)S(t)) + \lambda_V (u_1 S(t) - (1 - \varepsilon)\beta VW - \mu V) \\ & + \lambda_I (\beta S(t)W(t) + (1 - \varepsilon)\beta VW - (\mu + \gamma + u_2)I(t)) + \lambda_T (u_2 I(t) - (\mu + \gamma_\tau)T) \\ & + \lambda_W (\nu I(t) - (u_3 + \sigma)W(t)) + \lambda_R (\gamma I(t) + \gamma_\tau T(t) - \mu R(t)), \end{aligned} \quad (2.61)$$

where $\lambda_S, \lambda_V, \lambda_I, \lambda_T, \lambda_W$ and λ_R are the associated adjoints for the states S, V, I, T, W and R respectively.

Given an optimal control triple $(u^*(t), u_2^*(t), u_3^*(t))$ together with corresponding states $(S^*, V^*, I^*, T^*, W^*, R^*)$ that minimizes $J(u_1, u_2, u_3)$ over U , there exists adjoint variables

$\lambda_S, \lambda_V, \lambda_I, \lambda_T, \lambda_W$ and λ_R satisfying

$$\begin{aligned}
\frac{d\lambda_S}{dt} &= -A_1 + \lambda_S(\beta W + u_1) - \lambda_V u_1 - \lambda_I \beta W, \\
\frac{d\lambda_V}{dt} &= \lambda_V((1 - \varepsilon)\beta W + \mu) - \lambda_I(1 - \varepsilon)\beta W, \\
\frac{d\lambda_I}{dt} &= -A_2 + \lambda_I(\mu + \gamma + u_2) - \lambda_I u_2 - \lambda_W \nu - \lambda_R \gamma, \\
\frac{d\lambda_T}{dt} &= \lambda_T(\mu + \gamma_\tau) - \lambda_R \gamma_\tau, \\
\frac{d\lambda_W}{dt} &= -A_3 + \lambda_S S \beta + \lambda_V(1 - \varepsilon)V \beta - \lambda_I(\beta S + (1 - \varepsilon)\beta V) + \lambda_W(\sigma + u_2), \\
\frac{d\lambda_R}{dt} &= -\lambda_R \mu,
\end{aligned} \tag{2.62}$$

together with transversality conditions

$$\lambda_k(t_f) = 0, \quad \text{for } k = S, V, I, T, W \text{ and } R.$$

Note that the differential equations (2.62) governing the adjoint variables were obtained by differentiating the Hamiltonian function (2.61) with respect to the corresponding states as follows:

$$-\frac{d\lambda_k}{dt} = \frac{dH}{dk}.$$

Consider now the optimality conditions

$$0 = \frac{\partial H}{\partial u_1}, \quad 0 = \frac{\partial H}{\partial u_2} \quad \text{and} \quad 0 = \frac{\partial H}{\partial u_3}. \tag{2.63}$$

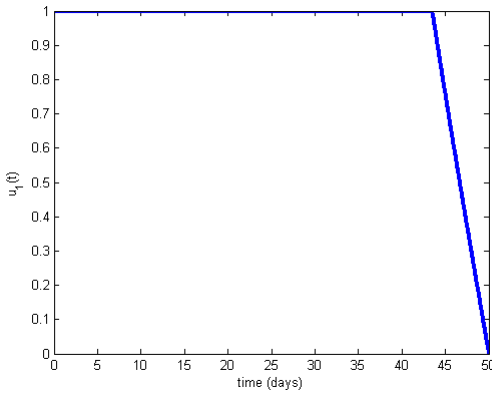
By solving for u_1 in the optimality conditions and subsequently taking bounds into account, we obtain

$$u_1^* = \min \{1, S(\lambda_S - \lambda_V)/(2C_1)\}. \tag{2.64}$$

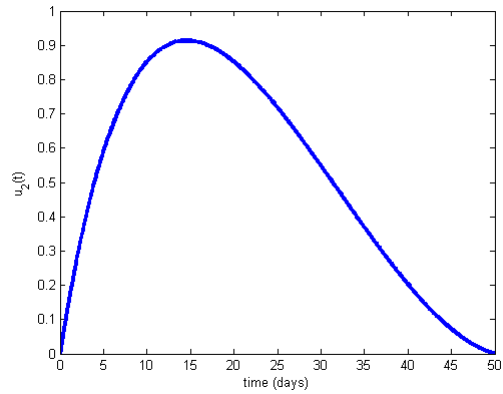
Similarly, we obtain that

$$u_2^* = \min \{1, I(\lambda_I - \lambda_T)/(2C_2)\}, \quad u_3^* = \min \{1, W\lambda_W/(2C_3)\}. \tag{2.65}$$

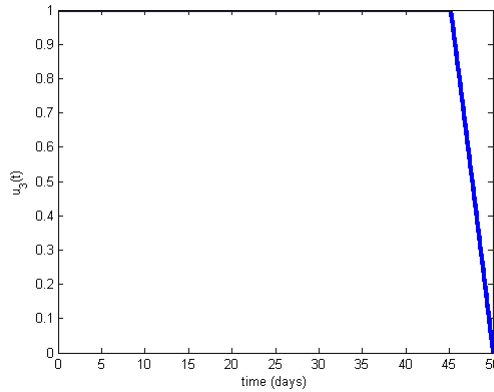
These results demonstrate that there exist an optimal control triple (u_1^*, u_2^*, u_3^*) that can reduce the spread of waterborne disease using multiple control intervention with minimum cost. Since



(a) Plot of $u_1(t)$ vs. time.



(b) Plot of $u_2(t)$ vs. time.



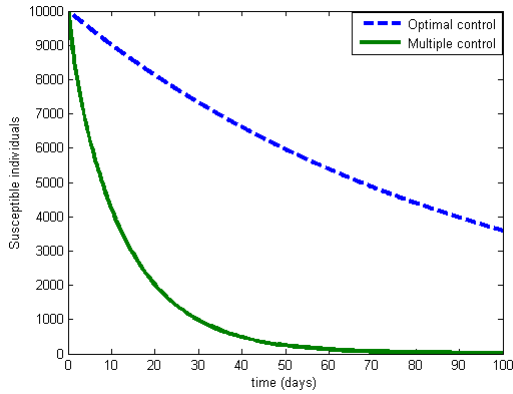
(c) Plot of $u_3(t)$ vs. time.

Figure 2.4:

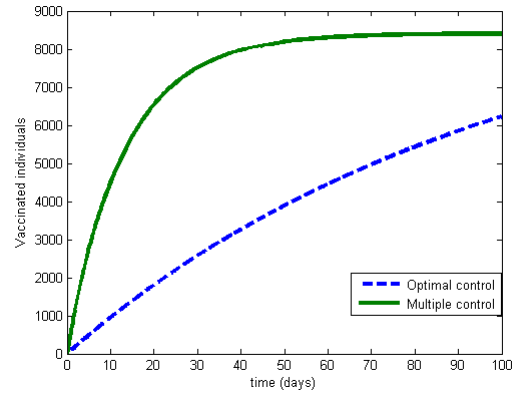
the optimal control triple is parameter dependent, to determine their magnitudes for the period of the outbreak we resort to numerical simulations using published data. The numerical solution of the optimal control triple are obtained using the parameter values in Table 2.1 together with the following cost factors : $A_1 = 6.00$, $A_2 = 2.00$, $A_3 = 100.00$, $C_1 = 10.00$, $C_2 = 10.00$, $C_3 = 10.00$ which are taken from [59]. We used the forward-backward algorithm of [49, 59] to obtain the optimal control triple that minimize the cost functional, and they are shown in Figures 2.4(a) – 2.4(c). Figures 2.4(a) and 2.4(c) suggest that it is optimal to begin vaccinating and providing clean water from the onset of the outbreak (or as soon as possible) and to continue vaccinating and purifying contaminated water with maximal effort until the outbreak ends. This is realistic since vaccination and water purification are preventive strategies and

they are highly recommended from the onset of the outbreak (even before the outbreak). On the other hand, Figure 2.4(b) suggests that it is optimal to treat individuals immediately as they get infected. The optimal treatment is also reasonable since treatment can only take place when someone is already infected and prompt treatment is highly recommended [78, 87].

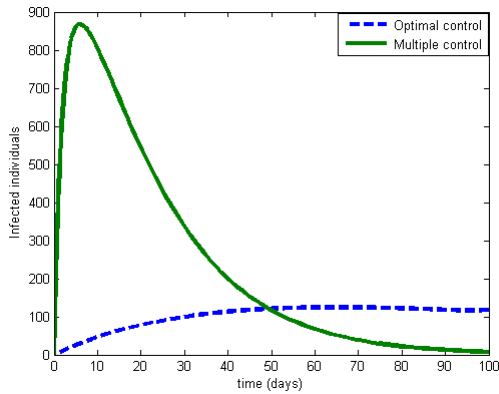
A simple demonstration of the impact of the optimal control triple on the dynamics of waterborne disease is given in Figures 2.5(a)–2.5(d). The Figures are obtained by solving the multiple control model numerically for two different sets of control parameters values: (i) using the optimal control triple, and (ii) using the control parameter values given in Table 2.1. From the Figures, we observe a big difference between the solutions of the model for the two cases. This reveals the impact of the optimal control triple on the dynamics of the disease. For instance, Figure 2.5(c) reveals that the maximum number of infected individuals when the optimal control triple is implemented is about one hundred, while the maximum number of infected individuals when the multiple control is considered is about nine hundred. This shows that the optimal control triple does not only minimize the cost of implementing the control, but also keeps the number of infected individual very low throughout the duration of the outbreak. A similar huge impact can be seen in the number of susceptible, vaccinated and treated individuals. Note that the reason for this huge impact can be traced back to our parameter values of the control parameters and optimal control triple. For example, the multiple control takes a vaccination rate $\phi = 0.070$, while the optimal control triple suggests that $\phi = u_1^* = 1.000$ from the onset of the outbreak. Similar results can also be seen for treatment and water purification. Finally, Figure 2.5(d) show that at most 30 people can be treated at each point in time during the outbreak under multiple control whereas more than 90 people can be treated when optimal control is considered.



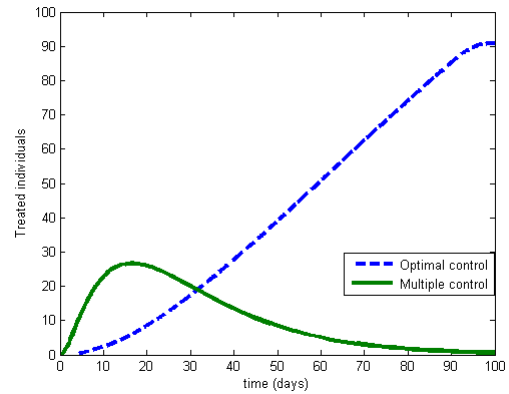
(a) Plot of $S(t)$ vs. time.



(b) Plot of $V(t)$ vs. time.



(c) Plot of $I(t)$ vs. time.



(d) Plot of $T(t)$ vs. time.

Figure 2.5: Graphical representation of $S(t)$, $V(t)$, $I(t)$ and $T(t)$ vs. time (t) in the presence of the multiple control intervention strategy and optimal control strategy.

2.8 Discussion

Dynamics and control intervention strategies for waterborne disease in a homogeneous mixing population/community have been explored. Our analyses have shown that significant information concerning the dynamics of waterborne disease can be obtained by analysing an appropriate mathematical epidemiological model.

In the absence of any control intervention strategy, we have shown that it is possible for the waterborne disease to be eradicated from the entire population provided the basic reproduction number \mathcal{R}_0 is less than unity. This can happen if the infected individuals begin to practice

healthy living like staying away from contaminated water, boiling water before drinking, proper sewage disposal etc. On the other hand, if $\mathcal{R}_0 > 1$, an outbreak which grows at a rate λ^+ might occur with a final outbreak size Z . This outbreak will persist in the entire population, since the endemic equilibrium is globally asymptotically stable. Furthermore, we discovered that seasonal variations have influence on the dynamics of the disease.

We investigated the benefits of introducing control intervention strategies such as vaccination, treatment, water purification and the multiple control intervention strategy by extending the control-free model accordingly. We computed the basic reproduction numbers for vaccination, treatment, water purification and the multiple control intervention strategy models given respectively, as \mathcal{R}_0^v , \mathcal{R}_0^τ , \mathcal{R}_0^w and \mathcal{R}_0^c . Analyses of our models have shown that vaccination, treatment, water purification and multiple control intervention strategy reduce the number of secondary infections by factors E_v , E_τ , E_w and E_c respectively. Further analysis revealed that the multiple control intervention strategy has the greatest effects on reducing the number of secondary infections, followed by vaccination, water purification and then treatment. We further showed that the disease can be quickly eradicated by any of these control intervention strategies provided that the corresponding basic reproduction number is less than one. However, if the control is not effective enough such that $\mathcal{R}_0^v > 1$, $\mathcal{R}_0^\tau > 1$, $\mathcal{R}_0^w > 1$ or $\mathcal{R}_0^c > 1$, then an outbreak occurs. We discovered that each of the control intervention strategies reduces the outbreak growth rates. Further analysis revealed that the multiple control intervention strategy has the greatest impact on reducing the outbreak growth rate, followed by vaccination, water purification and then treatment.

We focused on analysing the multiple control model since it is the best among the single control and control-free models. Firstly, we investigated the effects of the control parameters d, ε, τ and ϕ in reducing the number of secondary infections in the presence of the multiple control intervention strategy by calculating the sensitivity index of \mathcal{R}_0^c with respect to the parameters. The results of the analysis revealed that each of the control parameters decreases the number of secondary infections in the presence of the multiple control intervention strategy. Furthermore, we discovered that vaccine efficacy is the most important control parameter followed by reduction in pathogen concentration, treatment rate and then vaccination rate. Secondly, we

investigated the best strategy to minimize the spread of waterborne disease using the multiple control with a minimum cost. By analysing an appropriate optimal control cost functional subject to the multiple control model, we obtained an optimal control triple (u_1^*, u_2^*, u_3^*) that reduces the spread of infections with a minimizes cost. The results of our optimal control analysis revealed that it is optimal to treat individuals immediately as they get infected and begin to vaccinate and provide clean water as soon as the outbreak starts and continue with maximal effort until the outbreak ends.

The dynamical behaviour of our models agree with the intuitive expectation of waterborne disease dynamics in real life. Thus, the models can be used to predict future evolution of waterborne disease in communities where the disease is endemic. It can also be used to study how to control waterborne disease with minimum cost using control intervention strategies such as vaccination, treatment and/or water purification.

Even though this study has provides new insights into the dynamics and control intervention strategies for waterborne disease in a homogeneous population setting, we acknowledge that it has some limitations. Firstly, we assumed that the total population is constant. This is not always true in real life especially for an outbreak that last for a long period of time. We also assumed homogeneity in disease transmission, but is not always true since heterogeneity is an essential part of epidemiology and has been shown to have influence on disease transmission [76, 23]. In reality, individuals in any society belong to different socio economic classes and can migrate from one locality to another, thus affecting the spread of the disease. All these aspects will be considered in our future work.

Chapter 3

Analysis of a waterborne disease model with socioeconomic classes

Waterborne diseases continues to pose serious public health problems in the world today. We formulate a 2-patch waterborne disease model such that each patch represents a particular socioeconomic class. Important mathematical features of the model such as the basic reproduction number, outbreak growth rate etc are obtained and analysed accordingly. The effects of considering socioeconomic classes on the transmission dynamics of the disease are determined. The disease free equilibrium and endemic equilibrium are derived and their stabilities investigated. Sensitivity analyses are carried out to determine the importance of model parameters to the disease transmission and prevalence. The analytical results are supported by numerical illustrations. We conclude by extending some of the results of the 2-patch model to the general n -patch model. The contents of this Chapter have been drafted for publication [21].

3.1 Introduction

Waterborne diseases such as cholera has remained a major public health problem in developing countries, where outbreaks continue to occur and are intensely interconnected with poverty, malnutrition and poor sanitation [39, 15, 18]. Approximately 700,000 children die due to dehydration every year from diarrhoea caused by unsafe water and poor sanitation [89]. According

to the World Health Organization [96], the cholera incidence has increased steadily since 2005. In 2011, 58 nations reported 589,854 cholera cases and 7728 deaths [98, 97]. Due to poor surveillance and under-reporting, the above statistics is likely less than the actual cases and deaths globally [65].

The position of an individual or group within a hierarchical social structure depends on occupation, education and income. This position is referred to as socioeconomic status (SES)[81]. Individuals in low socio-economic class (SEC) are characterized by poverty, malnutrition, poor sanitation and low standard of living whereas individuals in high SEC are known for high standard of living, quality education, good job with better income, clean environment and access to clean water. Apart from impoverished countries, low SEC individuals can also be found in places such as refugee camps, areas devastated by war, famine or natural disasters. While everyone is susceptible to waterborne disease, individuals in low SEC are likely to be more vulnerable to the disease [39]. As a result, the transmission dynamics of waterborne disease will vary across the SEC. Each society or community is made up of different socioeconomic classes. One of the methods of studying the dynamics of a disease is by formulating and analysing an appropriate mathematical epidemiological model of the disease. A mathematical epidemiological model for waterborne disease incorporating socioeconomic classes is expected to improve the understanding of the dynamics of the disease. Understanding this dynamics is necessary for defining control intervention strategy for the disease.

A number of mathematical models such as those by [12, 72, 19, 33, 36, 42, 84, 62, 64, 80, 39, 76] have explored the dynamics of waterborne disease. These works have contributed immensely to the understanding of the dynamics and control intervention strategy for waterborne diseases. To the best of our knowledge, the effects of socioeconomic classes on waterborne disease has not yet been explored. The aim of this study is to improve the understanding of the dynamics of waterborne disease by formulating an appropriate mathematical epidemiological model that incorporates socioeconomic classes.

This chapter is comprised of 5 sections. We start by presenting the general n -socioeconomic class model in Section 3.2. Next, we consider a special case of the model when $n = 2$ in Section 3.3. In Section 3.4, some of the results of the 2-socioeconomic class model are extended to the

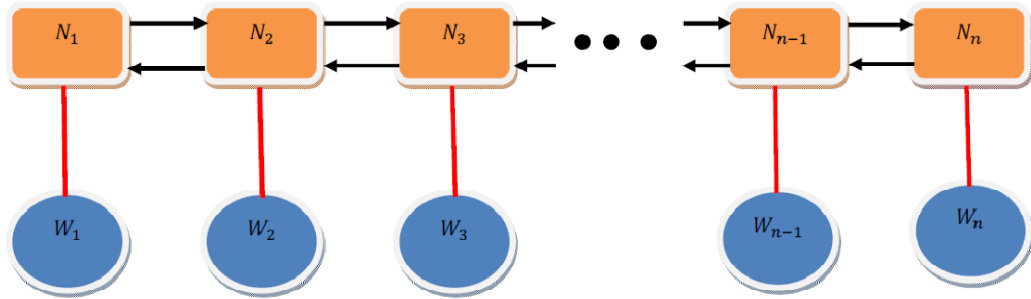


Figure 3.1: Schematic representation of n -socioeconomic classes in a population. Each of the yellow boxes represents human population in a SEC and each blue circle below it represents the water source for the corresponding class. The horizontal arrows indicate migration of individuals across socioeconomic classes as their socioeconomic status changes.

general n -socioeconomic class model. Finally, the discussion of the results are given in Section 3.5.

3.2 Model formulation

Let N be the total human population of a community at risk for waterborne disease infections. We partition N into n socioeconomic classes (SECs) or homogeneous subpopulations of size N_j . Each SEC is made up of susceptible S_j , infected I_j and recovered individuals R_j together with a compartment W_j that measures pathogen concentration in water reservoir. According to [84], waterborne disease can be transmitted through direct (person-to-person) transmission and indirect (water-to-person) transmission. Both direct and indirect transmissions have been shown to contribute to the spread of waterborne disease, but the relative importance of each type of transmission varies among outbreaks [62, 29]. Here we assume no person-to-person transmission and only consider transmission through contact with contaminated water, as it is often considered to be the main driver of waterborne disease outbreaks [64, 80]. As a result, secondary infections are generated when an infected individual sheds pathogens into the water source, which susceptible individuals subsequently come in contact with. Susceptible individ-

Table 3.1: Variables and parameters of the model (3.2) and their meanings

$N(t)$	total human population
$S_j(t)$	susceptible individuals in the j th SEC
$I_j(t)$	infected individuals in the j th SEC
$R_j(t)$	recovered individuals in the j th SEC
$W_j(t)$	measure of pathogen concentration in water reservoir of the j th SEC
b_j	contact rate between $S_j(t)$ and $W_j(t)$
β_j	scaled contact rate between $S_j(t)$ and $W_j(t)$
δ_{jk}	rate at which individuals migrate from $S_j(t)$ to $S_k(t)$
γ_j	recovery rate of $I_j(t)$
α_j	growth rate of pathogens in water source j
ν_j	shedding rate of pathogens by $I_j(t)$
ξ_j	decay rate of pathogens in water source j
μ	natural death rate

uals S_j become infected through contact with the contaminated water source W_j at rate b_j . Infected individuals I_j can contaminate the water source by shedding pathogens into it at rate ν_i and recover naturally at rate γ_j . Pathogens in the contaminated water source grow at rate α_j and decay at rate ξ_j . Natural death occurs in all the SECs at rate μ . The lower SECs have fewer resources to treat water, or to prevent shedding (such as rainwater washing feces into drinking water) than the higher SECs, who have in addition more access to clean water sources along with the ability to treat the water before drinking. Furthermore, recovery rates of the higher SECs would likely be greater than that of the lower SECs due to their ability to reach medical treatment in a timely manner. We assume that SEC 1 is the lowest class followed by SEC 2 in this order until SEC n , for $n > 2$. Based on these, we obtain the inequalities: $\beta_1 > \beta_2 > \dots > \beta_n$, $\nu_1 > \nu_2 > \dots > \nu_n$ and $\gamma_1 < \gamma_2 < \dots < \gamma_n$. Note that individuals can migrate from lower to higher SEC as they acquire more education or get a better paying job. On the other hand, some individuals may lose their jobs leaving them with lower income. In this case such individuals will come down to a lower SEC. As a result of these, we assume

that $S_j(t)$ migrate to $S_k(t)$ at the rate δ_{jk} . In particular, we assume that $S_j(t)$ can migrate to the next lower SEC $S_{j-1}(t)$ or to the next higher SEC $S_{j+1}(t)$. We are excluding jump in the system to ensure a smooth migration. However, the policy makers and society may encourage more individuals to migrate from lower to higher SEC through provision of bursary for education, job creation and some welfare packages. We do not consider change in SEC of $I_j(t)$ and $R_j(t)$. This is because $I_j(t)$ will concentrate on getting well first before thinking of education, job or income while migration of $R_j(t)$ will not affect the spread of infection. Putting these formulations and assumptions together, we obtain the model

$$\begin{aligned}
\dot{S}_1(t) &= \mu N_1(t) - \beta_1 S_1(t) W_1(t) - \mu S_1(t) - \delta_{12} S_1(t) + \delta_{21} S_2(t), \\
\dot{I}_1(t) &= \beta_1 S_1(t) W_1(t) - (\mu + \gamma_1) I_1(t), \\
\dot{W}_1(t) &= \nu_1 I_1(t) - \sigma_1 W_1(t), \\
\dot{R}_1(t) &= \gamma_1 I_1(t) - \mu R_1(t), \\
\dot{S}_2(t) &= \mu N_2(t) - \beta_2 S_2(t) W_2(t) - \mu S_2(t) - \sum_{j=1}^3 \delta_{2j} S_2(t) + \sum_{j=1}^3 \delta_{j2} S_j(t), \\
\dot{I}_2(t) &= \beta_2 S_2(t) W_2(t) - (\mu + \gamma_2) I_2(t), \\
\dot{W}_2(t) &= \nu_2 I_2(t) - \sigma_2 W_2(t), \\
\dot{R}_2(t) &= \gamma_2 I_2(t) - \mu R_2(t), \\
&\vdots = \vdots \\
\dot{S}_n(t) &= \mu N_n(t) - \beta_n S_n(t) W_n(t) - \mu S_n(t) - \sum_{j=n-1}^n \delta_{nj} S_n(t) + \sum_{j=n-1}^n \delta_{jn} S_j(t), \\
\dot{I}_n(t) &= \beta_n S_n(t) W_n(t) - (\mu + \gamma_n) I_n(t), \\
\dot{W}_n(t) &= \nu_n I_n(t) - \sigma_n W_n(t), \\
\dot{R}_n(t) &= \gamma_n I_n(t) - \mu R_n(t).
\end{aligned} \tag{3.1}$$

where $\sigma_j = \xi_j - \alpha_j > 0$, $j = 1, 2, \dots, n$ and $\delta_{jj} = \delta_{kk} = 0 \forall j, k$. By rescaling model (3.1) as follows: $i_j = I_j/N_j$, $s_j = S_j/N_j$, $r_j = R_j/N_j$, $w_j = \sigma_j W_j/(\nu_j N_j)$ and $\beta_j = b_j \nu_j N_j / \sigma_j$, we

obtain a non-dimensionless version of it given by

$$\begin{aligned}
\dot{s}_1(t) &= \mu - \beta_1 s_1 w_1 - \mu s_1 - \delta_{12} s_1 + \delta_{21} s_2, \\
\dot{i}_1(t) &= \beta_1 s_1 w_1 - (\mu + \gamma_1) i_1, \\
\dot{w}_1(t) &= \sigma_1 (i_1 - w_1), \\
\dot{r}_1(t) &= \gamma_1 i_1 - \mu r_1, \\
\dot{s}_2(t) &= \mu - \beta_2 s_2 w_2 - \mu s_2 - \sum_{j=1}^3 \delta_{2j} s_2 + \sum_{j=1}^3 \delta_{j2} s_j, \\
\dot{i}_2(t) &= \beta_2 s_2 w_2 - (\mu + \gamma_2) i_2, \\
\dot{w}_2(t) &= \sigma_2 (i_2 - w_2), \\
\dot{r}_2(t) &= \gamma_2 i_2 - \mu r_2, \\
&\vdots = \vdots \\
\dot{s}_n(t) &= \mu - \beta_n s_n w_n - \mu s_n - \sum_{j=n-1}^n \delta_{nj} s_n + \sum_{j=n-1}^n \delta_{jn} s_j, \\
\dot{i}_n(t) &= \beta_n s_n w_n - (\mu + \gamma_n) i_n, \\
\dot{w}_n(t) &= \sigma_n (i_n - w_n), \\
\dot{r}_n(t) &= \gamma_n i_n - \mu r_n.
\end{aligned} \tag{3.2}$$

All parameters are assumed positive and can be found in Table (3.1). The initial conditions are assumed as follows:

$$s_j(0) > 0, \quad i_j(0) \geq 0, \quad w_j(0) \geq 0, \quad r_j(0) \geq 0. \tag{3.3}$$

Based on the inequalities $\beta_1 > \beta_2 > \dots > \beta_n$, $\nu_1 > \nu_2 > \dots > \nu_n$ and $\gamma_1 < \gamma_2 < \dots < \gamma_n$, we assume that moving from j th SEC to a higher $(j+1)$ th SEC decreases contact rate β_j and shedding rate ν_j by a factor $p < 1$ and $q < 1$ respectively, and increases the recovery rate γ_j by a factor $c > 1$. Thus, we can rewrite β_j , ν_j and γ_j as follows:

$$\beta_j = p^{j-1} \beta_1, \quad \nu_j = q^{j-1} \nu_1, \quad \gamma_j = c^{j-1} \gamma_1, \tag{3.4}$$

where $0 < p, q < 1$ and $c > 1$.

Let $\bar{s} = (s_1(t), s_2(t), \dots, s_n(t))$, $\bar{i} = (i_1(t), i_2(t), \dots, i_n(t))$, $\bar{w} = (w_1(t), w_2(t), \dots, w_n(t))$ and

$\bar{r} = (r_1(t), r_2(t), \dots, r_n(t))$. The feasible region of model (3.2) is given by

$$\Omega = \Omega_H \times \Omega_P \subset \mathbb{R}_+^{3n} \times \mathbb{R}_+^n, \quad (3.5)$$

where

$$\Omega_P = \{\bar{w} \in \mathbb{R}_+^n \quad : \quad w_j \leq 1\},$$

is the feasible region of the pathogen components and

$$\Omega_H = \{(\bar{s}, \bar{i}, \bar{r}) \in \mathbb{R}_+^{3n} \quad : \quad \sum_{j=1}^n (s_j + i_j + r_j) = n\},$$

is the feasible region of the human components. Therefore, model (3.2) is well-posed mathematically and epidemiologically. Hence, it is sufficient to study the dynamics of (3.2) in Ω .

3.3 SIWR model with two socioeconomic classes

In this section, we consider the case where there are only two SECs in the community. The analysis of this special case gives insight into the dynamics of the general n -SECs model (3.2) which is our aim in this paper. Setting $n = 2$ in (3.2) gives

$$\begin{aligned} \dot{s}_1 &= \mu - \beta_1 s_1 w_1 - \mu s_1 - \delta_{12} s_1 + \delta_{21} s_2, \\ \dot{i}_1 &= \beta_1 s_1 w_1 - (\mu + \gamma_1) i_1, \\ \dot{w}_1 &= \sigma_1 (i_1 - w_1), \\ \dot{r}_1 &= \gamma_1 i_1 - \mu r_1, \\ \dot{s}_2 &= \mu - p\beta_1 s_2 w_2 - \mu s_2 - \delta_{21} s_2 + \delta_{12} s_1, \\ \dot{i}_2 &= p\beta_1 s_2 w_2 - (\mu + c\gamma_1) i_2, \\ \dot{w}_2 &= \sigma_2 (i_2 - w_2), \\ \dot{r}_2 &= c\gamma_1 i_2 - \mu r_2. \end{aligned} \quad (3.6)$$

The subscript 1 is used to emphasis SEC 1 while the subscript 2 is used to emphasis SEC 2.

3.3.1 The basic reproduction number

Model (3.6) has a unique disease free equilibrium (DFE) given by

$$(s_1^0, i_1^0, w_1^0, w_2^0, i_2^0, w_2^0) = (2\delta_{21}/(\delta_{12} + \delta_{21}), 0, 0, 2\delta_{12}/(\delta_{12} + \delta_{21}), 0, 0). \quad (3.7)$$

The s_1^0 and s_2^0 can also be rewritten as $s_1^0 = \delta_{21}/(1 + \delta_{12}/\delta_{21})$ and $s_2^0 = \delta_{12}/(1 + \delta_{21}/\delta_{12})$. Obviously, the DFE depends on the migration rates across the SECs in such a way that $s_1^0 = s_2^0 \iff \delta_{21} = \delta_{12}$, $s_1^0 > s_2^0 \iff \delta_{21} > \delta_{12}$ and $s_1^0 < s_2^0 \iff \delta_{21} < \delta_{12}$. If $\delta_{12} = \delta_{21}$, then the DFE becomes

$$(s_1^0, i_1^0, w_1^0, s_2^0, i_2^0, w_2^0) = (1, 0, 0, 1, 0, 0). \quad (3.8)$$

The basic reproduction number measures the expected number of secondary infections that result from introducing a single infected individual into a completely susceptible population. We compute the basic reproduction number of model (3.6) using the next generation matrix approach of van den Driessche and Watmough [90]. The next generation matrices of model (3.6) are

$$\mathcal{F} = \begin{pmatrix} 0 & 0 & \beta_1 s_1^0 & 0 \\ 0 & 0 & 0 & 0 \\ 0 & 0 & 0 & p\beta_1 s_2^0 \\ 0 & 0 & 0 & 0 \end{pmatrix}, \quad \mathcal{V} = \begin{pmatrix} \mu + \gamma_1 & 0 & 0 & 0 \\ -\sigma_1 & \sigma_1 & 0 & 0 \\ 0 & 0 & \mu + c\gamma_1 & 0 \\ 0 & 0 & -\sigma_2 & \sigma_2 \end{pmatrix}.$$

Then

$$\mathcal{F}\mathcal{V}^{-1} = \begin{pmatrix} \mathcal{R}_1 & \beta_1 s_1^0/\sigma_1 & 0 & 0 \\ 0 & 0 & 0 & 0 \\ 0 & 0 & \mathcal{R}_2 & p\beta_1 s_2^0/\sigma_2 \\ 0 & 0 & 0 & 0 \end{pmatrix}, \quad (3.9)$$

where

$$\mathcal{R}_1 = 2\beta_1\delta_{21}/((\mu + \gamma_1)(\delta_{21} + \delta_{12})), \quad \mathcal{R}_2 = 2p\beta_1\delta_{12}/((\mu + c\gamma_1)(\delta_{21} + \delta_{12})). \quad (3.10)$$

The matrix $\mathcal{F}\mathcal{V}^{-1}$ has two positive eigenvalues given by

$$\lambda = \mathcal{R}_1, \quad \lambda = \mathcal{R}_2. \quad (3.11)$$

Thus, the basic reproduction number \mathcal{R}^* of the entire population in the presence of the two SECs is the largest of these two eigenvalues which can be written as

$$\mathcal{R}^* = \max \{ \mathcal{R}_1, \mathcal{R}_2 \}. \quad (3.12)$$

These threshold quantities \mathcal{R}_1 and \mathcal{R}_2 are the basic reproduction number/type reproduction number for SEC 1 and SEC 2 respectively [75, 37]. Since $\mathcal{R}^* = \max\{\mathcal{R}_1, \mathcal{R}_2\}$, it implies that one of the SECs is driving the outbreak. Therefore, we need to identify the SEC that is driving the outbreak so that control interventions can be properly implemented to reduce the chances of outbreak.

3.3.2 The dominant SEC

To determine the SEC that is driving the outbreak (i.e., the dominant SEC), it is necessary to investigate the relationship between \mathcal{R}_1 and \mathcal{R}_2 . We investigate the relationship between \mathcal{R}_1 and \mathcal{R}_2 for the following cases: (i) $\delta_{21} = \delta_{12}$ (ii) $\delta_{21} > \delta_{12}$ (iii) $\delta_{21} < \delta_{12}$.

We begin with the case (i) $\delta_{21} = \delta_{12}$, a situation where individuals migrate across the two SECs at equal rate. For this case, \mathcal{R}_1 and \mathcal{R}_2 become

$$\mathcal{R}_1 = \beta_1 / (\mu + \gamma_1), \quad \mathcal{R}_2 = p\beta_1 / (\mu + c\gamma_1). \quad (3.13)$$

From equation (3.13), we have that

$$\mathcal{R}_2 < \mathcal{R}_1, \quad (3.14)$$

since $0 < p < 1$ and $c > 1$. This implies that $\mathcal{R}^* = \mathcal{R}_1$ under the assumption of uniform migration rates, suggesting that the outbreak is been driven by the lower SEC 1. Therefore, for this case, the SEC 1 should be the target of control intervention strategies in order to effectively reduce the spread of the disease.

Case (ii), $\delta_{12} < \delta_{21}$, a situation where more individuals are migrating from high to low SEC.

For this second case, \mathcal{R}_1 and \mathcal{R}_2 become

$$\mathcal{R}_1 = \frac{2\beta_1\delta_{21}}{(\mu + \gamma_1)(\delta_{12} + \delta_{21})}, \quad \mathcal{R}_2 = \frac{2p\beta_1\delta_{12}}{(\mu + c\gamma_1)(\delta_{12} + \delta_{21})}. \quad (3.15)$$

We can show that

$$\mathcal{R}_2 < \mathcal{R}_1.$$

This implies that the same results that hold under the assumption of uniform migration rates also hold for this case when more individuals are migrating from high to low SEC.

Case (iii), $\delta_{12} > \delta_{21}$, a situation where more individuals are migrating from low to high SEC. Unlike in the previous cases, the analysis of this case will be carried out under the assumption for the two extreme ends: when there is a very small difference between the two SECs (i.e., $(p, c) \rightarrow 1$) and when there is a very big difference between the two SECs (i.e., $p \rightarrow 0, c \rightarrow \infty$). This is because the basic reproduction numbers are parameter dependent, making it difficult to compute. From the analysis, we obtain

$$\mathcal{R}_1 < \mathcal{R}_2 \quad \text{as } (p, c) \rightarrow 1, \quad (3.16)$$

$$\mathcal{R}_2 < \mathcal{R}_1 \quad \text{as } p \rightarrow 0, c \rightarrow \infty. \quad (3.17)$$

From these results, we observe that when there is a very small difference between the two SECs, there will be more secondary infections in SEC 2. On the other hand, when there is a very big difference between the two SECs, there will be more secondary infections in SEC 1.

3.3.3 Homogeneous version of model (3.6)

In order to determine the effects of SECs, we compare the dynamics of the SECs model (3.6) with the homogeneous version of the model. The homogeneous version of the model (3.6) is obtained by considering the entire population as a homogeneous mixing population without recognizing different SECs. When we consider homogeneity, model (3.6) reduces to

$$\begin{aligned} \dot{s} &= \mu - \beta sw - \mu s, \\ \dot{i} &= \beta sw - (\mu + \gamma)i, \\ \dot{w} &= \sigma(i - w), \\ \dot{r} &= \gamma i - \mu r, \end{aligned} \quad (3.18)$$

where

$$\beta = \sum_{j=1}^2 \beta_1 p^{j-1} N_j / N, \quad \gamma = \sum_{j=1}^2 \gamma_1 c^{j-1} N_j / N, \quad \sigma = \sum_{j=1}^2 \sigma_j N_j / N.$$

The DFE and the basic reproduction number of the homogeneous model (3.18) are given by

$$(s^0, i^0, w^0) = (1, 0, 0), \quad (3.19)$$

and

$$\mathcal{R}_0 = \beta / (\mu + \gamma), \quad (3.20)$$

respectively.

3.3.4 Relationship between \mathcal{R}_1 , \mathcal{R}_2 and \mathcal{R}_0

Here, we investigate the relationship between \mathcal{R}_1 , \mathcal{R}_2 and \mathcal{R}_0 in order to determine the effects of considering SECs in the transmission dynamics of waterborne disease. Using a similar reasoning as in the previous section, we investigate the relationship between \mathcal{R}_1 , \mathcal{R}_2 and \mathcal{R}_0 for the following cases: (i) $\delta_{21} = \delta_{12}$ (ii) $\delta_{21} > \delta_{12}$ (iii) $\delta_{21} < \delta_{12}$.

For the first case $\delta_{21} = \delta_{12}$, we need to compare \mathcal{R}_0 with \mathcal{R}_1 and \mathcal{R}_2 . Comparing \mathcal{R}_0 and \mathcal{R}_2 , we obtain

$$\mathcal{R}_0 - \mathcal{R}_2 = \frac{\beta_1 N_1}{(\mu N + \gamma_1 N_1 + c \gamma_1 N_2)(\mu + c \gamma_1)} [(\mu + c \gamma_1) - p(\mu + \gamma_1)] > 0,$$

so,

$$\mathcal{R}_2 < \mathcal{R}_0. \quad (3.21)$$

Next, comparing \mathcal{R}_0 and \mathcal{R}_1 gives

$$\mathcal{R}_0 - \mathcal{R}_1 = \frac{\beta_1 N_2}{(N\mu + \gamma_1 N_1 + c \gamma_1 N_2)(\mu + \gamma_1)} [p(\mu + \gamma_1) - (\mu + c \gamma_1)] < 0.$$

This implies that

$$\mathcal{R}_0 < \mathcal{R}_1. \quad (3.22)$$

Thus, from equations (3.21) and (3.22), we have that

$$\mathcal{R}_2 < \mathcal{R}_0 < \mathcal{R}_1. \quad (3.23)$$

The inequality (3.23) shows that if individuals migrate across the SECs at equal rate, then secondary infections will be dominated in the lower SEC followed by the homogeneous mixing population case and finally the higher SEC.

For the remaining two cases i.e., $\delta_{12} < \delta_{21}$ and $\delta_{12} > \delta_{21}$, we compare \mathcal{R}_0 and \mathcal{R}_1 to obtain

$$\mathcal{R}_0 - \mathcal{R}_1 = \beta_1 \left[\frac{N_1 + pN_2}{N\mu + \gamma_1 N_1 + c\gamma_1 N_2} - \frac{2\delta_{21}}{(\mu + \gamma_1)(\delta_{12} + \delta_{21})} \right]. \quad (3.24)$$

Taking limits of (3.24) gives

$$\begin{aligned} \lim_{p,c \rightarrow 1} (\mathcal{R}_0 - \mathcal{R}_1) &< 0, \quad \text{if, } \delta_{12} < \delta_{21}, \\ \lim_{p,c \rightarrow 1} (\mathcal{R}_0 - \mathcal{R}_1) &> 0, \quad \text{if, } \delta_{12} > \delta_{21}. \end{aligned}$$

Similarly, by comparing \mathcal{R}_0 and \mathcal{R}_2 we have

$$\begin{aligned} \lim_{p,c \rightarrow 1} (\mathcal{R}_0 - \mathcal{R}_2) &< 0, \quad \text{if, } \delta_{12} < \delta_{21}, \\ \lim_{p,c \rightarrow 1} (\mathcal{R}_0 - \mathcal{R}_2) &> 0, \quad \text{if, } \delta_{12} > \delta_{21}. \end{aligned}$$

These results suggest that migration rates (δ_{12}, δ_{21}) have some influence on the dynamics of waterborne disease.

3.3.5 Stability analysis

The stability at the DFE determines the short-term dynamics of a disease, whereas its long-term dynamics are characterized by the stability at the endemic equilibrium [52]. In this section, we investigate the stability at the DFE and the endemic equilibrium (EE) of model (3.6) in order to determine both the short-term and long-term dynamics of waterborne disease in the presence of different SECs.

Stability of the disease free equilibrium

Theorem 3.3.1. *The DFE (3.7) of model (3.6) is both locally and globally asymptotically stable provided $\mathcal{R}^* < 1$.*

The proof of the theorem for the general case is given in Appendix ???. Theorem 3.3.1 implies that waterborne disease will be eradicated from the entire population in the presence of different SECs provided $\mathcal{R}^* < 1$.

Theorem 3.3.2. *The DFE (3.19) of the homogeneous model (3.18) is both locally and globally asymptotically stable provided $\mathcal{R}_0 < 1$.*

The proof of Theorem 3.3.2 can be established using a similar approach given in Appendix ???.

Stability of the Endemic equilibrium

When $\mathcal{R}^* > 1$, a unique endemic equilibrium (EE) given by

$$(s_1^*, s_1^*, w_1^*, s_2^*, i_2^*, w_2^*) = (1/\mathcal{R}_1, \mu(1 - s_1^*)/(\mu + \gamma_1), i_1^*, 1/\mathcal{R}_2, \mu(1 - s_2^*)/(\mu + c\gamma_1), i_2^*), (3.25)$$

exists for model (3.6). Note that at the EE (3.25), $\delta_{12}s_1 = \delta_{21}s_2$. Therefore, we investigate the global stability of the EE when $\delta_{12}s_1 = \delta_{21}s_2$.

Theorem 3.3.3. *The unique EE (3.25) is globally asymptotically stable if $\delta_{12}s_1 = \delta_{21}s_2$.*

The proof of Theorem 3.3.3 for the general case is given in Appendix 3.6.1. This implies that the disease can persist when different SECs are considered provided $\delta_{12}s_1 = \delta_{21}s_2$. Biologically, $\delta_{12}s_1 = \delta_{21}s_2$ means that equal number of individuals migrate in and out of the two SECs. Thus, migration of individuals across the SECs is at equilibrium and we have shown that both DFE and EE occur when this happen. However, when $\delta_{12}s_1 \neq \delta_{21}s_2$, it means more individuals will be migrating into either of the two SECs. Furthermore, we will see later that migration have significant influence on the dynamics of waterborne disease. Therefore, it will be interesting to know the extent migration will affect the long-term dynamics of the system by investigating the stability at the EE when $\delta_{12}s_1 \neq \delta_{21}s_2$. This will be part of our future work.

Similarly, when $\mathcal{R}_0 > 1$, a unique EE exists in the homogeneous model (3.18) and is given by

$$(s^*, i^*, w^*) = (1/\mathcal{R}_0, \mu(1 - s^*)/(\gamma + \mu), i^*). (3.26)$$

Theorem 3.3.4. *The unique EE (3.26) is globally asymptotically stable.*

We do not present the proof of Theorem 3.3.4 since the global stability of a similar model with multiple transmission pathways has been done in [84] by constructing an appropriate Lyapunov function. Alternatively, the proof of Theorem 3.3.4 can be established using a method based on monotone dynamical systems, as developed in [51, 83].

3.3.6 Outbreak growth rate

If $\mathcal{R}^* > 1$, the DFE (3.7) becomes unstable and a waterborne disease outbreak occurs. Determining the rate at which this outbreak grows is necessary for understanding the dynamics of the disease as well as informing the public health for proper management of the outbreak. The positive (dominant) eigenvalue of the Jacobian at the DFE is typically referred to as the outbreak growth rate [84]. The Jacobian matrix of (3.6) evaluated at the DFE is given by

$$J^0 = \begin{pmatrix} -\delta_{12} & \mu & -\beta_1 s_1^0 & \delta_{21} & 0 & 0 \\ 0 & -(\mu + \gamma_1) & \beta_1 s_1^0 & 0 & 0 & 0 \\ 0 & \sigma_1 & -\sigma_1 & 0 & 0 & 0 \\ \delta_{12} & 0 & 0 & -\delta_{21} & \mu & -p\beta_1 s_2^0 \\ 0 & 0 & 0 & 0 & -(\mu + c\gamma_1) & p\beta_1 s_2^0 \\ 0 & 0 & 0 & 0 & \sigma_2 & -\sigma_2 \end{pmatrix}. \quad (3.27)$$

The Jacobian matrix (3.27) has five distinct eigenvalues given by

$$\lambda^{(i)} = -(\delta_{12} + \delta_{21}), \quad (3.28)$$

$$\lambda_1^- = \frac{1}{2} \left[-(\mu + \gamma_1 + \sigma_1) - \sqrt{(\mu + \gamma_1 + \sigma_1)^2 - 4\sigma_1(\mu + \gamma_1)(1 - \mathcal{R}_1)} \right], \quad (3.29)$$

$$\lambda_1^+ = \frac{1}{2} \left[-(\mu + \gamma_1 + \sigma_1) + \sqrt{(\mu + \gamma_1 + \sigma_1)^2 - 4\sigma_1(\mu + \gamma_1)(1 - \mathcal{R}_1)} \right], \quad (3.30)$$

$$\lambda_2^- = \frac{1}{2} \left[-(\mu + c\gamma_1 + \sigma_2) - \sqrt{(\mu + c\gamma_1 + \sigma_2)^2 - 4\sigma_2(\mu + c\gamma_1)(1 - \mathcal{R}_2)} \right], \quad (3.31)$$

$$\lambda_2^+ = \frac{1}{2} \left[-(\mu + c\gamma_1 + \sigma_2) + \sqrt{(\mu + c\gamma_1 + \sigma_2)^2 - 4\sigma_2(\mu + c\gamma_1)(1 - \mathcal{R}_2)} \right]. \quad (3.32)$$

We can easily observe that $\lambda^{(i)}, \lambda_1^-, \lambda_2^-$ are negative, while λ_1^+ and λ_2^+ are positive whenever $\mathcal{R}^* > 1$. Thus, the outbreak growth rate of the entire population when the two SECs are considered is given by

$$\lambda^* = \max \{ \lambda_1^+, \lambda_2^+ \}. \quad (3.33)$$

The quantities λ_1^+ and λ_2^+ represent the outbreak growth rate of SEC 1 and SEC 2 respectively. We observe from the above equations that if $\mathcal{R}_1 = 1$ and $\mathcal{R}_2 = 1$, then the outbreak growth rate vanishes. On the other hand, if $\mathcal{R}_1 < 1$ and $\mathcal{R}_2 < 1$, then all the eigenvalues have negative real part. This implies that the model is locally asymptotically stable if $\mathcal{R}_1 < 1$ and $\mathcal{R}_2 < 1$. Thus waterborne disease can be eliminated from the entire population if the initial size of the infected population is in the basin of attraction of the DFE. This confirms that to have any chances of outbreak, the basic reproduction number must be greater than unity. The value of $\lambda^* > 0$ represents the steepness of the ascending infection curve (with respect to time). Hence, a higher λ^* implies a more severe disease outbreak. Equation (3.33) suggests that one of the SECs is still driving the outbreak at this endemic stage (i.e., when the basic reproduction numbers are greater than unity). Analyses of basic reproduction numbers \mathcal{R}_1 , \mathcal{R}_2 and \mathcal{R}_0 have shed light on the dynamics of waterborne disease in the presence of SECs. Therefore, at the endemic stage of the outbreak, there is a need to determine the SEC where the outbreak will be more severe as well as investigate the effects of considering SECs.

Using a similar argument as in the case of the basic reproduction numbers, we determine the SEC that is driving the outbreak at this endemic stage for the following cases: (i) $\delta_{21} = \delta_{12}$ (ii) $\delta_{21} > \delta_{12}$ (iii) $\delta_{21} < \delta_{12}$.

Next, we obtain the relationship between λ_1^+ and λ_2^+ . Since pathogen in water can decay naturally, we assume that $\sigma_j = \sigma$. Let $M = \mu + \gamma_1 + \sigma$. We rewrite equations (3.30) and (3.32) as

$$(2\lambda_1^+ + M)^2 = M^2 - 4\sigma(\mu + \gamma_1)(1 - \mathcal{R}_1), \quad (3.34)$$

$$(2\lambda_2^+ + M)^2 = M^2 - 4\gamma_1\lambda_2^+(c - 1) - 4\sigma(\mu + c\gamma_1)(1 - \mathcal{R}_2), \quad (3.35)$$

respectively. Subtracting equation (3.35) from (3.34) and simplifying gives

$$(2\lambda_1^+ + M)^2 - (2\lambda_2^+ + M)^2 = 4\gamma_1(c - 1)(\lambda_2^+ + \sigma) + 8\sigma\beta_1(\delta_{21} - p\delta_{12})/(\delta_{21} + \delta_{12}). \quad (3.36)$$

When $\delta_{12} = \delta_{21}$, we have

$$\lambda_2^+ < \lambda_1^+.$$

This shows that under the assumption of equal migration rates between the SECs, the outbreak will grow faster (i.e., a more severe disease outbreak) in the SEC 1. For the remaining cases when $\delta_{12} \neq \delta_{21}$, taking limits of (3.36) gives

$$\begin{aligned}\lambda_1^+ &< \lambda_2^+ \text{ as } (p, c) \longrightarrow 1, \text{ if } \delta_{12} > \delta_{21}, \\ \lambda_1^+ &> \lambda_2^+ \text{ as } (p, c) \longrightarrow 1, \text{ if } \delta_{12} < \delta_{21}.\end{aligned}$$

These results show that it is possible to have a greater outbreak growth rate in SEC 2 when more individuals migrates from SEC 2 to SEC 1, otherwise outbreak will be dominated in the SEC 1.

We determine the effects of SECs at the endemic stage of the outbreak by comparing λ_1^+ and λ_2^+ with the outbreak growth rate of the homogeneous model (5.16). The outbreak growth rate of the homogeneous model (3.18) is given by

$$\lambda^+ = \frac{1}{2} \left[-(\mu + \gamma + \sigma) + \sqrt{(\mu + \gamma + \sigma)^2 - 4\sigma(\mu + \gamma)(1 - \mathcal{R}_0)} \right]. \quad (3.37)$$

Comparing λ_1^+ and λ^+ , we have that

$$(2\lambda_1^+ + M)^2 - (2\lambda^+ + M)^2 = 4(\gamma - \gamma_1)(\lambda^+ + \sigma) + 4\sigma(2\delta_{21}\beta_1 - (\delta_{21} + \delta_{12})\beta)/(\delta_{21} + \delta_{12}).$$

Thus, we obtain

$$\lambda^+ < \lambda_1^+, \quad \text{if } \delta_{12} \leq \delta_{21}.$$

By a similar reasoning, comparing λ_2^+ and λ^+ gives

$$(2\lambda_2^+ + M)^2 - (2\lambda^+ + M)^2 = 4(c\gamma_1 - \gamma)(\lambda^+ + \sigma) + 4\sigma(2p\delta_{21}\beta_1 - (\delta_{21} + \delta_{12})\beta)/(\delta_{21} + \delta_{12}).$$

Hence, we obtain

$$\lambda_2^+ < \lambda^+, \quad \text{if } \delta_{21} \leq \delta_{12}.$$

These show that considering SECs also has impact on the dynamics of waterborne disease at the endemic stage of the outbreaks.

Table 3.2: Parameter values for numerical simulations with reference

Parameter	Symbol	Value	Reference
Total contact rate	$\beta_1 + \beta_2$	0.30 day ⁻¹	[76]
Birth/death rate	μ	0.02 day ⁻¹	[76]
Recovery rate in SEC 1	γ_1	0.0793 day ⁻¹	[84]
Net decay rate of pathogen in water	σ_j	0.0333 day ⁻¹	[84]
Rate of migration from SEC 1 to SEC 2	δ_{12}	0.022	[30]
Rate of migration from SEC 2 to SEC 1	δ_{21}	0.015	[30]

3.3.7 Model simulations

Analytical results for the SEC model (3.6) gives an insight into the dynamics of waterborne disease in the presence of SECs. In particular, we determine the relationship between the basic reproduction numbers ($\mathcal{R}_0, \mathcal{R}_1, \mathcal{R}_2$) and outbreak growth rates ($\lambda^+, \lambda_1^+, \lambda_2^+$) for the two extreme cases: when there is a very small difference between the SECs (i.e., $p, c \rightarrow 1$) and when there is a very big difference between the SECs (i.e., $p \rightarrow 0, c \rightarrow \infty$). It is not enough to draw conclusions based on these two extreme cases because they are not the only cases in real life. Other cases where p, c are between these two extreme cases are difficult to calculate analytically as the mathematical features involve are parameter dependent.

To quantitatively represent the dynamics of waterborne disease in the presence of SECs, we resort to the use of parameter values that can best represent possible real life scenarios emanating from our analytical results to carry out the numerical simulations. Such results will improve the understanding of the dynamics of the disease, hence, we can draw conclusions from it. Parameter values used are chosen from published data. These parameter values are given in Table 3.2. The constants p and c are estimated such that $\beta_1 \sim \beta_2$ and $\gamma_1 \sim \gamma_2$. Particularity, we take $p = 0.8657$ and $c = 1.050$.

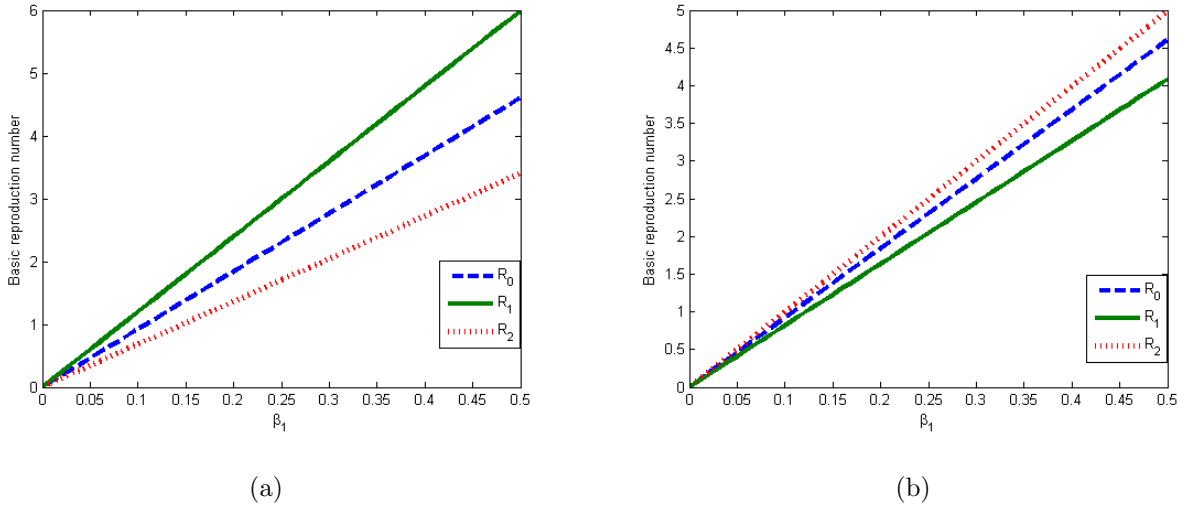


Figure 3.2: Numerical illustrations of the effects of δ_{12} and δ_{21} on the basic reproduction numbers using the parameter values in table 3.2 (a) plot of $\mathcal{R}_0, \mathcal{R}_1, \mathcal{R}_2$ vs β_1 for $\delta_{12} = 0.015$, $\delta_{21} = 0.022$ (b) plot of $\mathcal{R}_0, \mathcal{R}_1, \mathcal{R}_2$ vs β_1 for $\delta_{12} = 0.022$, $\delta_{21} = 0.015$.

Effects of migration of individuals across SECs

Here, we investigate the effects of migration of individuals across SECs on the dynamics of the disease. We can achieve this by either solving the SEC model (3.6) numerically or by comparing the mathematical features of SEC model (3.6) with that of the homogeneous model (3.18). Numerical simulations of the basic reproduction numbers ($\mathcal{R}_1, \mathcal{R}_2, \mathcal{R}_0$) are given in Figures 3.2(a) and 3.2(b). We perform the numerical simulation by fixing every other parameter and varying only δ_{12} or δ_{21} as shown in the Figures. These Figures reveal the effects of considering SECs. From the Figures, we discover that considering SECs can lead to more secondary infections if greater number of individuals migrate from SEC 2 to SEC 1 or less secondary infections if greater number of individuals migrate from SEC 1 to SEC 2. This shows that it is possible for secondary infections to be dominated by either of the SECs as migration rate changes even when the differences in transmission of the disease between the two SECs are neither too small nor too big. We also notice that considering SECs can lead to more or less secondary infections when the differences in transmission of the disease between the two SECs are neither too small nor too big.

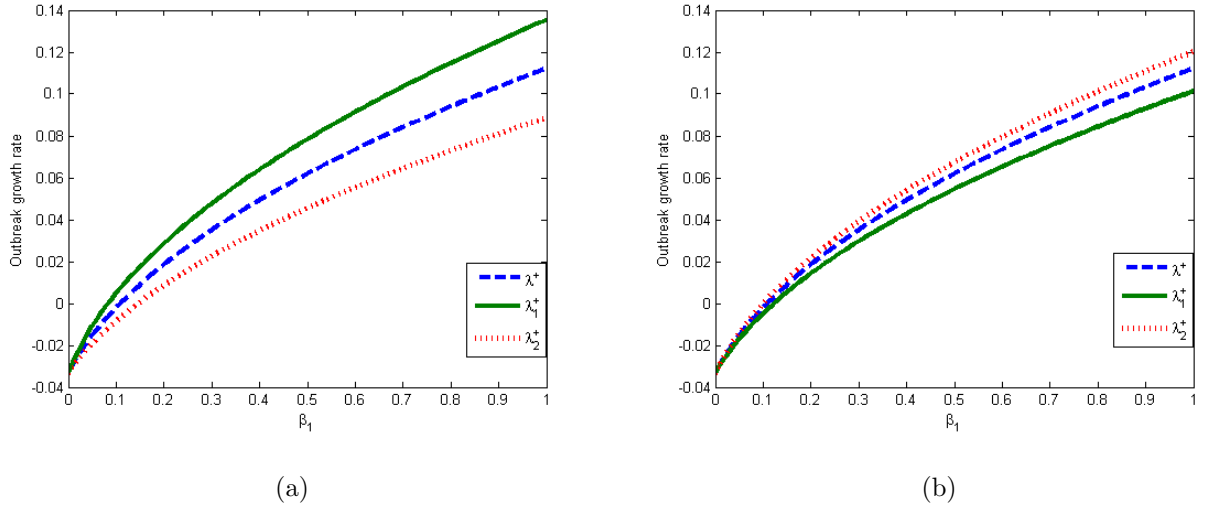
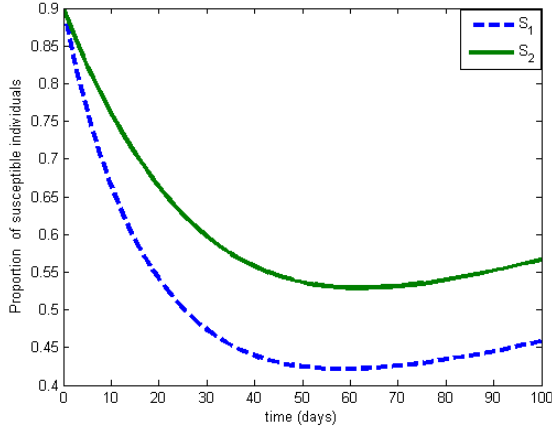


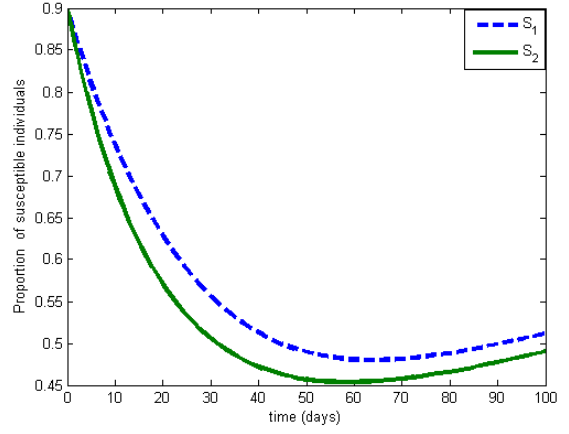
Figure 3.3: Numerical illustrations of the effects of δ_{12} and δ_{21} on the outbreak growth rates (a) plot of $\lambda^+, \lambda_1^+, \lambda_2^+$ vs β_1 for $\delta_{12} = 0.015$, $\delta_{21} = 0.022$ (b) plot of $\lambda^+, \lambda_1^+, \lambda_2^+$ vs β_1 for $\delta_{12} = 0.022$, $\delta_{21} = 0.015$.

Next, we perform numerical illustrations of the outbreak growth rates using the same parameter values used for the basic reproduction numbers. The numerical illustrations of the outbreak growth rates given in Figures 3.3(a) and 3.3(b) reveal the effects of considering SECs at the endemic stage of the outbreak. Similar to our analytical results, we notice that considering SECs can lead to a more severe outbreaks (greater outbreak growth rate) which will be driven by SEC 1 if more individuals migrate from SEC 2 to SEC 1 or a less severe outbreaks which will be driven by SEC 2 if more individuals migrate from SEC 1 to SEC.

To investigate the effects of migration rate on the number of susceptible and infected individuals, we solve the SEC model (3.6) numerically for the same parameter values used above. We notice from the results shown in Figures 3.4 and 3.5 that the dynamics of the SEC model (3.6) also depends on the migration rate across the SECs. Specifically, we observe that the number of infected and susceptible individuals in SEC 1 are greater when more individuals migrate from SEC 2 to SEC 1, while the number of infected and susceptible individuals in SEC 2 are greater when more individuals migrate from SEC 1 to SEC 2.

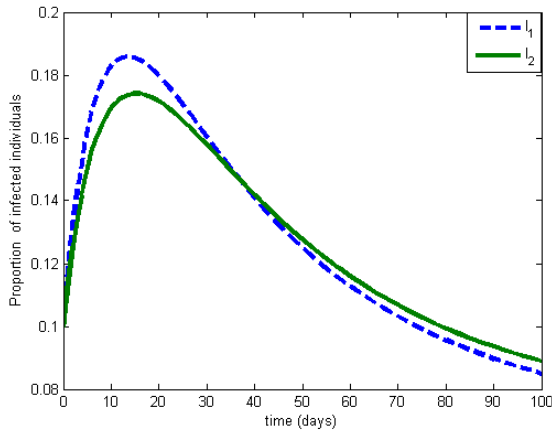


(a)

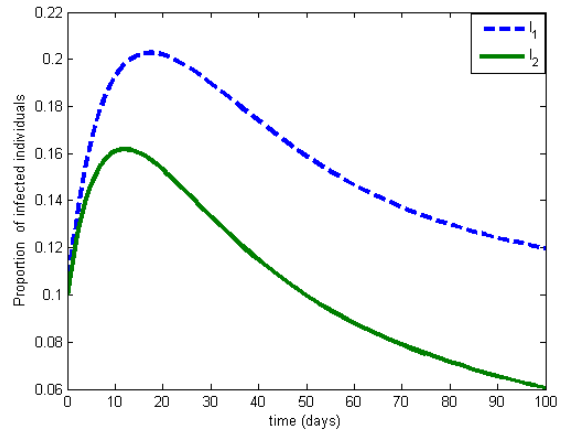


(b)

Figure 3.4: Plot of proportion of susceptible individuals vs. time for (a) $\delta_{12} = 0.022$, $\delta_{21} = 0.015$ (b) $\delta_{12} = 0.015$, $\delta_{21} = 0.022$.



(a)



(b)

Figure 3.5: Plot of proportion of infected individuals vs. time for (a) $\delta_{12} = 0.022$, $\delta_{21} = 0.015$ (b) $\delta_{12} = 0.015$, $\delta_{21} = 0.022$.

3.3.8 Sensitivity analysis

To understand the relative importance of the different parameters (factors) responsible for disease transmission as well as its prevalence, it is necessary to carry out sensitivity analysis of the basic reproduction number and endemic equilibrium. According to [17], the initial disease transmission is directly related to basic reproduction number whereas disease prevalence is directly related to endemic equilibrium point, specifically to the magnitudes of the infected classes. We calculate the sensitivity indices of the basic reproduction numbers (\mathcal{R}_0 , \mathcal{R}_1 , \mathcal{R}_2), and the endemic equilibrium points, (s^*, i^*, w^*) and $(s_1^*, s_2^*, i_1^*, i_2^*, w_1^*, w_2^*)$, with respect to the parameters in the model. These indices reveal to us the importance of each parameter to disease transmission and prevalence. They are the parameters that should be taken into consideration while defining control strategy.

Definition[17]. The normalized forward sensitivity index of a variable, u , that depends differentially on a parameter, ρ , is defined as:

$$\Upsilon_{\rho}^u = \frac{\partial u}{\partial \rho} \times \frac{\rho}{u}. \quad (3.38)$$

When $\Upsilon_{\rho}^u > 0$, we say that ρ increases the value of u as its value increases, while if $\Upsilon_{\rho}^u < 0$ we say that ρ decreases the value of u as its value increases.

Sensitivity indices of the basic reproduction numbers

Since we have an explicit formula for the basic reproduction numbers (\mathcal{R}_0 , \mathcal{R}_1 , \mathcal{R}_2), we can derive an analytical expression for the sensitivity indices of these basic reproduction numbers with respect to each of the parameters of the model. For example, the sensitivity index of \mathcal{R}_1 with respect to β_1 is given by,

$$\Upsilon_{\beta_1}^{\mathcal{R}_1} = \frac{\partial \mathcal{R}_1}{\partial \beta_1} \times \frac{\beta_1}{\mathcal{R}_1} = 1.000, \quad (3.39)$$

and is independent of any parameter. We notice that some of the sensitivity indices are independent of parameters while others are parameter dependent. Those that are parameter dependent are calculated using the parameter values in Table 3.2. The remaining sensitivity indices of the basic reproduction numbers are given in Table 3.3.

For the \mathcal{R}_0 , we observe from Table 3.3, that the most sensitive parameter is β_1 , followed by β_2 , γ_2 , γ_1 and then μ . Hence one of the most important parameters for \mathcal{R}_0 is the contact rate in SEC2 with sensitivity index of 0.5360. Since $\Upsilon_{\beta_1}^{\mathcal{R}_0} = 0.5360$, decreasing (or increasing) the β_1 by 10% also decreases (or increases) \mathcal{R}_0 by 5.36%.

For the SEC 1, we observe that the most sensitive parameters for the sensitivity index of \mathcal{R}_1 is also β_1 with each having a sensitivity index of magnitude 1, followed by γ_1 , δ_{12} and δ_{21} and then μ . We can see that the sensitivity index of \mathcal{R}_1 with respect to δ_{12} has a positive sign while the sensitivity index of \mathcal{R}_1 with respect to δ_{21} has a negative sign. This implies that the rate at which individuals migrate from SEC 1 decreases \mathcal{R}_1 while the rate at which individuals migrate into SEC 1 increases \mathcal{R}_1 .

Similarly, for the SEC 2, the most sensitive parameters for the sensitivity index of \mathcal{R}_2 is β_2 with each having a sensitivity index of magnitude 1. Other important parameters are γ_2 followed by δ_{12} and then δ_{21} and then μ . We also discover that the rate at which individuals migrate from SEC 2 (δ_{21}) decreases \mathcal{R}_2 while the the rate at which individuals migrate into SEC 2 (δ_{12}) increases it. The sign of the sensitivity indices of \mathcal{R}_0 , \mathcal{R}_1 and \mathcal{R}_2 with respect to each of the parameters agrees with intuitive expectation.

We also observe that

$$\Upsilon_{\beta_1}^{\mathcal{R}_0} + \Upsilon_{\beta_2}^{\mathcal{R}_0} = \Upsilon_{\beta_1}^{\mathcal{R}_1} = \Upsilon_{\beta_2}^{\mathcal{R}_2} = 1. \quad (3.40)$$

From the above results, we notice that the most important parameters for the basic reproduction numbers are β_1 and β_2 having sensitivity indices of magnitude 1.000. This implies that decreasing (or increasing) any of these two parameters by 10% increases (or decreases) the corresponding basic reproduction number by 10%.

The magnitude of sensitivity index of \mathcal{R}_1 and \mathcal{R}_2 with respect to the rates of migration (δ_{12} , δ_{21}) across SECs is always less than that of \mathcal{R}_1 and \mathcal{R}_2 with respect to the parameters (β_1 and β_2). From

$$\Upsilon_{\delta_{12}}^{\mathcal{R}_1} = \frac{\delta_{12}}{\mathcal{R}_1} \frac{\partial \mathcal{R}_1}{\partial \delta_{12}} = \frac{-\delta_{12}}{\delta_{21} + \delta_{12}}, \quad \Upsilon_{\delta_{21}}^{\mathcal{R}_2} = \frac{\delta_{21}}{\mathcal{R}_2} \frac{\partial \mathcal{R}_2}{\partial \delta_{21}} = \frac{-\delta_{21}}{\delta_{21} + \delta_{12}} \quad (3.41)$$

$$\Upsilon_{\delta_{21}}^{\mathcal{R}_1} = \frac{\delta_{21}}{\mathcal{R}_1} \frac{\partial \mathcal{R}_1}{\partial \delta_{21}} = \frac{\delta_{12}}{\delta_{21} + \delta_{12}}, \quad \Upsilon_{\delta_{12}}^{\mathcal{R}_2} = \frac{\delta_{12}}{\mathcal{R}_2} \frac{\partial \mathcal{R}_2}{\partial \delta_{12}} = \frac{\delta_{21}}{\delta_{21} + \delta_{12}} \quad (3.42)$$

Table 3.3: Sensitivity index of \mathcal{R}_0 , \mathcal{R}_1 and \mathcal{R}_2

Parameter	\mathcal{R}_0	\mathcal{R}_1	\mathcal{R}_2
β_1	0.5360	1.000	0.000
β_2	0.4640	0.000	1.000
γ_1	-0.3915	-0.7986	0.000
γ_2	-0.4111	0.000	-0.8063
μ	-0.1975	-0.2014	-0.1937
δ_{12}	0.000	-0.5946	0.4054
δ_{21}	0.000	0.5946	-0.4054

it is clear that the magnitudes of $\Upsilon_{\delta_{12}}^{\mathcal{R}_1}$, $\Upsilon_{\delta_{21}}^{\mathcal{R}_1}$, $\Upsilon_{\delta_{12}}^{\mathcal{R}_2}$ and $\Upsilon_{\delta_{21}}^{\mathcal{R}_2}$ are less than 1. Even though migration rates (δ_{21}, δ_{12}) across the SECs have some influence on the spread of infection, this result shows that their influence on \mathcal{R}_1 and \mathcal{R}_2 is less than that of contact rates (β_1, β_2). Therefore, for effective control of the disease in each of the SECs, we should control the contact rates first before controlling the migration rates. From equations (3.41) and (3.42), we observe that

$$\Upsilon_{\delta_{21}}^{\mathcal{R}_1} = -\Upsilon_{\delta_{12}}^{\mathcal{R}_1}, \quad \Upsilon_{\delta_{21}}^{\mathcal{R}_2} = -\Upsilon_{\delta_{12}}^{\mathcal{R}_2}. \quad (3.43)$$

This shows that δ_{21} and δ_{12} have equal but opposite impact on \mathcal{R}_1 and \mathcal{R}_2 . Another important parameter for the basic reproduction number is μ having sensitivity indices as follows: $\Upsilon_{\mu}^{\mathcal{R}_0} = -0.1975$, $\Upsilon_{\mu}^{\mathcal{R}_1} = -0.2014$ and $\Upsilon_{\mu}^{\mathcal{R}_2} = -0.1937$.

Sensitivity indices of the endemic equilibrium

Since we have an explicit formula for the endemic equilibrium, we can also derive an analytical expression for its sensitivity indices with respect to each of the parameters described in Table 3.2. For example, the sensitivity index of s_1^* with respect to β_1 is given by,

$$\Upsilon_{\beta_1}^{s_1^*} = \frac{\partial s_1^*}{\partial \beta_1} \times \frac{\beta_1}{s_1^*} = -1.000. \quad (3.44)$$

The remaining sensitivity indices of the EE (3.26) and EE (3.25) with respect to the parameters of the models are given in Table 3.4.

From Table 3.3 and 3.4 we notice some interesting relationships among the sensitivity indices. We observe that the sensitivity index of s^* with respect to any of the parameter ρ of the model (3.18) is the negative of the sensitivity index of \mathcal{R}_0 with respect to the same parameter ρ , i.e.,

$$\Upsilon_{\rho}^{s^*} = -\Upsilon_{\rho}^{\mathcal{R}_0}, \quad (3.45)$$

irrespective of parameter value or population size. This shows that any parameter ρ will have an equal but opposite influence on s^* and \mathcal{R}_0 . Similarly, the sensitivity index of s_1^* and \mathcal{R}_1 , s_2^* and \mathcal{R}_2 also have the same relations:

$$\Upsilon_{\rho}^{s_1^*} = -\Upsilon_{\rho}^{\mathcal{R}_1}, \quad \Upsilon_{\rho}^{s_2^*} = -\Upsilon_{\rho}^{\mathcal{R}_2}, \quad (3.46)$$

where ρ is any of the parameters described in Table 3.2 except δ_{12} and δ_{21} which are independent of the EE. Next, we observe that

$$\Upsilon_{\rho}^{i^*} = \Upsilon_{\rho}^{w^*}, \quad \Upsilon_{\rho}^{i_1^*} = \Upsilon_{\rho}^{w_1^*}, \quad \Upsilon_{\rho}^{i_2^*} = \Upsilon_{\rho}^{w_2^*}, \quad (3.47)$$

for all parameters. This is obvious, since $i^* = w^*$, $i_1^* = w_1^*$, $i_2^* = w_2^*$. Note that equation (3.43) also holds for i_1^*, i_2^*, w_1^* and w_2^* i.e.,

$$\Upsilon_{\delta_{21}}^{i_1^*} = -\Upsilon_{\delta_{12}}^{i_1^*}, \quad \Upsilon_{\delta_{21}}^{i_2^*} = -\Upsilon_{\delta_{12}}^{i_2^*}, \quad \Upsilon_{\delta_{21}}^{w_1^*} = -\Upsilon_{\delta_{12}}^{w_1^*}, \quad \Upsilon_{\delta_{21}}^{w_2^*} = -\Upsilon_{\delta_{12}}^{w_2^*}, \quad (3.48)$$

showing that δ_{21} and δ_{12} have equal but opposite impact on i_1^*, i_2^*, w_1^* and w_2^* . Having established the above relationships, we proceed to interpret the results of the sensitivity indices of the EE (3.25) and EE (3.26) described in Table 3.4.

The most sensitive parameter for i^* is μ with sensitivity index of -2.0411. Since $\Upsilon_{\mu}^{i^*} = -2.0411$, decreasing (or increasing) μ by 10% will increase (or decrease) i^* by 20.411%. Other important parameters are β_1 , β_2 followed by γ_2 and then γ_1 . Similar results also holds for w^* , since $i^* = w^*$.

We examine the sensitivity indices of i_1^*, w_1^*, i_2^* and w_2^* to assess the effects of SECs in the prevalence of the disease. The most sensitive parameters for i_1^* is γ_1 with sensitivity index of

Table 3.4: Sensitivity index of the endemic equilibrium

Parameter	S^*	I^*	W^*	S_1^*	S_2^*	I_1^*	I_2^*	W_1^*	W_2^*
β_1	-0.5360	-1.1143	-1.1143	-1.000	0.000	-0.0826	0.000	-0.0826	0.000
β_2	-0.4640	-0.9646	-0.9646	0.000	-1.000	0.000	-0.0321	0.000	-0.0321
γ_1	0.3915	0.0124	0.0124	0.7986	0.000	-3.3502	0.000	-3.3502	0.000
γ_2	0.4111	0.0130	0.0130	0.000	0.8063	0.000	-2.1434	0.000	-2.1434
μ	0.1975	-2.0411	-2.041	0.2014	0.1937	0.1551	0.4852	0.1551	0.4852
δ_{12}	0.000	0.000	0.000	0.000	0.000	-1.8998	0.6722	-1.8998	0.6722
δ_{21}	0.000	0.000	0.000	0.000	0.000	1.8998	-0.6722	1.8998	-0.6722

magnitude 3.3502 followed by δ_{12} and δ_{21} , μ and then β_1 . For i_2^* , we discover that the most important parameters for i_2^* is γ_2 with sensitivity index of magnitude 2.1434 followed by δ_{12} and δ_{21} , μ and then β_2 . The same result in i_1^* , i_2^* also hold for w_1^* , w_2^* since $\Upsilon_\rho^{i_1^*} = \Upsilon_\rho^{w_1^*}$ and $\Upsilon_\rho^{i_2^*} = \Upsilon_\rho^{w_2^*}$ for any parameter ρ of the model. This suggests that to effectively reduce the prevalence of infection in the entire community at endemic stage of the outbreak, equal attention should be given to treatment of infected individual and water purification.

3.4 The n -socioeconomic class model

In this section, we shall extend several results obtained in the 2-SEC model (3.6) to the more general n -SEC model (3.2).

3.4.1 Disease free equilibrium for the n -SEC model

The unique DFE for the n -SEC model (3.2) is given by

$$E_n^0 = (s_1^0, i_1^0, w_1^0, s_2^0, i_2^0, w_2^0, \dots, s_n^0, i_n^0, w_n^0), \quad (3.49)$$

where $s_1^0 = n/(1 + \frac{\delta_{12}}{\delta_{21}} + \frac{\delta_{12} \delta_{23}}{\delta_{21} \delta_{32}} + \frac{\delta_{12} \delta_{23} \delta_{34}}{\delta_{21} \delta_{32} \delta_{43}} + \dots + \frac{\delta_{12} \delta_{23} \delta_{34} \dots \delta_{n-1} n}{\delta_{21} \delta_{32} \delta_{43} \dots \delta_n n-1})$, $s_2^0 = \frac{\delta_{12}}{\delta_{21}} s_1^0$, $s_3^0 = \frac{\delta_{12} \delta_{23}}{\delta_{21} \delta_{32}} s_1^0$, $s_4^0 = \frac{\delta_{12} \delta_{23} \delta_{34}}{\delta_{21} \delta_{32} \delta_{43}} s_1^0$, \dots , $s_n^0 = \frac{\delta_{12} \delta_{23} \delta_{34} \dots \delta_{n-1} n}{\delta_{21} \delta_{32} \delta_{43} \dots \delta_n n-1} s_1^0$, $(i_1^0, i_2^0, \dots, i_n^0) = (0, 0, 0, \dots, 0)$, and $(w_1^0, w_2^0, \dots, w_n^0) = (0, 0, 0, \dots, 0)$. If $\delta_{jk} = \delta_{kj}$ (i.e., rates of migration in and out of any SEC are equal), then the DFE (3.49) becomes

$$(s_1^0, i_1^0, w_1^0, s_2^0, i_2^0, w_2^0, \dots, s_n^0, i_n^0, w_n^0) = (1, 0, 0, 1, 0, 0, \dots, 1, 0, 0). \quad (3.50)$$

As we have seen earlier in the case $n = 2$, this special case will also be important for our analysis in this general case. Note that the homogeneous version of model (3.2) is still (3.18) except that

$$\beta = \beta_1 \sum_{j=1}^n p^{j-1} N_j / N, \quad \gamma = \gamma_1 \sum_{j=1}^n c^{j-1} N_j / N, \quad \sigma = \sum_{j=1}^n \sigma_j N_j / N. \quad (3.51)$$

3.4.2 The basic reproduction number for the n -SEC model

Since we have an explicit expression for the DFE of the n -SEC model, we can also derive the basic reproduction number of the model using similar approach in the case $n = 2$. Using the approach, the basic reproduction number of model (3.2) becomes

$$\mathcal{R}^* = \max\{\mathcal{R}_j\}, \quad j = 1, 2, 3, \dots, n, \quad (3.52)$$

where

$$\mathcal{R}_j = \frac{p^{j-1} \beta_1}{(\mu + c^{j-1} \gamma_1)} \frac{\delta_{12} \delta_{23} \delta_{34} \dots \delta_{j-1} j}{\delta_{21} \delta_{32} \delta_{43} \dots \delta_j j-1} s_1^0. \quad (3.53)$$

Note that the threshold quantity \mathcal{R}_j is the basic reproduction number of the SEC j of model (3.2).

Remark: $\mathcal{R}_j \rightarrow 0$ as $j \rightarrow \infty$. Therefore, n should be chosen appropriately. The subscript j is used to emphasize the SEC j .

To determine which of the SECs is driving the outbreaks for this general n -SEC model, we consider the following cases:

Case i: $\delta_{jk} = \delta_{kj}$. For this case, the basic reproduction number (3.53) becomes

$$\mathcal{R}_j = p^{j-1} \beta_1 / (\mu + c^{j-1} \gamma_1). \quad (3.54)$$

We can easily show that

$$\mathcal{R}_{j+1} < \mathcal{R}_j, \quad j = 1, 2, 3, \dots, n. \quad (3.55)$$

This result demonstrates that under equal migration rate across the SECs, secondary infections will be dominated by the lowest SEC. Therefore, the lower the SEC is driving the outbreak for this case.

Case ii: $\delta_{jk} < \delta_{kj}$ for $j < k$, i.e., a situation where more individuals migrate from higher to lower SECs. For this case, similar analysis shows that (3.55) also hold.

Case iii: $\delta_{jk} > \delta_{kj}$ for $j < k$, i.e., when more individuals migrate from lower to higher SECs. For this case, similar argument reveals that

$$\mathcal{R}_j < \mathcal{R}_{j+1}, \quad \text{as } (p, c) \longrightarrow 1 \quad (3.56)$$

holds. These show that infections can be dominated in any SEC (lower or higher) if more individuals migrate into it. Individuals in such SEC will therefore be more vulnerable to the disease. Hence, such SEC will be the major target of control interventions to minimize the spread of the disease. These results are also consistent with the 2-SEC model.

Next we investigate the effects of migration rate δ_{jk} on the dynamics of model (3.2) by considering the same cases presented above. Note that the basic reproduction number of the homogeneous model (3.18) remains

$$\mathcal{R}_0 = \beta/(\mu + \gamma),$$

except that β and γ are now given by (3.51).

Case i: $\delta_{jk} = \delta_{kj}$. Comparing \mathcal{R}_0 and \mathcal{R}_i , we have

$$\mathcal{R}_0 - \mathcal{R}_i = \beta_1 \left(\frac{(\sum_{j=1}^n p^{j-1} N_j)(\mu + \gamma_1 c^{j-1}) - p^{j-1}(\mu N + \gamma_1 \sum_{j=1}^n c^{j-1} N_j)}{(\mu N + \gamma_1 \sum_{j=1}^n c^{j-1} N_j)(\mu + \gamma_1 c^{j-1})} \right). \quad (3.57)$$

Taking limits of equation (3.57) gives

$$\mathcal{R}_0 = \mathcal{R}_j, \quad \text{as } (p, c) \longrightarrow 1. \quad (3.58)$$

However, from equation (3.57), we observe that

$$\mathcal{R}_0 > \mathcal{R}_j, \iff \left(\sum_{j=1}^n p^{j-1} N_j \right) (\mu + \gamma_1 c^{j-1}) > p^{j-1} (\mu N + \gamma_1 \sum_{j=1}^n c^{j-1} N_j), \quad (3.59)$$

$$\mathcal{R}_0 < \mathcal{R}_j, \iff \left(\sum_{j=1}^n p^{j-1} N_j \right) (\mu + \gamma_1 c^{j-1}) < p^{j-1} (\mu N + \gamma_1 \sum_{j=1}^n c^{j-1} N_j), \quad (3.60)$$

$$\mathcal{R}_0 = \mathcal{R}_j, \iff \left(\sum_{j=1}^n p^{j-1} N_j \right) (\mu + \gamma_1 c^{j-1}) = p^{j-1} (\mu N + \gamma_1 \sum_{j=1}^n c^{j-1} N_j). \quad (3.61)$$

For the case $\delta_{jk} \neq \delta_{kj}$ for $j < k$, similar inequalities as above can also be derived.

3.4.3 Outbreak growth rate for the n -SEC model

If $\mathcal{R}_j > 1$, a disease outbreak occurs in each of the SECs. The outbreak growth rate of the general SEC model (3.2) is given by

$$\lambda^* = \max\{\lambda_j^+\} \quad (3.62)$$

where

$$\lambda_j^+ = \frac{1}{2} \left[-(\mu + c^{j-1} \gamma_1 + \sigma_j) + \sqrt{(\mu + c^{j-1} \gamma_1 - \sigma_j)^2 + 4\sigma(\mu + c^{j-1} \gamma_1) \mathcal{R}_j} \right] \quad (3.63)$$

is the outbreak growth rate for the j th SEC of the general model (3.2). We need to determine the SEC which is the main cause of the outbreak at this stage. Since $\mathcal{R}_{j+1} < \mathcal{R}_j$ when $\delta_{jk} \leq \delta_{kj}$, then it follows that

$$\lambda_{j+1}^+ < \lambda_j^+. \quad (3.64)$$

On the other hand, when $\delta_{jk} > \delta_{kj}$, we obtain

$$\lambda_j^+ < \lambda_{j+1}^+, \text{ as } (p, c) \longrightarrow 1. \quad (3.65)$$

Next, to determine the effects of considering SECs, we investigate the relationship between λ^+ and λ_j^+ . Note that the outbreak growth rate λ^+ for the homogeneous model (3.18) remains

$$\lambda^+ = \frac{1}{2} \left[-(\mu + \gamma + \sigma) + \sqrt{(\mu + \gamma - \sigma)^2 + 4\sigma(\mu + \gamma) \mathcal{R}_0} \right], \quad (3.66)$$

where β and γ are given in equation (3.51). Let $B = \mu + \gamma_1 c^{j-1} + \sigma_j$ and $\sigma_j = \sigma$, from equations (3.63) and (3.66), we get

$$(2\lambda^+ + B)^2 - (2\lambda_j^+ + B)^2 = 4\lambda^+(\gamma - \gamma_j) + 4\sigma(\mu + \gamma)(\mathcal{R}_0 - 1) - 4\sigma(\mu + \gamma_j)(1 - \mathcal{R}_j). \quad (3.67)$$

From this we obtain the following inequalities:

$$\lambda^+ > \lambda_j^+ \iff 4\lambda^+(\gamma - \gamma_j) + 4\sigma(\mu + \gamma)(\mathcal{R}_0 - 1) > 4\sigma(\mu + \gamma_j)(1 - \mathcal{R}_j),$$

$$\lambda^+ < \lambda_j^+ \iff 4\lambda^+(\gamma - \gamma_j) + 4\sigma(\mu + \gamma)(\mathcal{R}_0 - 1) < 4\sigma(\mu + \gamma_j)(1 - \mathcal{R}_j),$$

$$\lambda^+ = \lambda_j^+ \iff 4\lambda^+(\gamma - \gamma_j) + 4\sigma(\mu + \gamma)(\mathcal{R}_0 - 1) = 4\sigma(\mu + \gamma_j)(1 - \mathcal{R}_j).$$

The above inequalities gives the conditions under which outbreak growth rate will dominated when SECs are considered or not.

3.5 Discussion

It is believed that the socioeconomic status of individuals in any community does affect the spread of infection in the community. We investigated the effects of socioeconomic classes in the spread of waterborne disease in a community by formulating an n -patch waterborne disease model where each patch represents a SEC. From the n -patch model, we derived a homogeneous version of the model when SECs are not considered and compared the results with that of n -patch model.

We began our analyses with that of n -patch model for a special case when there are only two SECs in the community and determined the important epidemiological threshold quantities known as the basic reproduction numbers \mathcal{R}_1 , \mathcal{R}_2 and \mathcal{R}_0 for SEC 1, SEC 2 and the homogeneous model respectively. We showed that the infections can be completely eradicated from the population when SECs are considered provided the basic reproduction number is less than unity. However, when the basic reproduction number is greater than unity, we discovered that an outbreak will occur and determine the rate at which the outbreak will be spreading in the

community. We showed that the long-term dynamics of the outbreak can be described by stability arguments. Specifically, we proved that the endemic equilibrium is globally asymptotically stable by finding an appropriate Lyapunov function.

We discovered that under the assumption of equal migration rates, the number of secondary infections generated by an infected individual in SEC 1 will always dominate that of SEC 2. Similarly, under the same assumption, we proved that there will be greater outbreak growth rate in the SEC 1. Therefore, we conclude that under this assumption, the SEC 1 will be the the main cause of outbreak in the population when SECs are considered irrespective of the magnitude of the outbreak. To effectively minimize the chances of outbreak in this case, we recommended that the SEC 1 should be the target of control interventions.

However, if more individuals migrate from SEC 1 to SEC 2, we discovered that the number of secondary infections generated by an infected individual in SEC 2 will dominate that of SEC 1. On the contrary, we observed that the number of secondary infections generated by an infected individual in SEC 1 will dominate that of SEC 2 when more individuals migrate from SEC 2 to SEC 1. At the endemic stage of the outbreak when the basic reproduction number is greater than unity, we discovered that considering SECs can lead to a greater outbreak growth rate if more individuals migrate from SEC 2 to SEC 1 or a less outbreak growth rate if more individuals migrate from SEC 1 to SEC 2. Therefore, any of the SECs where majority of the individuals is moving into is will be in a higher risk of contacting the infection. Thus, we recommended that such SEC will be the target of control interventions to effectively minimize the chances of outbreak.

The important parameters relative to initial disease transmission and prevalence were determined by calculating the sensitivity indices of the basic reproduction numbers and endemic equilibria. We discovered that rate of immigration and emmigration into any SEC has equal but opposite impact on the initial disease transmission and prevalence. When SECs are considered, we discovered that contact rates (β_1, β_2) , shedding rates (ν_1, ν_2) and net decay rate of pathogen concentration in water reservoirs σ have greatest influence on the initial disease transmission in each of the SEC 1 and SEC 2. However, when SECs are not considered, we showed that the net decay rate σ has the greatest influence on the initial disease transmission

in the entire community. Thus, these parameters should be put into consideration in order to effectively define better control intervention strategies.

We identify important parameters relative to prevalence of the disease in the presence or absence of SECs. We discovered that recovery rate γ_1 is the most important parameter relative to prevalence of the disease in SEC 1, while the most important parameters relative to prevalence of the disease in SEC 2 is recovery rate γ_2 . In the absence of migration due to socioeconomic reasons, we found out that birth/death rate is the most important parameter relative to prevalence of the disease. These suggested that it is more effective to reduce the prevalence of the disease in the entire community by controlling these parameters.

Finally, we extended the results of the 2-SEC model to the general n -SEC model. The dynamical behaviour of our model agrees with the intuitive expectation of waterborne disease dynamics in real life. As a result, the model can be used to study the dynamics of waterborne diseases as well as predict future waterborne disease outbreak in communities where the disease is endemic. Based on this study we conclude that socioeconomic status of individuals plays a very significant role in improving the understanding of transmission of waterborne disease in order to define appropriate control intervention strategies that reduce the spread of the infection.

3.6 Appendix to Chapter 3

Theorem 3.6.1. *The DFE of model (3.2) is globally asymptotically stable if $\mathcal{R}^* < 1$.*

Proof. We only need to show that (3.2) satisfies conditions (H1) and (H2) of Theorem 1.4.9 when $\mathcal{R}^* < 1$. In model (2.41), let $X_1 = (s_1, r_1, s_2, r_2, \dots, s_n, r_n)$, $X_2 = (i_1, w_1, i_2, w_2, \dots, i_n, w_n)$ and $X_1^* = (s_1^0, 0, s_2^0, 0, \dots, s_n^0, 0)$ as described in equation (3.49). The infected compartments

$G(X_1, X_2)$ are given by

$$G(X_1, X_2) = \begin{pmatrix} \beta_1 s_1 w_1 - (\mu + \gamma_1) i_1 \\ \sigma_1 (i_1 - w_1) \\ p \beta_1 s_2 w_2 - (\mu + c \gamma_1) i_2 \\ \sigma_2 (i_2 - w_2) \\ \dots \\ p^{n-1} \beta_1 s_n w_n - (\mu + c^{n-1} \gamma_1) i_n \\ \sigma_n (i_n - w_n) \end{pmatrix}.$$

The $G(X_1, X_2)$ can be rewritten in the form of

$$G(X_1, X_2) = AX_2 - \hat{G}(X_1, X_2)$$

where

$$A = \begin{pmatrix} -(\mu + \gamma_1) & \beta_1 s_1^0 & 0 & 0 & 0 & 0 & \dots & 0 & 0 \\ \sigma_1 & -\sigma_1 & 0 & 0 & 0 & 0 & \dots & 0 & 0 \\ 0 & 0 & -(\mu + c \gamma_1) & p \beta_1 s_2^0 & 0 & 0 & \dots & 0 & 0 \\ 0 & 0 & \sigma_2 & -\sigma_2 & 0 & 0 & \dots & 0 & 0 \\ \vdots & \vdots & & & & & \ddots & & \\ 0 & 0 & 0 & 0 & 0 & 0 & \dots & -(\mu + c^{n-1} \gamma_1) & p^{n-1} \beta_1 s_n^0 \\ 0 & 0 & 0 & 0 & 0 & 0 & \dots & \sigma_n & -\sigma_n \end{pmatrix}$$

and

$$\hat{G}(X_1, X_2) = \begin{pmatrix} \beta_1 w_1 (s_1^0 - s_1) \\ 0 \\ p \beta_1 w_2 (s_2^0 - s_2) \\ 0 \\ \vdots \\ p^{n-1} \beta_1 w_n (s_n^0 - s_n) \\ 0 \end{pmatrix}.$$

It is obvious that $\hat{G}(X_1, X_2) \geq 0$, since $s_j \leq s_j^0$ for $j = 1, 2, \dots, n$. The global stability of the

system

$$\frac{dX_1}{dt} = F(X_1, 0) = \begin{pmatrix} \mu + \delta_{21}s_2(t) - (\delta_{12} + \mu)s_1(t) \\ -\mu r_1(t) \\ \mu + \delta_{12}s_1(t) + \delta_{32}s_3(t) - (\delta_{21} + \delta_{23} + \mu)s_2(t) \\ -\mu r_2(t) \\ \vdots \\ \mu + \delta_{n-1} s_{n-1}(t) - (\delta_{n-1} - \mu)s_n(t) \\ -\mu r_n(t) \end{pmatrix} \quad (3.68)$$

can be easily verified as follows: $F(X_1, 0)$ is linear ordinary differential equations and solving it gives

$$\begin{aligned} s_1(t) &= \frac{(\mu r_1(0) - \delta_{21}r_2(0))e^{-\mu t}}{\delta_{12} - \mu} + \delta_{21}/\delta_{12} + A_1 e^{-\delta_{12}t}, \\ r_1(t) &= r_1(0)e^{-\mu t}, \\ s_2(t) &= \frac{(\mu r_2(0) - \delta_{21}r_1(0) - \delta_{32}r_3(0))e^{-\mu t}}{\delta_{21} + \delta_{32} - \mu} + \frac{\delta_{12} + \delta_{32}}{\delta_{21} + \delta_{23}} + A_2 e^{-(\delta_{21} + \delta_{23})t}, \\ r_2(t) &= r_2(0)e^{-\mu t}, \\ &\vdots \\ s_n(t) &= \frac{(\mu r_n(0) - \delta_{n-1} r_{n-1}(0))e^{-\mu t}}{\delta_{n-1} - \mu} + \frac{\delta_{n-1}}{\delta_{n-1}} + A_n e^{-\delta_{n-1}t}, \\ r_n(t) &= r_n(0)e^{-\mu t}, \end{aligned}$$

where A_1, A_2, \dots, A_n are constants. Clearly,

$$(s_1(t), r_1(t), s_2(t), r_2(t), \dots, s_n(t), r_n(t)) \longrightarrow (s_1^0, 0, s_2^0, 0, \dots, s_n^0, 0).$$

Therefore, X_1^* is globally asymptotically stable. Hence, the DFE (3.49) of the n -SEC model is globally asymptotically stable provided $\mathcal{R}^* < 1$. \square

This shows that the disease can be eradicated from the entire population irrespective of the migration rates when SECs are considered provided $\mathcal{R}^* < 1$. This does not mean that migration rates do not affect global stability of the DFE/short-term dynamics of the disease. Note that if our target is to eradicate the disease from only the SEC j , we require $\mathcal{R}_j < 1$, not necessary $\mathcal{R}^* < 1$.

3.6.1 Stability of the endemic equilibrium

When $\mathcal{R}_j > 1$, a unique endemic equilibrium (EE) given by

$$(s_1^*, i_1^*, w_1^*, \dots, s_n^*, i_n^*, w_n^*) = \left(\frac{1}{\mathcal{R}_1}, \frac{\mu(1-s_1^*)}{\mu + \gamma_1}, i_1^*, \dots, \frac{1}{\mathcal{R}_n}, \frac{\mu(1-s_n^*)}{\mu + c^{n-1}\gamma_1}, i_n^* \right), \quad (3.69)$$

exists for model (2.41). Note that at the EE (3.69), there is a uniform migration rates such that each of the SECs has a constant population size N_j . Therefore, we investigate the global stability of the EE when $N_j(t)$ is constant.

Theorem 3.6.2. *The unique EE of the n -SEC model is globally asymptotically stable if $N_j(t)$ is constant.*

Proof. Let Ω be the feasible region of model (3.2). Let $x(t) = (s_1(t), i_1(t), w_1(t), \dots, s_n(t), i_n(t), w_n(t))$ be any solution of (3.2) in Ω such that $(i_1(t), w_1(t), \dots, i_n(t), w_n(t)) \neq (0, 0, \dots, 0, 0)$ and $x^* = (s_1^*, i_1^*, w_1^*, \dots, s_n^*, i_n^*, w_n^*)$. We show that as $t \rightarrow \infty$, $x(t) \rightarrow x^*$. Consider the Lyapunov function

$$V = \sum_{k=1}^n \left[(s_k - s_k^* \log s_k) + (i_k - i_k^* \log i_k) + \frac{(\mu + c^{k-1}\gamma_1)}{\sigma} (w_k - w_k^* \log w_k) \right], \quad (3.70)$$

which is similar to the type considered in [44, 43, 84]. Note that V is continuous and has a global minimum at the EE. The time derivative of V is

$$\begin{aligned} \dot{V} &= \sum_{k=1}^n \left[\left(1 - \frac{s_k^*}{s_k}\right) \dot{s}_k + \left(1 - \frac{i_k^*}{i_k}\right) \dot{i}_k + \frac{(\mu + c^{k-1}\gamma_1)}{\sigma} \left(1 - \frac{w_k^*}{w_k}\right) \dot{w}_k \right], \\ &= \sum_{k=1}^n \left[\mu \left(2 - s_k - \frac{s_k^*}{s_k}\right) + \beta_k^o s_k^* i_k^* \left(1 - \frac{s_k w_k}{s_k^* i_k} - \frac{i_k}{w_k}\right) \right], \\ &= \sum_{k=1}^n \left[-\mu \left(\frac{i_k}{w_k} + \frac{s_k w_k}{s_k^* i_k} + \frac{s_k^*}{s_k} - 3\right) - \mu s_k^* \left(\frac{i_k}{w_k} - 1 + \frac{s_k}{s_k^*} \left(\frac{w_k}{i_k} - 1\right)\right) \right], \\ &= \sum_{k=1}^n \left[-\mu(1 - s_k^*) \left(\frac{i_k}{w_k} + \frac{s_k w_k}{s_k^* i_k} + \frac{s_k^*}{s_k} - 3\right) - \mu s_k^* \left(\frac{s_k^*}{s_k} + \frac{s_k}{s_k^*} - 2\right) \right], \\ &\leq 0. \end{aligned}$$

The last inequality follows from the fact that the geometric mean is less than or equal to the arithmetic mean. Thus, we have $1 = \sqrt{\frac{s_k^*}{s_k} \frac{s_k}{s_k^*}} \leq \frac{1}{2} \left(\frac{s_k^*}{s_k} + \frac{s_k}{s_k^*}\right) \implies \frac{s_k^*}{s_k} + \frac{s_k}{s_k^*} - 2 \geq 0$. Similarly,

we can show that $\frac{i_k}{w_k} + \frac{s_k w_k}{s_k^* i_k} + \frac{s_k^*}{s_k} - 3 \geq 0$. Let L denote the set of points where \dot{V} is zero. As $t \rightarrow \infty$, $x(t)$ approaches the largest invariant set in L [47]. Meanwhile the fixed point $\{x^*\}$ is the only invariant set in L . This completes the proof. \square

This implies that the disease can persist in the population when migration rate of individuals across the SECs are at equilibrium provided that $\mathcal{R}_j > 1$.

Chapter 4

On the mathematical analysis and application of a waterborne disease model with multiple water sources

Waterborne disease is one of the major health problems facing the world today especially in developing countries where there is limited access to clean water. We formulate a waterborne disease model for a community where individuals are exposed to multiple contaminated water sources. The fundamental mathematical features of the model such as the basic reproduction number \mathcal{R}_0 , outbreak growth rate and final epidemic size are obtained and analysed accordingly. The global stability analysis of the disease free equilibrium and endemic equilibrium are performed. We verify our analytical predictions by investigating the recent cholera outbreak in Haiti. The model is later extended by considering vaccination as a possible control intervention strategy. Sensitivity analysis is carried out to determine how important each parameter is in relation to disease transmission. An optimal control problem is constructed to investigate the existence of an optimal control function that controls the spread of the disease with minimum cost. The contents of this Chapter have been submitted for publication [22].

4.1 Introduction

Current statistics from WHO [92] reveals that approximately 1.1 billion people globally do not have access to improved water supply sources whereas around 700,000 children die every year from diarrhoea caused by unsafe water and poor sanitation [89]. A number of waterborne disease outbreaks occur in rural communities where there is limited access to clean water. Most of these rural communities are exposed to multiple contaminated water sources like streams, rivers, dams, wells, lakes, and ponds etc as their major sources of water. Each of these contaminated water sources contains different percentages of pathogen concentration. Considering multiple contaminated water sources to study the dynamics of waterborne disease for such a community becomes apparent. This will certainly make the model complex and difficult to analyse mathematically unlike when single water source is considered. Note that the basic mathematical analysis involving computation of basic reproduction number, outbreak growth rate, final outbreak size, stability of disease free equilibrium and endemic equilibrium depend on the measures of pathogens in water sources available. Furthermore, determining the appropriate contact rate, shedding rate and evaluating the effectiveness of control intervention strategy also depend on the water sources the individuals are exposed to. Therefore, it is our intention to seek to understand the dynamics of waterborne disease in the presence of multiple water sources by analysing these important mathematical epidemiological features of the model for the case of multiple water sources. By rigorously analysing some of these important mathematical epidemiological features of the model, we will determine the impact of considering multiple water sources. This will also deepen our understanding of the dynamics of the disease. For a simple demonstration of the applicability of the multiple water sources model, we consider the model to investigate the cholera outbreak in Haiti. Using the parameter values from the literature and by adjusting the two main key parameters in the model, we are able to fit the model to the number of reported cases of hospitalization in Haiti from 30 October 2010 to 24 December 2012.

To define better control measures that will reduce the spread of the disease, it is necessary to extend the model by introducing control intervention strategies such as vaccination. Sensitivity

analysis is also necessary to determine how important each of the model parameters is for disease transmission and prevalence. Even though vaccination is one the most effective control intervention strategies for reducing the spread of waterborne disease, most of the communities where this disease is endemic could not afford effective vaccination due to limited resources [59, 65]. It is necessary to understand how to reduce the spread of waterborne disease using vaccination with minimum cost. To effect this analysis we invoke optimal control theory which has been a useful mathematical tool in determining the appropriate control intervention strategy to reduce the spread of an infection with minimum cost [49, 2, 59, 85]. We also utilise numerical simulations which is a very useful tool which can be use to support analytical predictions.

Dynamics of waterborne disease is made up of two subsystems: human and pathogens in water. The nature of interaction that exists between human and pathogens in water and the transmission pathways that lead to waterborne disease have been an issue of concern over the years. Some authors [84, 62] have considered multiple transmission pathways with linear or non-linear interactions. For the purpose of this study, we will consider a single interaction whereby infections are generated only through person-water contact. We pursue this approach as contact with contaminated water has been shown to be the major driving force of some waterborne disease outbreaks [19, 36, 64, 80, 65]. While these and many other studies [12, 72, 29, 33, 42] on waterborne disease have contributed immensely to understanding their dynamics, to the best of our knowledge, none of those studies considered a homogeneous population where individuals are exposed to multiple contaminated water sources. The aim of this study is to use a mathematical epidemiological model to deepen our understanding on the dynamics of waterborne disease for a community where individuals are exposed to multiple contaminated water sources and furthermore determine appropriate vaccination measures that will reduce the spread of the disease with minimum cost.

4.2 Model formulation

Figure 4.1 represents the flow diagram for the model we will analyse in this paper. The model consists of the standard SIR model under the assumption of constant population size [5, 84],

together with compartments W_1, W_2, \dots, W_n that measure pathogen concentration in water sources $1, 2, \dots, n$ respectively. As usual, we consider a total human population N and partition it into susceptible $S(t)$, infected $I(t)$ and recovered individuals $R(t)$. We assume that individuals are exposed to the n distinct water reservoirs (sources). Even though individuals are exposed to multiple contaminated water sources, they are not likely to have equal access to each of the water sources. As a result, we assume that susceptible individuals $S(t)$ become infected through contact with any of the contaminated water sources $1, 2, \dots, n$ at rate $\beta_1, \beta_2, \dots, \beta_n$ respectively. Infected individuals $I(t)$ can in turn contaminate the water sources $1, 2, \dots, n$ by shedding pathogens into them at rate $\nu_1, \nu_2, \dots, \nu_n$ respectively. An infected individual generates secondary infections by first shedding pathogens into the water sources, which susceptible individuals subsequently come in contact with. Infected individuals $I(t)$ recover naturally at rate γ . We assume that recovered individuals $R(t)$ have immunity against reinfection throughout the duration of the outbreak. Natural death occurs in all the above human compartments at rate μ . Pathogens in water reservoirs can decay as well as grow naturally. As a result, we assume that each of the concentration of pathogens in each of the compartments $W_i(t)$ increases through natural generation of pathogens in the water reservoirs at rate α and decreases through natural decay of pathogens at rate ξ . Putting all these assumptions and formulations together, we obtain

$$\begin{aligned}
\dot{S}(t) &= \mu N(t) - S(t) \sum_{i=1}^n \beta_i W_i(t) - \mu S(t), \\
\dot{I}(t) &= S(t) \sum_{i=1}^n \beta_i W_i(t) - (\mu + \gamma) I(t), \\
\dot{W}_1(t) &= \nu_1 I(t) - \sigma W_1(t), \\
\dot{W}_2(t) &= \nu_2 I(t) - \sigma W_2(t), \\
&\vdots \\
\dot{W}_n(t) &= \nu_n I(t) - \sigma W_n(t), \\
\dot{R}(t) &= \gamma I(t) - \mu R(t),
\end{aligned} \tag{4.1}$$

where $\sigma = \xi - \alpha > 0$. Note that $\beta = \sum_{i=1}^n \beta_i$ is the effective contact rate with all the contaminated water sources, $\nu = \sum_{i=1}^n \nu_i$ is the effective shedding rate into all the contaminated

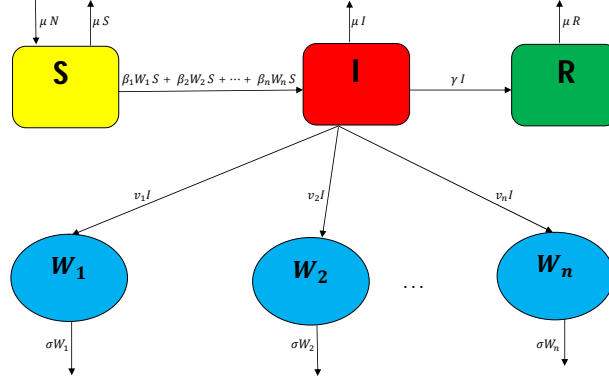


Figure 4.1: Flow chart of the waterborne disease model (4.1) .

water sources and the force of infection is given by $\sum_{i=1}^n \beta_i W_i(t)$ [54]. The initial conditions are assumed as follows:

$$S(0) > 0, \quad I(0) \geq 0, \quad W(0) \geq 0, \quad R(0) \geq 0, \quad (4.2)$$

where $W = (W_1, W_2, \dots, W_n)$.

4.3 Model analysis

4.3.1 Existence of solutions

Theorem 4.3.1. *All solutions $(S(t), I(t), W(t), R(t))$ of the model (4.1) are positive and bounded for all $t > 0$ with the initial conditions (4.2). Furthermore, all the solutions will enter the feasible region*

$$\Phi = \Phi_H \times \Phi_P, \quad (4.3)$$

where

$$\Phi_H = \left\{ (S, I, R) \in \mathbb{R}_+^3 : S + I + R = N, \quad 0 \leq S, I \leq N, \quad 0 \leq R \leq \gamma N / \mu \right\},$$

is the feasible region of human components and

$$\Phi_P = \left\{ (W_1, W_2, \dots, W_n) \in \mathbb{R}_+^n : 0 \leq W_i \leq N \nu_i / \sigma, \quad 0 \leq \sum_{i=1}^n W_i \leq N \sum_{i=1}^n \nu_i / \sigma \right\}$$

is the feasible region of pathogen components.

Theorem 4.3.1 can be established using a similar approach as in [101]. The feasible region Φ is a positively invariant region, hence model (4.1) will be considered mathematically and epidemiologically well posed in Φ .

4.3.2 The basic reproduction number

Model (4.1) has a disease free equilibrium (DFE) given by

$$(S^0, I^0, W^0) = (N, 0, \bar{0}), \quad (4.4)$$

where $\bar{0} = (0, 0, \dots, 0)$ (n time). The basic reproduction number \mathcal{R}_0 is defined as the expected number of secondary infections that result from introducing a single infected individual into an otherwise susceptible population. We determine the basic reproduction number of (4.1) using the next generation matrix approach of van den driessche and watmough [90]. The associated next generation matrices are

$$\mathcal{F} = \begin{pmatrix} 0 & \beta_1 N & \beta_2 N & \dots & \beta_n N \\ 0 & 0 & 0 & \dots & 0 \\ \vdots & \vdots & & & \\ 0 & 0 & & \dots & 0 \end{pmatrix}, \quad \mathcal{V} = \begin{pmatrix} \mu + \gamma & 0 & 0 & \dots & 0 \\ -\nu_1 & \sigma & 0 & & 0 \\ -\nu_2 & 0 & \sigma & & 0 \\ \vdots & & & \ddots & \\ -\nu_n & 0 & \dots & 0 & \sigma \end{pmatrix}. \quad (4.5)$$

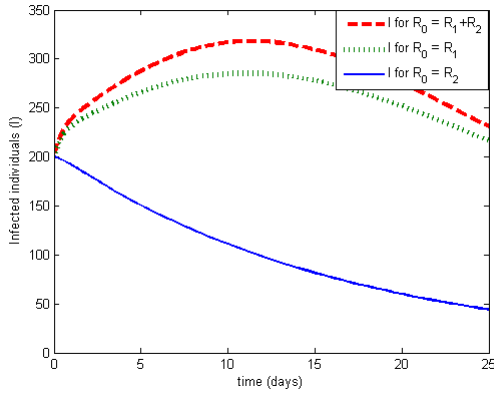
The basic reproduction number is the spectral radius of $\mathcal{F}\mathcal{V}^{-1}$, which is given by

$$\mathcal{R}_0 = N \sum_{i=1}^n \nu_i \beta_i / (\sigma(\gamma + \mu)). \quad (4.6)$$

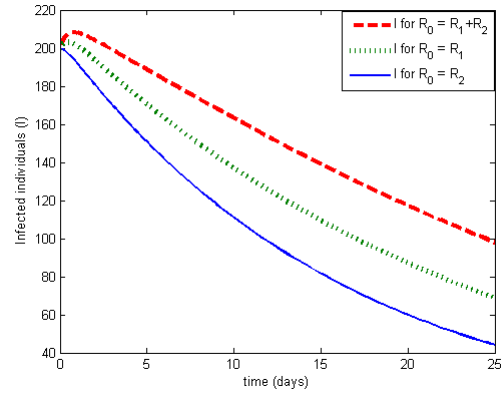
The basic reproduction number (4.6) for the case of multiple contaminated water sources can be re-written as

$$\mathcal{R}_0 = \sum_{i=1}^n \mathcal{R}_i \quad (4.7)$$

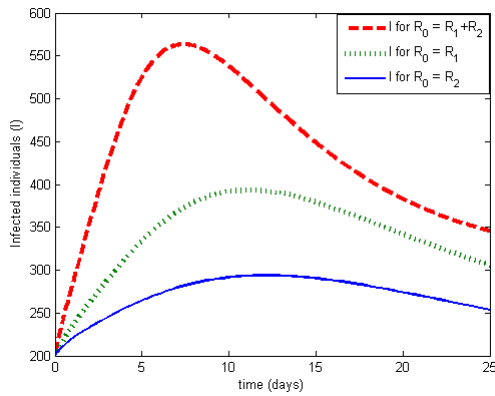
where $\mathcal{R}_i = N\nu_i\beta_i/(\sigma(\gamma + \mu))$ is the basic reproduction number of model (4.1) due to the i th contaminated water source only. This result implies that the basic reproduction number \mathcal{R}_0 in



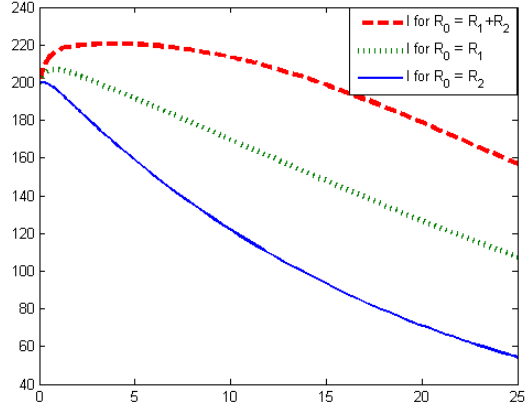
(a)



(b)



(c)



(d)

Figure 4.2: Numerical illustrations showing the contributions of contaminated water sources to the number of infected individuals (a) $\mathcal{R}_0 > 1, \mathcal{R}_2 < 1 < \mathcal{R}_1$ (b) $\mathcal{R}_0 < 1, \mathcal{R}_2 < \mathcal{R}_1 < 1$ (c) $\mathcal{R}_0 > 1, 1 < \mathcal{R}_2 < \mathcal{R}_1$. (d) $\mathcal{R}_0 > 1, \mathcal{R}_2 < \mathcal{R}_1 < 1$.

the presence of multiple contaminated water sources is the sum of basic reproduction numbers \mathcal{R}_i due to each contaminated water source in the community. This suggests that the higher the number of water sources available to the population, the greater the basic reproduction number. This results in an increase in the number of infected individuals. Figures 4.2(a), 4.2(b), 4.2(c) and 4.2(d) reveal that each \mathcal{R}_i (whether $\mathcal{R}_i < 1$ or $\mathcal{R}_i > 1$) has some influence on the dynamics of waterborne disease (increasing the number of infected individuals). Also from the Figures, it seems that when $\mathcal{R}_0 < 1$, infected individuals $I(t) \rightarrow 0$ (disease free equilibrium) as $t \rightarrow \infty$. We confirm this by showing that the disease free equilibrium is globally asymptotically stable when $\mathcal{R}_0 < 1$. On the contrary, when $\mathcal{R}_0 > 1$, we cannot make a general conclusion about the behaviour of the infected individuals I .

To determine the effects of considering multiple water sources, it is necessary to obtain the single water source version of model (4.1) and consequently compare some of its mathematical features with that of the multiple water sources model. The single water source version of model (4.1) is given by

$$\begin{aligned}
\dot{S}(t) &= \mu N(t) - \beta S(t)\bar{W}(t) - \mu S(t), \\
\dot{I}(t) &= \beta S(t)\bar{W}(t) - (\mu + \gamma)I(t), \\
\dot{\bar{W}}(t) &= \nu I(t) - \sigma \bar{W}(t), \\
\dot{R}(t) &= \gamma I(t) - \mu R(t),
\end{aligned} \tag{4.8}$$

where $\bar{W} = \sum_{i=1}^n W_i/n$. This single water source model can also be regarded as a special case ($n = 1$) of the multiple water source model (4.1). Thus any result that holds in (4.1) will also hold in (4.8), but not vice versa. Therefore, we shall also be exploring how to extend the results that hold in the single water source model (4.8) to the multiple water source model (4.1).

The basic reproduction number for the model (4.8) is

$$\mathcal{R}_0^s = N\nu\beta/(\sigma(\gamma + \mu)). \tag{4.9}$$

We can show that

$$\mathcal{R}_0 < \mathcal{R}_0^s. \tag{4.10}$$

This implies that the number of secondary infections generated by an individual in the presence of single water source is more than that generated in the presence of multiple water sources.

Since a multiple water sources model is more realistic, we can say that the basic reproduction number will be over estimated when the single water source is considered.

4.3.3 Stability of the disease free equilibrium

The stability at the DFE determines the short-term dynamics of a disease [52]. Therefore, to determine the short-term dynamics of the multiple water sources model, it is necessary to investigate the stability of the DFE.

Theorem 4.3.2. *The DFE of the model (4.1) is locally asymptotically stable, when $\mathcal{R}_0 < 1$. \square*

The proof of Theorem 4.3.2 follows from Theorem 2 of van den Driessche and Watmough [90]. Epidemiologically, Theorem 4.3.2 implies that waterborne disease can be eliminated from the community where there are multiple contaminated water sources (when $\mathcal{R}_0 < 1$) if the initial size of the subpopulation is in the basin of attraction of the DFE (4.4). On the contrary, the disease will be established in the population when $\mathcal{R}_0 > 1$. To ensure that eradication of the disease is independent of the initial size of the subpopulation, we prove that the DFE is globally asymptotically stable. This is established using a global stability result by Castillo-Chavez et al. [13] which is stated in Theorem 1.4.9.

Theorem 4.3.3. *The DFE of the model (4.1) is globally asymptotically stable, provided $\mathcal{R}_0 < 1$.*

Proof. We need to show that model (4.1) satisfies conditions (H1) and (H2) in Theorem 1.4.9. From (4.1), $X_1 = S$, $X_2 = (I, W)$ and $X_1^* = N$. The system

$$\frac{dX_1}{dt} = F(X_1, 0) = \mu N - \mu S$$

is linear and solving this linear ordinary differential equation gives

$$S(t) = N - (N - S(0))e^{-\mu t}.$$

Clearly, $S(t) \rightarrow N$ as $t \rightarrow \infty$, provided $\mu > 0$. Thus, X_1^* is globally asymptotically stable.

Next, applying Theorem 1.4.9 to model (4.1) gives

$$G(X_1, X_2) = \begin{pmatrix} S \sum_{i=1}^n \beta_i W_i - (\mu + \gamma)I \\ \nu_1 I - \sigma W_1 \\ \nu_2 I - \sigma W_2 \\ \vdots \\ \nu_n I - \sigma W_n \end{pmatrix},$$

and

$$A = \begin{pmatrix} -(\mu + \gamma) & \beta_1 N & \beta_2 N & \beta_3 N & \dots & \beta_n N \\ \nu_1 & -\sigma & 0 & 0 & \dots & 0 \\ \nu_2 & 0 & -\sigma & 0 & \dots & 0 \\ \vdots & & & & & \\ \nu_n & 0 & 0 & 0 & \dots & -\sigma \end{pmatrix}$$

is clearly an M -matrix with non negative off diagonal elements. Meanwhile, we have that

$$\hat{G}(X_1, X_2) = \begin{pmatrix} \sum_{i=1}^n \beta_i W_i (N - S) \\ \bar{0} \end{pmatrix} \geq 0,$$

since $N \geq S$. Hence, the DFE (4.1) is globally asymptotically stable provided $\mathcal{R}_0 < 1$. \square

The epidemiological implication of this is that waterborne disease can be eradicated from the entire community where individuals are exposed to multiple contaminated water sources irrespective of the initial sizes of the subpopulation provided $\mathcal{R}_0 < 1$. Similarly, we can show that the DFE of the single water source model (4.8) is globally asymptotically stable provided $\mathcal{R}_0^s < 1$. This shows that the disease can also be eradicated from the entire community where individuals are exposed to a single water source when $\mathcal{R}_0^s < 1$.

4.3.4 Outbreak growth rate

If $\mathcal{R}_0 > 1$, then the DFE (4.4) becomes unstable and a disease outbreak occurs. The positive (dominant) eigenvalue of the Jacobian at the DFE is referred to as the outbreak growth rate

[84]. The Jacobian matrix J^0 of model (4.1) evaluated at the DFE (4.4) is given by

$$J^0 = \begin{pmatrix} -\mu & 0 & -\beta_1 N & -\beta_2 N & -\beta_3 N & \dots & -\beta_n N \\ 0 & -(\mu + \gamma) & \beta_1 N & \beta_2 N & \beta_3 N & \dots & \beta_n N \\ 0 & \nu_1 & -\sigma & 0 & 0 & \dots & 0 \\ 0 & \nu_2 & 0 & -\sigma & 0 & \dots & 0 \\ \vdots & \vdots & & & & & \\ 0 & \nu_n & 0 & 0 & 0 & \dots & -\sigma \end{pmatrix}. \quad (4.11)$$

The Jacobian J^0 has $n+2$ negative eigenvalues and one positive eigenvalue which automatically becomes the outbreak growth rate and is given by

$$\lambda^+ = \frac{1}{2} \left(-(\gamma + \mu + \sigma) + \sqrt{[(\gamma + \mu - \sigma)^2 + 4\sigma(\gamma + \mu)\mathcal{R}_0]} \right). \quad (4.12)$$

Note that the value of $\lambda^+ > 0$ represents the steepness of the ascending infection curve (with respect to time). Therefore, a higher λ^+ implies a more severe disease outbreak.

Similarly, when $\mathcal{R}_0^s > 1$, the outbreak growth rate of single water source model (4.8) is

$$\lambda_s^+ = \frac{1}{2} \left(-(\gamma + \mu + \sigma) + \sqrt{[(\gamma + \mu - \sigma)^2 + 4\sigma(\gamma + \mu)\mathcal{R}_0^s]} \right). \quad (4.13)$$

Since $\mathcal{R}_0 < \mathcal{R}_0^s$, it is easy to observe that

$$\lambda^+ < \lambda_s^+. \quad (4.14)$$

This shows that the outbreak growth rate will also be over estimated when a single water source is considered. Note that if $\mathcal{R}_0 < 1$, then the real part of $\lambda^+ < 0$. This implies that outbreaks will not occur whenever $\mathcal{R}_0 < 1$. However, we have that all the eigenvalues of the Jacobian matrix of model (4.1) evaluated at the DFE are negative or have negative real parts when $\mathcal{R}_0 < 1$. Thus, the DFE of model (4.1) is locally asymptotically stable when $\mathcal{R}_0 < 1$ confirming Theorem 4.3.2.

4.3.5 Final outbreak size

Whenever an infectious disease outbreak emerges in any human population, the likely magnitude of the outbreak, often called the expected final outbreak size of the epidemic, is very

important in understanding the dynamics of the disease [57]. The final outbreak size denoted by Z of the SIR models together with some other related models is given by the relation

$$Z = 1 - \exp(-\mathcal{R}_0 Z). \quad (4.15)$$

We show that the final outbreak size relation (4.15) also holds for model (4.1). We consider the same approach used in [57, 84].

Proposition 4.3.4. *Let $\mu = 0$ and $\mathcal{R}_0 > 1$. Let $S(0)$ denote the initial susceptible population and $W_i(0)$ the initial pathogen level in the water reservoir i . As $S(0) \rightarrow N$ and $W_i(0) \rightarrow 0$, the final outbreak size Z of system (4.1) satisfies the relation (4.15).*

Proof. Consider a function

$$F(t) = \log S(t) + R(t) \sum_{i=1}^n \nu_i \beta_i / (\sigma \gamma) - \sum_{i=1}^n \beta_i W_i(t) / \sigma. \quad (4.16)$$

The derivative of F with respect to time t along the solution trajectories of model (4.1) gives

$$\begin{aligned} \dot{F}(t) &= - \sum_{i=1}^n \beta_i W_i(t) + I(t) \sum_{i=1}^n \nu_i \beta_i / \sigma - \sum_{i=1}^n \beta_i (\nu_i I(t) - \sigma W_i(t)) / \sigma, \\ &= 0. \end{aligned}$$

Thus, F is constant along solution trajectories of model (4.1). Since $\mu = 0$, then $S(t)$ decreases monotonically to a limit \bar{S} and $R(t)$ increases monotonically to a limit \bar{R} . By lemma 2 of [84], $I(t) \rightarrow 0$ and $W_i(t) \rightarrow 0$. Since $N = S(t) + I(t) + R(t)$, we have that $\bar{S} = N - \bar{R}$. Taking limits of (4.16) gives

$$\lim_{t \rightarrow \infty} F(t) = \log(N - \bar{R}) + \bar{R} \sum_{i=1}^n \nu_i \beta_i / (\sigma \gamma).$$

At $t = 0$, we obtain

$$F(0) = \log S(0) + R(0) \sum_{i=1}^n \nu_i \beta_i / (\sigma \gamma) - \sum_{i=1}^n \beta_i W_i(0) / \sigma.$$

Since F is constant along solution trajectories, $\lim_{t \rightarrow \infty} F(t) = F(0) = 0$, so

$$\log \left(\frac{N - \bar{R}}{S(0)} \right) + (\bar{R} - R(0)) \sum_{i=1}^n \nu_i \beta_i / (\sigma \gamma) + \sum_{i=1}^n \beta_i W_i(0) / \sigma = 0. \quad (4.17)$$

Next, let $S(0) \rightarrow N$ and $W_i(0) \rightarrow 0$. Note that $I(0) \rightarrow 0$ and $R(0) \rightarrow 0$ whenever $S(0) \rightarrow N$, thus equation (4.17) becomes

$$\log \left(1 - \frac{\bar{R}}{N} \right) + \frac{\bar{R}}{N} \frac{N}{\sigma\gamma} \sum_{i=1}^n \nu_i \beta_i / (\sigma\gamma) = 0. \quad (4.18)$$

Finally, letting $\bar{R}/N = Z$ and noting that $\mathcal{R}_0 = N \sum_{i=1}^n \nu_i \beta_i / (\sigma\gamma)$ when $\mu = 0$, gives the desired result. \square

By assuming $\mu = 0$, it means that there is no recruitment nor birth/death in the population. Biologically, this assumption will lead to the disease outbreaks to die off in time. The case when $\mu \neq 0$ will be part of our future work.

Similarly, the final outbreak size relation

$$Z_s = 1 - \exp(-\mathcal{R}_0^s Z_s) \quad (4.19)$$

also holds for the single water source model (4.8) where Z_s is the final outbreak size of the model. Comparing the two relations, we can see that

$$Z < Z_s. \quad (4.20)$$

This demonstrates that the final outbreak size will also be over estimated when the single water source is considered.

4.3.6 Stability of the endemic equilibrium

The stability at the DFE determines the short-term dynamics of a disease, whereas its long-term dynamics are characterized by the stability at the endemic equilibrium (EE) [52]. Thus, to determine the long-term dynamics of the multiple water sources model, it is necessary to investigate the stability at the EE. When $\mathcal{R}_0 > 1$, a unique EE exists in the model (4.1) and is given by

$$(S^e, I^e, W_1^e, \dots, W_n^e) = (N/\mathcal{R}_0, \mu N(\mathcal{R}_0 - 1)/[(\gamma + \mu)\mathcal{R}_0], \nu_1 I^e/\sigma, \dots, \nu_n I^e/\sigma). \quad (4.21)$$

Also, when $\mathcal{R}_0^s > 1$, a unique EE exists in the single water source model (4.8) and its global stability can be established using the Lyapunov function of the type considered in [84].

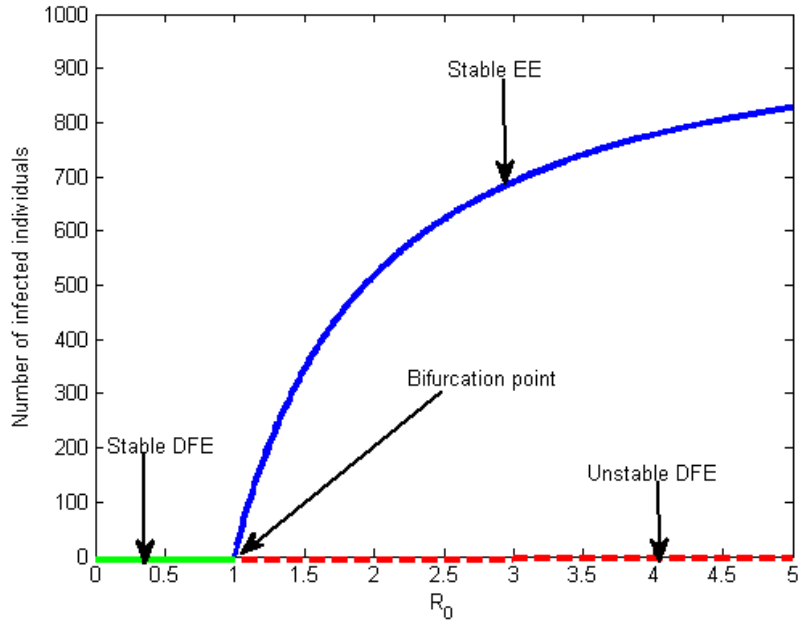


Figure 4.3: The bifurcation diagram of $I(t)$ vs. \mathcal{R}_0 for the DFE and the positive EE.

4.3.7 Bifurcation diagram

We summarize our stability analysis results by sketching a bifurcation diagram of $I(t)$ vs. \mathcal{R}_0 for model (4.1). The diagram is presented in Figure 4.3. The bifurcation diagram illustrates the stability exchange at $\mathcal{R}_0 = 1$ for the two biologically feasible equilibria: the DFE and the positive EE. Note that the biologically non-feasible equilibria are not shown on the diagram [52].

4.4 A case study: the Haiti cholera outbreak

We have seen that multiple water sources have a significant influence on the dynamics of waterborne disease. To demonstrate how realistic the multiple water sources model (4.1) is, we use the model to investigate the recent cholera outbreak in Haiti. According to the Ministry of Public Health and Population (MSPP), the cholera outbreak in Haiti started on October 21, 2010 [63, 60]. By August 4, 2013, 669,396 cases and 8,217 deaths have been reported since the beginning of the outbreak [15]. In this section, we will use our model to fit the data for

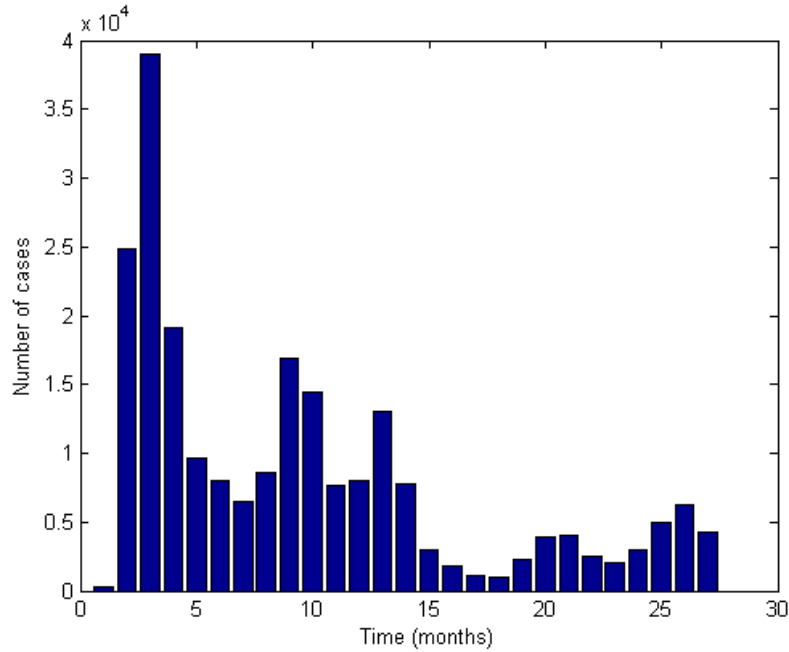


Figure 4.4: Bar chart representing the number of reported hospitalized cholera cases in Haiti from October 30, 2010, to December 24, 2012 [60].

the number of reported hospitalized cholera cases in Haiti from October 30, 2010, to December 24, 2012 [60]. The number of reported hospitalized cholera cases in Haiti for each month from October 30, 2010, to December 24, 2012 is given in Figure 4.4. From the onset of the epidemic in October, 2010, there was a steady increase in the number of cases (at least for the first three months). This was expected as most of the individuals in Haiti have not been previously exposed to the infection, considering that Cholera had not been reported in the country for decades [63].

To obtain reasonable results, we choose the parameter values as follows: We take $n = 2$ and assume that W_1 measures the pathogen concentration of the unimproved water source in the rural area in Haiti and W_2 measures the pathogen concentration of the unimproved water source in the urban area in Haiti. This is because approximately 49% and 90% of Haiti's population in rural areas do not have access to improved drinking water sources and sanitation facilities respectively while, 15% and 76% of Haiti's population living in urban areas also do not have access to improved drinking water sources and sanitation facilities respectively [16]. The

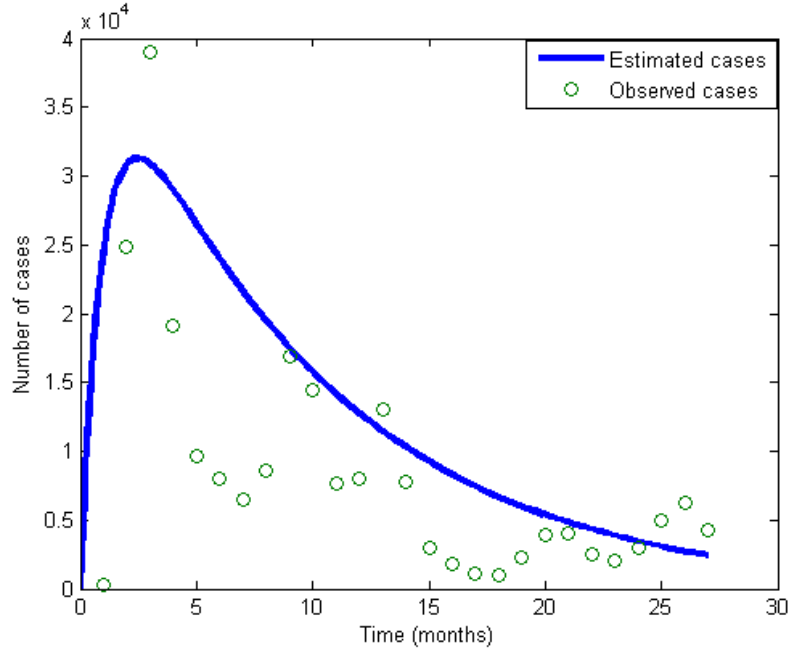


Figure 4.5: Model fitting for the number of reported hospitalized cholera cases in Haiti from October 30, 2010 to December 24, 2012.

population of Haiti is taken from 2009 Haiti population data before the outbreak started [14] while the birth rate is estimated from [16]. The remaining parameter values are chosen from published data and realistic ranges and can be found in Table 4.2. The results of incorporating these parameter values for our model to fit the number of reported hospitalized cholera cases in Haiti from October 30, 2010 to December 24, 2012 is shown in Figure 4.5.

Repeated seasonal outbreak is one of the characteristics of cholera [80]. We can see from Figure 4.5 that, following the initial epidemic wave, the number of reported hospitalized cholera cases seems to be affected by the seasonal variation. To improve the prediction capability of our model, we must take these seasonal variations into consideration. We can do this by substituting the contact rate β_i in our model (4.1) by a sine function:

$$\beta_i(t) = \beta_i (1 + \delta \sin(2\pi t / (365\rho))), \quad (4.22)$$

where β_i is the mean contact rate, δ describes the relative amplitude of seasonal variations and ρ is a scaling factor. The result of considering seasonal variations in our model to fit the number of reported hospitalized cholera cases in Haiti from October 30, 2010 to December 24, 2012 is

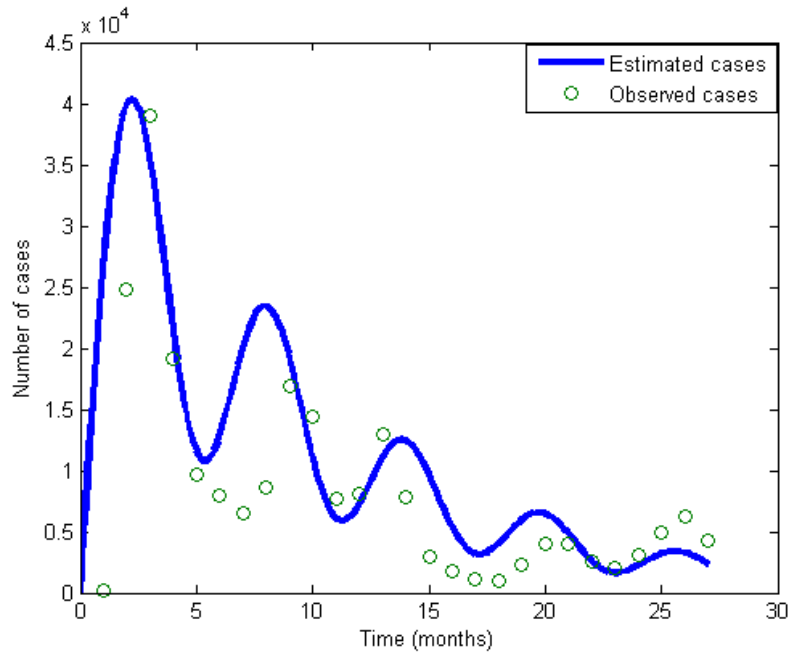


Figure 4.6: Model fitting for the number of reported hospitalized cholera cases in Haiti from October 30, 2010 to December 24, 2012 putting seasonality into consideration.

given in Figure 4.6. Obviously, Figure 4.6 gives a better fit to the data for cholera outbreak in Haiti. This shows that our model can be used as an accurate analytical prediction for cholera dynamics in Haiti. We expect that model (4.1) can also be used to carry out similar studies in other cholera-endemic countries (using different parameter values).

4.5 Vaccination model

We have seen that a waterborne disease model that takes multiple water sources into consideration is an accurate model for investigating the dynamics of the disease and making predictions of future outbreak. We now consider modifying the model to study how to reduce the spread of the disease using vaccination as a control intervention strategy.

In this section, we formulate a vaccination model by extending the multiple water sources model (4.1) to study the effects of vaccination in curtailing the epidemic. According to Brauer [9], vaccination may mean either an inoculation which decreases susceptibility to infection or an

education program such as encouragement of better hygiene practices or social distancing from contaminated water reservoirs. However, it only reaches a fraction of the susceptible population and so is imperfect in nature. For vaccination as a control intervention strategy, we consider the following equations

$$\begin{aligned}
\dot{S}(t) &= \mu N(t) + (1 - u_1)\omega V - S(t) \sum_{i=1}^n \beta_i W_i(t) - (\mu + u_2)S(t), \\
\dot{V}(t) &= u_2 S(t) - (1 - u_1)\omega V - (1 - \varepsilon)V \sum_{i=1}^n \beta_i W_i(t) - \mu V(t), \\
\dot{I}(t) &= S(t) \sum_{i=1}^n \beta_i W_i(t) + (1 - \varepsilon)V \sum_{i=1}^n \beta_i W_i(t) - (\mu + \gamma)I(t), \\
\dot{W}_1(t) &= \nu_1 I(t) - \sigma W_1(t), \\
\dot{W}_2(t) &= \nu_2 I(t) - \sigma W_2(t), \\
&\vdots \\
\dot{W}_n(t) &= \nu_n I(t) - \sigma W_n(t), \\
\dot{R}(t) &= \gamma I(t) - \mu R(t),
\end{aligned} \tag{4.23}$$

where V is vaccinated individuals, ω is rate at which the vaccine wanes and ε is vaccine efficacy. Note that $\varepsilon \in [0, 1]$; if $\varepsilon = 0$, then the vaccine is useless, if $\varepsilon = 1$, the vaccine is 100% effective, and if $0 < \varepsilon < 1$, the vaccine is imperfect or leaky [85, 61]. We use the following control variables: $u_1(t)$ to account for controlling the rate at which vaccine wanes and $u_2(t)$ measures the rate of vaccination [85]. Causes of vaccine waning are associated with: nutritional status, concurrent infection, immune status, seasonal influence, food/water access, age, exposure level, improper storage of vaccine, use of vaccine after expiration, improper dosage, improper timing etc. Therefore, to effectively control vaccine wane, it is necessary and sufficient to control the causes. Proper administration of vaccination so that it reaches all the susceptible individuals at the proper time is also crucial. These are the motivations for introducing controls on vaccine waning and the vaccination rate.

4.5.1 Analysis of the vaccination model

The DFE and the basic reproduction number of the vaccination model (4.23) are given by

$$(S_v^0, V_v^0, I_v^0, W_v^0) = \left(\frac{((1-u_1)\omega + \mu)N}{(1-u_1)\omega + u_2 + \mu}, \frac{u_2N}{(1-u_1)\omega + u_2 + \mu}, 0, \bar{0} \right), \quad (4.24)$$

and

$$\mathcal{R}_0^v = E_0^v \mathcal{R}_0, \quad (4.25)$$

respectively, where

$$E_0^v = \frac{(1-u_1)\omega + \mu + (1-\varepsilon)u_2}{(1-u_1)\omega + \mu + u_2}. \quad (4.26)$$

The threshold quantity \mathcal{R}_0^v represents the number of secondary infections that results from introducing a single infected individual into an otherwise susceptible population in the presence of vaccination [85, 84]. By elementary algebraic calculations, we can easily show that the following equations

$$E_0^v < 1 \iff \mathcal{R}_0^v < \mathcal{R}_0, \quad \forall 0 < u_2, \varepsilon \leq 1, \quad (4.27)$$

$$E_0^v = 1 \iff \mathcal{R}_0^v = \mathcal{R}_0, \quad \text{for } \varepsilon = 0 \text{ or } u_2 = 0, \quad (4.28)$$

hold. From the definition of the basic reproduction number, we deduce that equation (4.27) implies that vaccination decreases the number of secondary infections by a factor E_0^v . Noting that $u_2 = 0$ implies that no individual is vaccinated and $\varepsilon = 0$ means that vaccine is useless [61, 85], then (4.28) implies that vaccination has no effect on or vaccination imparts no immunity to the population. However, from the above discussion, we can see that $\mathcal{R}_0^v \leq \mathcal{R}_0$. This implies that vaccination will always have a positive effect on the number of secondary infections in the community.

We have shown in Theorem 4.3.3 that if $\mathcal{R}_0 < 1$, then disease can be eradicated from the entire population. Since the disease may not develop into an epidemic if $\mathcal{R}_0 < 1$, therefore vaccination may not be necessary to eradicate the disease. However, we should note that introducing vaccination would lead to eradication of the disease faster. To determine the short-term dynamics of waterborne disease in the presence of vaccination, it is necessary to investigate

the stability of the vaccination model at the DFE (4.24). We consider a similar approach used in the proof of Theorem 4.3.3 and conclude as follows:

Theorem 4.5.1. *The DFE (4.24) of the vaccination model is globally asymptotically stable, provided $\mathcal{R}_0^v < 1$. \square*

Epidemiologically, Theorem 4.5.1 implies that waterborne disease can be eradicated from the entire population using vaccination as a control intervention strategy provided that $\mathcal{R}_0^v < 1$. On the other hand, if $\mathcal{R}_0 > 1$, we determine the necessary conditions for slowing down the spread of a waterborne disease outbreak. We show later that each of the control parameters ω, u_1, u_2 and ϕ has some influence in decreasing the vaccination-induced basic reproduction number \mathcal{R}_0^v . Thus, a necessary condition for slowing down the spread of a waterborne disease outbreak is $E_0^v < 1$ which occurs when $0 < \omega, u_1, u_2, \varepsilon < 1$.

Since waterborne disease vaccines have different efficacies [63], it is necessary to determine the optimal vaccine efficacy and vaccination rate for controlling the epidemic. By setting $\mathcal{R}_0^v = 1$ and solving for ε and u_2 , we obtain the threshold proportion for optimal intervention, as

$$\varepsilon^c = \frac{((1 - u_1)\omega + \mu)(\mathcal{R}_0 - 1) + u_2(1 + \mathcal{R}_0)}{u_2\mathcal{R}_0}, \quad u_2^c = \frac{((1 - u_1)\omega + \mu)(\mathcal{R}_0 - 1)}{1 - (1 - \varepsilon)\mathcal{R}_0}. \quad (4.29)$$

The threshold value u_2^c exists if $1 < \mathcal{R}_0 < \frac{1}{1-\varepsilon}$. Hence, vaccination can effectively control the outbreak if $\varepsilon^c < \varepsilon$ or $u_2^c < u_2$ ($\mathcal{R}_0^v < 1$). In contrast, the disease can persist when $\varepsilon^c > \varepsilon$ or $u_2^c > u_2$ ($\mathcal{R}_0^v > 1$).

Suppose that vaccination is not strong enough such that $\mathcal{R}_0^v > 1$, and an outbreak can occur. The outbreak growth rate of the vaccination model (4.23) is given by

$$\lambda_v^+ = \frac{1}{2} \left(-(\gamma + \mu + \sigma) + \sqrt{[(\gamma + \mu - \sigma)^2 + 4\sigma(\gamma + \mu)\mathcal{R}_0^v]} \right). \quad (4.30)$$

Clearly,

$$\lambda_v^+ \leq \lambda^+. \quad (4.31)$$

This shows that vaccination reduces the outbreak growth rate. The above results suggest that vaccination has some influence in reducing the spread of infections provided that $0 <$

$\omega, u_1, u_2, \varepsilon < 1$. Practically, the strength and the success of vaccination would be limited by social, political and economic factors as well as available resources. Therefore, proper management is a necessity to achieve the best result.

4.5.2 Sensitivity analysis

To determine the relative importance of the different factors responsible for disease transmission and prevalence, it is necessary to carry out sensitivity analysis. Sensitivity analysis is used mainly to determine the robustness of model predictions to parameter values [17]. This analysis is crucial since there are usually errors in data collection and assumed parameter values. We utilise it to determine the parameters that have a high impact on the basic reproduction numbers ($\mathcal{R}_0, \mathcal{R}_0^s, \mathcal{R}_0^v$). Such parameters should be the target of control intervention strategies in order to minimize the spread of infections. We determine the sensitivity indices of $\mathcal{R}_0, \mathcal{R}_0^s$ and \mathcal{R}_0^v with respect to the parameters in the model using the normalized forward sensitivity index [17]. These indices demonstrate how important each parameter is to disease transmission and prevalence. For instance, the sensitivity index of \mathcal{R}_0 with respect to β_1 denoted by $\Upsilon_{\beta_1}^{\mathcal{R}_0}$ is given by

$$\Upsilon_{\beta_1}^{\mathcal{R}_0} = \frac{\beta_1}{\mathcal{R}_0} \frac{\partial \mathcal{R}_0}{\partial \beta_1} = \frac{\nu_1 \beta_1}{\nu_1 \beta_1 + \nu_1 \beta_1}. \quad (4.32)$$

Since $\Upsilon_{\beta_1}^{\mathcal{R}_0}$ is parameter dependent, to determine its magnitude we resort to parameter values as shown in Table 4.2.

The parameter values in Table 4.2 are estimated as follows: Since the effective contact rate $\beta = \sum_{i=1}^n \beta_i$, we choose β_i such that β is an approximation of the parameter values in the literature [84]. Similar reasoning also holds for shedding rate since the effective shedding rate $\nu = \sum_{i=1}^n \nu_i$. The remaining parameter values i.e., birth/death rate μ , recovery rate γ , net decay of pathogen in water sources ν , vaccine efficacy ε and wane rate of vaccine ω are taken from published data as shown in Table 4.2.

The sensitivity indices of $\mathcal{R}_0, \mathcal{R}_0^s$ and \mathcal{R}_0^v for the remaining parameters are given in Table 4.1. From the table we notice that the most sensitive parameter to the basic reproduction numbers is the net decay rate of pathogens in water reservoir σ with sensitivity index of -1.000

Table 4.1: Sensitivity index of \mathcal{R}_0 , \mathcal{R}_0^s and \mathcal{R}_0^v

Parameter	\mathcal{R}_0	\mathcal{R}_0^s	\mathcal{R}_0^v
β_1	0.6964	0.6737	0.6737
β_2	0.3036	0.3263	0.3263
ν_1	0.6964	0.5263	0.5263
ν_2	0.3036	0.4737	0.4737
σ	-1.0000	-1.0000	-1.0000
μ	-0.000666	-0.000666	0.0068
γ	-0.9993	-0.9993	-0.9993

followed by recovery rate γ , then partial contact and shedding rates $(\beta_1, \beta_2, \nu_1, \nu_2)$ and finally the birth/death rate μ . This illustrates that decreasing (or increasing) σ by 10% decreases (or increases) the corresponding basic reproduction number by 10%. This also reveals the importance of considering multiple water sources in the dynamics of the disease.

Next, we determine the effects of each of the control parameters u_1, ω, ε and u_2 in reducing the spread of the disease, by computing the sensitivity index of \mathcal{R}_0^v with respect to each of the parameters. The sensitivity index of \mathcal{R}_0^v with respect to the parameters u_1, ω, ε and u_2 denoted by $\Upsilon_{\omega}^{\mathcal{R}_0^v}, \Upsilon_{u_1}^{\mathcal{R}_0^v}, \Upsilon_{\varepsilon}^{\mathcal{R}_0^v}$ and $\Upsilon_{u_2}^{\mathcal{R}_0^v}$ respectively, are given by

$$\Upsilon_{\varepsilon}^{\mathcal{R}_0^v} = \frac{\varepsilon}{\mathcal{R}_0^v} \frac{\partial \mathcal{R}_0^v}{\partial \varepsilon} = \frac{-u_2 \varepsilon}{((1-u_1)\omega + \mu + u_2)E_0^v} < 0, \quad (4.33)$$

$$\Upsilon_{\omega}^{\mathcal{R}_0^v} = \frac{\omega}{\mathcal{R}_0^v} \frac{\partial \mathcal{R}_0^v}{\partial \omega} = \frac{(1-u_1)\omega}{((1-u_1)\omega + \mu + u_2)} \Upsilon_{\varepsilon}^{\mathcal{R}_0^v} > 0, \quad (4.34)$$

$$\Upsilon_{u_1}^{\mathcal{R}_0^v} = \frac{u_1}{\mathcal{R}_0^v} \frac{\partial \mathcal{R}_0^v}{\partial u_1} = \frac{-\omega u_1}{((1-u_1)\omega + \mu + u_2)} \Upsilon_{\varepsilon}^{\mathcal{R}_0^v} < 0, \quad (4.35)$$

$$\Upsilon_{u_2}^{\mathcal{R}_0^v} = \frac{u_2}{\mathcal{R}_0^v} \frac{\partial \mathcal{R}_0^v}{\partial u_2} = \frac{-((1-u_1)\omega + \mu)}{((1-u_1)\omega + \mu + u_2)} \Upsilon_{\varepsilon}^{\mathcal{R}_0^v} < 0. \quad (4.36)$$

From the above equations, we discover that the magnitude of $\Upsilon_{\varepsilon}^{\mathcal{R}_0^v}$ is greater than the magnitude of each of $\Upsilon_{\omega}^{\mathcal{R}_0^v}, \Upsilon_{u_1}^{\mathcal{R}_0^v}$ and $\Upsilon_{u_2}^{\mathcal{R}_0^v}$ irrespective of the parameter values. Therefore, vaccine efficacy is the most sensitive control parameter. This shows that vaccine efficacy has the greatest impact in reducing the spread of the infections, thus it must be taken into consideration while

Table 4.2: Parameter values for numerical simulations with reference

Parameter	Symbol	Value	Reference
Contact rate with W_1	β_1	0.002172 day ⁻¹	assumed
Contact rate with W_2	β_2	0.001052 day ⁻¹	assumed
Shedding rate into W_1	ν_1	0.015 cells ml ⁻³ day ⁻¹	assumed
Shedding rate into W_2	ν_2	0.0135 cells ml ⁻³ day ⁻¹	assumed
Birth/death rate	μ	0.0001 day ⁻¹	[19]
Recovery rate of I	γ	0.015 day ⁻¹	[38]
Net decay rate of pathogen in water	σ	0.333 day ⁻¹	[19]
Efficacy of vaccine	ε	0.85	[65]
Wane rate of vaccine	ω	0.0019 day ⁻¹	[55, 42]

defining control intervention strategy for maximum result. To determine the magnitude of the sensitivity index, we also use the parameter values in Table 4.2 to obtain

$$\Upsilon_{\omega}^{\mathcal{R}_0^v} = 0.7882, \quad \Upsilon_{u_1}^{\mathcal{R}_0^v} = -0.1436, \quad \Upsilon_{\varepsilon}^{\mathcal{R}_0^v} = -5.2970, \quad \Upsilon_{u_2}^{\mathcal{R}_0^v} = -0.0549. \quad (4.37)$$

Equation (4.37) reveals that ε is the most sensitive parameter followed by ω then u_1 and u_2 . Since $\mathcal{R}_0^v = E_0^v \mathcal{R}_0$ and the parameters u_1, ω, ε and u_2 are independent of \mathcal{R}_0 , we can demonstrate that

$$\Upsilon_{\omega}^{\mathcal{R}_0^v} = \Upsilon_{\omega}^{E_0^v}, \quad \Upsilon_{u_1}^{\mathcal{R}_0^v} = \Upsilon_{u_1}^{E_0^v}, \quad \Upsilon_{\varepsilon}^{\mathcal{R}_0^v} = \Upsilon_{\varepsilon}^{E_0^v}, \quad \Upsilon_{u_2}^{\mathcal{R}_0^v} = \Upsilon_{u_2}^{E_0^v}, \quad (4.38)$$

for parameters $0 \leq u_1, u_2, \varepsilon, \omega, \leq 1$ where $\Upsilon_{\omega}^{E_0^v}, \Upsilon_{u_1}^{E_0^v}, \Upsilon_{\varepsilon}^{E_0^v}$ and $\Upsilon_{u_2}^{E_0^v}$ denote the sensitivity index of E_0^v with respect to the parameters ω, u_1, ε and u_2 respectively. For example, the sensitivity index of \mathcal{R}_0^v with respect to ω is given by

$$\Upsilon_{\omega}^{\mathcal{R}_0^v} = \frac{\omega}{\mathcal{R}_0^v} \frac{\partial \mathcal{R}_0^v}{\partial \omega} = \frac{\omega}{\mathcal{R}_0 E_0^v} \frac{\mathcal{R}_0 \partial E_0^v}{\partial \omega} = \frac{\omega}{E_0^v} \frac{\partial E_0^v}{\partial \omega} = \Upsilon_{\omega}^{E_0^v}. \quad (4.39)$$

Similarly, we can show that $\Upsilon_{u_1}^{\mathcal{R}_0^v} = \Upsilon_{u_1}^{E_0^v}$, $\Upsilon_{\varepsilon}^{\mathcal{R}_0^v} = \Upsilon_{\varepsilon}^{E_0^v}$ and $\Upsilon_{u_2}^{\mathcal{R}_0^v} = \Upsilon_{u_2}^{E_0^v}$. This testifies that the efficacy of the control parameters can also be determined by calculating the sensitivity index E_0^v with respect to the control parameters.

4.5.3 Optimal control problem

We have seen that it is possible to reduce the spread of waterborne disease using vaccination for a community where individuals are exposed to multiple contaminated water sources. Here, we formulate an optimal control problem subject to the vaccination model (4.23) in order to determine appropriate vaccination that will reduce the epidemic with minimum cost for such communities. Some waterborne diseases such as cholera have vaccines that can offer 85–90 % protection for a period of six months [65]. Even though such high quality vaccines are available, affordability remains the greatest challenge to most communities where the disease is endemic. Since the vaccine can guarantee protection for only six months, it means that after six months the vaccinated individuals become susceptible to the disease. Therefore controlling the rate at which the vaccine wanes becomes necessary, but it also requires money. The cost of effective vaccination also includes funds needed for hiring qualified health workers, transportations, public awareness and fund for other logistics. As a result, there is need for vaccination that will reduce the spread of waterborne disease with minimum cost. Optimal control theory can help us obtain such an appropriate vaccination that can give protection for quite a reasonable longer duration with a minimum cost.

The optimal control problem is to minimize the cost functional

$$J(u_1, u_2) = \int_0^{t_f} [A_1 I(t) + B_1 S(t) + C_1 u_1^2(t) + C_2 u_2^2(t)] dt \quad (4.40)$$

subject to the vaccination model (4.23), where the coefficients, A_1, B_1, C_1, C_2 , are balancing cost factors that transform the integral into money expended over a finite time t_f . This performance specification involves minimizing the number of susceptible and infected individuals, as well as the costs for implementing the controls. We consider non-linear quadratic expressions for measuring the control cost. Similar approaches for measuring control cost can also be found in [100, 2, 59, 85]. The existence of an optimal control pair (u_1^*, u_2^*) such that

$$J(u_1^*(t), u_2^*(t)) = \min \{J(u_1(t), u_2(t)) : (u_1(t), u_2(t)) \in U\}, \quad (4.41)$$

where $U = \{(u_1(t), u_2(t)) : (u_1(t), u_2(t)) \text{ are measurable, } 0 \leq (u_1(t), u_2(t)) \leq 1, t \in [0, t_f]\}$, is the control set follows from [32, 56]. The Pontryagin's Maximum Principle [71] gives the necessary conditions that an optimal control must satisfy. This principle converts (4.40) into

a problem of pointwise minimizing a Hamiltonian H , with respect to $u_1(t)$ and $u_2(t)$. The Hamiltonian obtained from the objective functional (4.40) and the governing dynamics of the vaccination model (4.23) is given by

$$\begin{aligned}
H = & A_1 I(t) + B_1 S(t) + C_1 u_1^2 + C_2 u_2^2 \\
& + \lambda_S \left(\mu N(t) + (1 - u_1) \omega V - S(t) \sum_{i=1}^n \beta_i W_i(t) - (\mu + u_2) S(t) \right) \\
& + \lambda_V \left(u_2 S(t) - (1 - u_1) \omega V - (1 - \varepsilon) V \sum_{i=1}^n \beta_i W_i(t) - \mu V(t) \right) \\
& + \lambda_I \left(S(t) \sum_{i=1}^n \beta_i W_i(t) + (1 - \varepsilon) V \sum_{i=1}^n \beta_i W_i(t) - (\mu + \gamma) I(t) \right) \\
& + \sum_{i=1}^n [\lambda_{W_i} (\nu_i I(t) - \sigma W_i(t))] + \lambda_R (\gamma I(t) - \mu R(t)),
\end{aligned} \tag{4.42}$$

where $\lambda_S, \lambda_V, \lambda_I, \lambda_{W_1}, \lambda_{W_2}, \dots, \lambda_{W_n}$ and λ_R are the associated adjoints for the states $S, V, I, W_1, W_2, \dots, W_n$ and R respectively.

Given the optimal control pair $(u_1^*(t), u_2^*(t))$ and solutions S^*, V^*, I^*, W^* and R^* of the corresponding state system (4.23) that minimizes $J(u_1, u_2)$ over U , there exists adjoint variables $\lambda_S, \lambda_V, \lambda_I, \lambda_{W_1}, \lambda_{W_2}, \dots, \lambda_{W_n}$ and λ_R satisfying

$$\begin{aligned}
\frac{d\lambda_S}{dt} &= -B_1 + \lambda_S \left[\sum_{i=1}^n \beta_i W_i + (\mu + u_2) \right] - \lambda_V u_2 - \lambda_I \sum_{i=1}^n \beta_i W_i, \\
\frac{d\lambda_V}{dt} &= -\lambda_S (1 - u_1) \omega + \lambda_V \left[(1 - u_1) \omega + (1 - \varepsilon) \sum_{i=1}^n \beta_i W_i + \mu \right] - \lambda_I (1 - \varepsilon) \sum_{i=1}^n \beta_i W_i, \\
\frac{d\lambda_I}{dt} &= -A_1 + \lambda_I (\mu + \gamma) - \sum_{i=1}^n \lambda_{W_i} \nu_i - \lambda_R \gamma, \\
\frac{d\lambda_{W_1}}{dt} &= \lambda_S S \beta_1 + \lambda_V (1 - \varepsilon) V \beta_1 - \lambda_I [S \beta_1 + (1 - \varepsilon) V \beta_1] + \lambda_{W_1} \sigma, \\
\frac{d\lambda_{W_2}}{dt} &= \lambda_S S \beta_2 + \lambda_V (1 - \varepsilon) V \beta_2 - \lambda_I [S \beta_2 + (1 - \varepsilon) V \beta_2] + \lambda_{W_2} \sigma, \\
&\vdots \\
\frac{d\lambda_{W_n}}{dt} &= \lambda_S S \beta_n + \lambda_V (1 - \varepsilon) V \beta_n - \lambda_I [S \beta_n + (1 - \varepsilon) V \beta_n] + \lambda_{W_n} \sigma, \\
\frac{d\lambda_R}{dt} &= -\lambda_R \mu.
\end{aligned}$$

together with transversality conditions

$$\lambda_k(t_f) = 0, \quad \text{where } k = S, V, I, W_1, W_2, \dots, W_n \text{ and } R. \quad (4.43)$$

These differential equations governing the adjoint variables were obtained by differentiating the Hamiltonian function (4.42) with respect to the corresponding states as follows:

$$-\frac{d\lambda_k}{dt} = \frac{dH}{dk}.$$

We now consider the optimality conditions

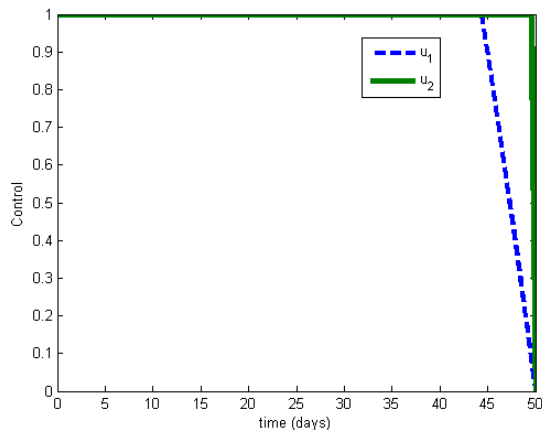
$$0 = \frac{\partial H}{\partial u_1} \quad \text{and} \quad 0 = \frac{\partial H}{\partial u_2}. \quad (4.44)$$

By solving for u_1 and u_2 in (4.44) and subsequently applying standard control arguments and bounds on the controls, we obtain

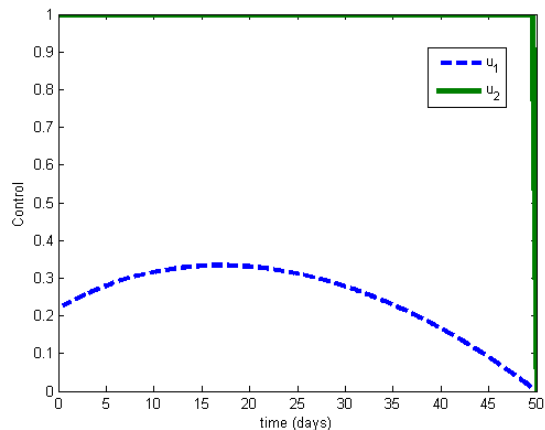
$$u_1^* = \min \{1, \omega V(\lambda_S - \lambda_V)/(2C_1)\}, \quad u_2^* = \min \{1, S(\lambda_S - \lambda_V)/(2C_2)\}. \quad (4.45)$$

The above results show that there exist optimal control functions u_1^* and u_2^* that minimize the spread of waterborne disease using vaccination with minimum cost. To understand the behaviour of u_1^* and u_2^* , we carry out numerical simulations of the optimality system.

The numerical results of the optimality system are obtained for different values of ω , while keeping the other parameters fixed in each of the simulations. The values of the cost factors: $A_1 = 6.00$, $B_1 = 6.00$, $C_1 = 10.00$, $C_2 = 10.00$ are taken from [49] while the remaining parameter values with references can be found in Table 4.2. The numerical results are obtained for two water sources i.e., $n = 2$. Numerical solutions of the optimal system which are made up of the state equations and adjoint equations are carried out using MatLab [86]. The algorithm is the forward-backward scheme described in [49, 59]. We obtain the two optimal control functions u_1^* and u_2^* that minimize the cost functional subject to the state equations as shown in Figures 4.7(a) and 4.7(b). To reduce the spread of infections with minimum cost, the results of our simulations in the Figures indicate the following: Firstly, the results suggest 100% vaccination rate (i.e., everybody to be vaccinated) from the onset of the outbreak irrespective of the wane rate ω . Since vaccination is a preventive control measure, the idea of vaccinating every individuals from the onset of the outbreak is reasonable and agrees with intuitive expectation.



(a) Plot of $u_1(t)$ and $u_2(t)$ vs t for $\omega = 0.03$.



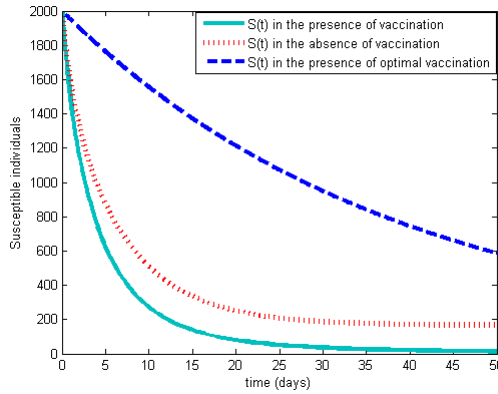
(b) Plot of $u_1(t)$ and $u_2(t)$ vs t for $\omega = 0.003$.

Figure 4.7: Graphical representation of the control functions $u_1(t)$ and $u_2(t)$ for two different values of vaccine wane rate ω .

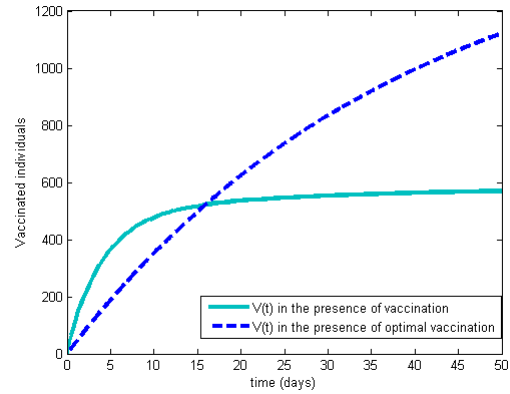
Secondly, Figure 4.7(a) suggests 100% control of vaccine wane from the onset of the outbreak when $\omega = 0.03$. On the other hand, when $\omega = 0.003$ [65] Figure 4.7(b) suggests at most 30% control over wane rate throughout the period of the outbreak. This means that more resources will be channelled toward controlling the vaccine wane rate as it is very big, but if the vaccine wane rate is very small, then less resources will be directed to control it. This suggestion is also reasonable and agrees with intuitive expectation.

We investigate the effects of this optimal vaccination on the $S(t)$, $V(t)$ and $I(t)$. By solving our models numerically, we were able to determine the impact of vaccination as well as optimal vaccination. From Figures 4.8(a) and 4.8(b), we observe that the number of susceptible and infected individuals in the absence of vaccination is always greater the number of susceptible and infected individuals in the presence of vaccination. This agrees with intuitive expectation since vaccination tends to reduce the number of susceptible individuals and hence leading to decrease in the number of infected individuals. However, we notice from Figure 4.8(a) that the number of susceptible individuals in the presence of optimal vaccination is greater than the number of susceptible individuals in the presence or absence vaccination at least for the first 50 days. This seems to be unusual, but we should realize that optimal vaccination is not necessarily the best vaccination but rather a good vaccination with minimum cost of implementation. Furthermore,

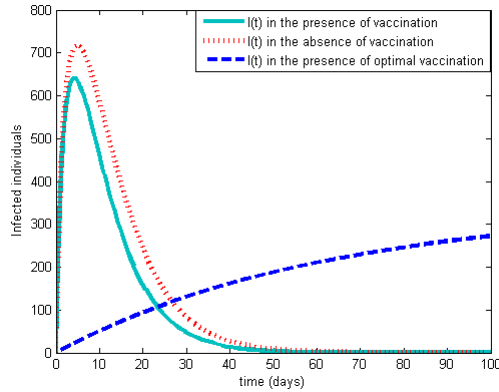
in Figure 4.8(c), we observe that the number of infected individuals in the presence or absence vaccination grow very fast for the first 5 days and then drop very fast as well while the number of infected individuals in the presence of optimal vaccination grows very slowly. This fast increase and decrease of the number of infected individuals in the presence or absence vaccination is regarded as the first epidemic wave. This is always the case whenever a waterborne disease outbreak occurs in an unprepared community. The first epidemic wave normally lead to many deaths/infections but after it, the number of deaths/infections will decrease as the remaining individual will start a healthy life style like purifying water before drinking, staying away from contaminated water sources and so on. This explain why the number of infected and susceptible individuals in the presence or absence vaccination decreases faster than the number of infected and susceptible individuals in the presence of optimal vaccination. Since we are optimizing the vaccination rate and control over vaccine wane rate, Figure 4.8(b) demonstrates that after the first 15 days of the outbreak, vaccinated individuals in the presence of optimal vaccination grows faster and becomes greater than the vaccinated individuals in the presence of vaccination only. From Figure 4.8(c) we also notice that the maximum number of infected individuals in the presence of optimal vaccination is less than the maximum number infected individuals in the presence or absence of vaccination at least for the period of the outbreak. This confirms the result in [20] that optimal control intervention tends to keep the number of infected individuals low to a certain level throughout the duration of the outbreak. As a result, one can better manage the outbreak in the presence of optimal vaccination. In other words, the health system will not suffer a shock as in the case of no vaccination or vaccination only.



(a) Plot of $S(t)$ vs. time.



(b) Plot of $V(t)$ vs. time.



(c) Plot of $I(t)$ vs. time.

Figure 4.8: Graphical representation of $S(t)$, $V(t)$ and $I(t)$ against time (t) in the presence or absence of vaccination or optimal vaccination.

4.6 Discussion

We formulated a mathematical epidemiological model for waterborne disease for a community where individuals are exposed to multiple contaminated water sources and showed that it is possible to control the spread of waterborne disease using vaccination with minimum cost. We considered the waterborne disease model (4.1) with multiple contaminated water sources and qualitatively determined some of its essential mathematical epidemiological features such as: the basic reproduction number \mathcal{R}_0 , the outbreak growth rate, stability of the DFE and EE. By analysing these mathematical features and comparing them with that of the single water source

model, we discovered some interesting relationships between the two models. For example, the basic reproduction number \mathcal{R}_0 , outbreak growth rate λ^+ and final outbreak size Z of the multiple water sources model were shown to be always less than that of the single water source model. Since the multiple water sources are more realistic, epidemiologically, this implies that these important features of the model will be under estimated, thus leading to poor prediction of an outbreak if the single water source model is considered for a community where there is more than one water source. These analyses also revealed that it is possible to extend some results of the single water source model to the multiple water source model. Furthermore, we discovered that it is possible for the disease to be eradicated from such community whenever $\mathcal{R}_0 < 1$ by proving that the disease free equilibrium of the multiple contaminated water source model (4.1) is globally asymptotic stable whenever $\mathcal{R}_0 < 1$. On the other hand, if $\mathcal{R}_0 > 1$, we determined a unique endemic equilibrium for the model and investigated its global asymptotically stability by constructing a suitable Lypunov function. We summarized the stability results of the model (4.1) with a bifurcation diagram that illustrates the stability exchange at $\mathcal{R}_0 = 1$.

Next, we verified how realistic our results are by using the multiple water source model (4.1) to investigate the recent cholera outbreak in Haiti. We fitted the model to the number of reported hospitalized cholera cases in Haiti from October 30, 2010 to December 24, 2012. Our analysis revealed that the analytical results are consistent with the cholera dynamics in Haiti. Thus, the multiple water source model (4.1) is applicable to the Haiti cholera outbreak. It can therefore be considered to provide insight into the future evolution of cholera dynamics in Haiti.

The analysis and results obtained from the multiple water source model (4.1) also enable us to study a control intervention strategy for waterborne disease. As a simple illustration, we considered the use of vaccination to control the disease by extending model (4.1). The vaccination-induced basic reproduction number \mathcal{R}_0^v was obtained. We discovered that the disease can be eradicated using vaccination if $\mathcal{R}_0^v < 1$. By proving that $\mathcal{R}_0^v < \mathcal{R}_0$, we discovered that vaccination reduces the number of secondary infections by a factor E_0^v . The quantity E_0^v is regarded as a measure of effectiveness of vaccination. We also discovered that the sensitivity indices of \mathcal{R}_0^v and E_0^v with respect to the control parameters ω, u_1, ε and u_2 are equal, suggesting that each of the parameters has the same effects on \mathcal{R}_0^v and E_0^v . Furthermore, we

discovered that each of the control parameters have some impact in decreasing the number of secondary infections. Further analysis revealed that vaccine efficacy ε is the most sensitive control parameter irrespective of parameter values. Through these analyses, we conclude that vaccination has influence in reducing the spread of waterborne disease in a community where individuals are exposed to multiple contaminated water sources such that an outbreak will not occur. Note that other types of control intervention strategies such as treatment of infected individuals, sanitation, sewage treatment, and provision of clean water/water sanitation, can be also incorporated into the model and similar analyses can be performed. Such information would provide useful guidelines for the public health administrations to effectively design better control intervention strategies.

Finally, we considered the cost of administering effective vaccination in such communities by constructing a suitable optimal control functional subject to the vaccination model. We determined the optimal control functions u_1^* and u_2^* that control the spread of waterborne disease in the community with minimum cost. The numerical illustration of the optimal control functions reveals that infection can be reduced with minimum cost through effective vaccination given at the onset of the outbreak.

This study explored the dynamics of waterborne disease in a community where individuals are exposed to multiple contaminated water sources as well as predicting some strategies to reduce the spread of the disease using vaccination with minimum cost. It is important to know that it still has some limitations. First, we assumed that the total human population is constant (i.e., the natural birth and death rates are always equal). This is not always true in the real world, especially when the outbreak lasted for a long period of time. Thus, considering a variable population will certainly affect our results especially the long-term dynamics of the disease. Moreover, we will expect to have a higher number of susceptible and infected individuals since waterborne disease affect mostly children, unlike when a constant population is considered. Next, as we mentioned earlier, vaccination is not the only control intervention strategy, so we may also consider some other control intervention strategies like treatment, provision of clean water, public health campaigns, quarantine etc. Finally, we note that one of the methods of controlling the rate at which a vaccine wanes is by considering pulse vaccination,

i.e., the repeated application of a vaccine over a defined age range [1, 82, 68]. As this has been successfully used to eliminate infections such as measles and polio, it can also be considered for waterborne diseases. All these are the subjects of future work.

Chapter 5

Heterogeneity and control intervention strategies of an n -patch waterborne disease model

We formulate an n -patch model that captures the essential dynamics of waterborne disease transmission in a meta-population setting to study the effects of heterogeneity on the spread of the disease. The effects of heterogeneity on some important mathematical features of the model such as the basic reproduction number, type reproduction number and final outbreak size are analysed accordingly. We conduct a real-world application of this model by using it to investigate the recent cholera outbreak in Haiti. The model is extended by introducing control intervention strategies such as vaccination, treatment and water purification, and analysed to determine the possible benefits of these intervention strategies. The contents of this Chapter have been submitted for publication [23].

5.1 Introduction

Waterborne diseases can be transmitted via person-water-person contact. This means that an infected individual will first shed pathogens into the water source and susceptible individuals can then contract the disease when they come in contact with the water source. In reality,

the transmission rate and shedding rate vary from one individual to another, hence leading to heterogeneity in transmission of waterborne diseases. Even though, in some of the theoretical studies on the dynamics and control intervention strategies [12, 72, 19, 29, 33, 36, 42, 84, 65, 52, 62, 64, 101] this is not taken into account, heterogeneity is crucial to understand the dynamics of the waterborne disease and how best to reduce the spread of the infection. Since most of the factors affecting the spread of waterborne diseases vary within and across a population, it is expected that most of the important mathematical features of waterborne disease models such as the basic reproduction number, the type reproduction number and the final outbreak size will also vary. Understanding the behaviour of each of these mathematical features is very important in defining better control intervention strategies that will reduce the spread of the disease. It is our interest in this study to explore the effects of heterogeneity on each of the mathematical feature of waterborne disease model and consequently define better control strategies that will reduce the spread of the disease.

To the best of our knowledge, the heterogeneity and control of waterborne disease for a meta-population have not yet been explored. A meta-population approach is one of the methods of considering heterogeneity to study the dynamics of waterborne diseases [76]. We consider this approach to study the dynamics of waterborne disease for a meta-population setting where individuals are exposed to multiple contaminated water sources. The remaining part of this chapter is organized as follows: The model we are going to discuss is formulated in Section 5.2 and its qualitative analyses is carried out in Section 5.3. In Section 5.4, we apply our model to investigate the recent cholera outbreak in Haiti. Analyses of the multiple control model which we obtain by introducing three controls simultaneously are presented in Section 5.5. The effects of each of the control intervention strategy are investigated in Section 5.6. We conclude the chapter by discussing our results in Section 5.7.

5.2 Model formulation

Consider a community where all the individuals are exposed to multiple contaminated water sources. Despite the fact that all the individuals are exposed to contaminated water sources,

studies have shown that some groups of individuals (especially children) are more vulnerable to infection. Some of the reasons for these differences might be due to hygienic practices of the individuals (like boiling water before drinking, washing hands after going to the toilet, proper washing of dishes and food before eating) and the level of the immune system of the individuals. Understanding the dynamics of waterborne diseases for such a community is complicated as homogeneous models cannot explain such situations. As a result, we resort to a multi-group model where individuals with the same activity level (hygiene practices, immune systems, etc.,) form a group or a patch.

To formulate the model, we consider a total human population N where individuals are exposed to m multiple water sources. We partition the population into n distinct subpopulations or patches based on the activity level. These populations are combined to form a meta-population model in which secondary infections are generated both within a given patch and between patches. The secondary infections within a patch occur when an individual from a patch sheds pathogens into water sources with which susceptible individuals from the same patch subsequently come into contact. However, if the susceptible individuals that come in contact with the pathogens shed from an individual are from different patches, we say that secondary infections between patches have occurred.

We partition N , the total human population of a community at risk for waterborne disease infections, into n patches or homogeneous sub-populations of size N_j such that each patch is made up of susceptible $S_j(t)$, infected $I_j(t)$ and recovered $R_j(t)$, individuals. The compartment W_k measures pathogen concentration in water reservoir k . In this study, we assume that there is no person to person transmission and only consider transmission through contact with contaminated water, as it is often considered to be the main driver of waterborne disease outbreaks [64, 80]. Susceptible individuals $S_j(t)$ become infected through contact with the contaminated water sources W_k at rate β_{jk} . Infected individuals $I_j(t)$ can contaminate the water sources by shedding pathogen into them at rate ν_{jk} and recover naturally at rate γ_j . Pathogens in the contaminated water source k grow naturally at rate α_k and decay at rate ξ_k . We assume that $\sigma_k = -(\alpha_k - \xi_k) < 0$ is the net decay rate of pathogens in the k^{th} water reservoir. Natural death occurs in all the patches at rate μ . Note that $j = 1, 2, \dots, n$ and

$k = 1, 2, \dots, m$. Putting these assumptions together, we obtain the model

$$\begin{aligned}
\dot{S}_1(t) &= \mu N_1(t) - S_1(t) \sum_{k=1}^m \beta_{1k} W_k(t) - \mu S_1(t), \\
\dot{I}_1(t) &= S_1(t) \sum_{k=1}^m \beta_{1k} W_k(t) - (\mu + \gamma_1) I_1(t), \\
\dot{R}_1(t) &= \gamma_1 I_1(t) - \mu R_1(t). \\
\\
\dot{S}_2(t) &= \mu N_2(t) - S_2(t) \sum_{k=1}^m \beta_{2k} W_k(t) - \mu S_2(t), \\
\dot{I}_2(t) &= S_2(t) \sum_{k=1}^m \beta_{2k} W_k(t) - (\mu + \gamma_1) I_2(t), \\
\dot{R}_2(t) &= \gamma_2 I_2(t) - \mu R_2(t). \\
\\
\dot{\vdots} &= \dot{\vdots} \\
\dot{S}_n(t) &= \mu N_n(t) - S_n(t) \sum_{k=1}^m \beta_{nk} W_k(t) - \mu S_n(t), \\
\dot{I}_n(t) &= S_n(t) \sum_{k=1}^m \beta_{nk} W_k(t) - (\mu + \gamma_n) I_n(t), \\
\dot{R}_n(t) &= \gamma_n I_n(t) - \mu R_n(t).
\end{aligned} \tag{5.1}$$

$$\begin{aligned}
\dot{W}_1(t) &= \sum_{j=1}^n \nu_{j1} I_j(t) - \sigma_1 W_1(t), \\
\dot{W}_2(t) &= \sum_{j=1}^n \nu_{j2} I_j(t) - \sigma_2 W_2(t), \\
\dot{\vdots} &= \dot{\vdots} \\
\dot{W}_m(t) &= \sum_{j=1}^n \nu_{jm} I_j(t) - \sigma_m W_m(t),
\end{aligned}$$

The model (5.1) can be written in compact form as

$$\begin{aligned}
\dot{S}_j(t) &= \mu N_j(t) - S_j(t) \sum_{k=1}^m b_{jk} W_k(t) - \mu S_j(t), \\
\dot{I}_j(t) &= S_j(t) \sum_{k=1}^m b_{jk} W_k(t) - (\mu + \gamma_j) I_j(t), \\
\dot{W}_k(t) &= \sum_{j=1}^n \theta_{jk} I_j(t) - \sigma_k W_k(t), \\
\dot{R}_j(t) &= \gamma_j I_j(t) - \mu R_j(t).
\end{aligned} \tag{5.2}$$

Variables and parameters of the model (5.2) with their meaning are given in Table 5.1. The force of infection in patch j is given by the linear term $\sum_{k=1}^m b_{jk} W_k$ [34, 54]. Note that model (5.2) is an extension of the model considered by Collins and Govinder [22] to study the dynamics of waterborne disease with multiple water sources.

A dimensionless version of model (5.2) is given by

$$\begin{aligned}
\dot{s}_j &= \mu - s_j \sum_{k=1}^m \beta_{jk} w_k - \mu s_j, \\
\dot{i}_j &= s_j \sum_{k=1}^m \beta_{jk} w_k - (\mu + \gamma_j) i_j, \\
\dot{w}_k &= \sigma_k \left(\sum_{j=1}^n \nu_{jk} i_j - w_k \right), \\
\dot{r}_j &= \gamma_j i_j - \mu r_j,
\end{aligned} \tag{5.3}$$

where $s_j = S_j/N_j$, $i_j = I_j/N_j$, $r_j = R_j/N_j$, $w_k = \sigma_k W_k / \sum_{j=1}^n \theta_{jk} N_j$, $\beta_{jk} = b_{jk} \sum_{p=1}^n \theta_{pk} N_p / \sigma_k$, $\nu_{jk} = \theta_{jk} N_j / \sum_{p=1}^n \theta_{pk} N_p$. Note that $\sum_{j=1}^n \nu_{jk} = 1$. Thus the parameter ν_{jk} can be interpreted as the proportion of total shedding from I_j into W_k while β_{jk} is the scaled contact rate of S_j with the water source W_k . Note that $\beta_j = \sum_{k=1}^m \beta_{jk}$ is the scaled effective contact rate of S_j with all the water sources and $\nu_j = \sum_{k=1}^m \nu_{jk}$ is the scaled effective proportion of total shedding from I_j into all the water sources.

Table 5.1: Variables and parameters for model (5.3)

Variables	Meaning
$N(t)$	total human population
$S_j(t)$	susceptible individuals in patch j
$I_j(t)$	infected individuals in patch j
$R_j(t)$	recovered individuals in patch j
$W_k(t)$	measure of pathogen concentration in water reservoir k
b_{jk}	partial contact rate of $S_j(t)$ with $W_k(t)$
b_j	effective contact rate of $S_j(t)$ with all the water sources
θ_{jk}	partial shedding rate of $I_j(t)$ into $W_k(t)$
θ_j	effective shedding rate of $I_j(t)$ into all the water sources
γ_j	recovery rate of I_j
σ_k	net decay rate of pathogen in water source k
μ	natural death rate of individuals

5.3 Model analysis

In this section, we carry out a qualitative analysis of model (5.3). The initial conditions are assumed as follows:

$$s_j(0) > 0, \quad i_j(0) \geq 0, \quad w_k(0) \geq 0, \quad r_j(0) \geq 0. \quad (5.4)$$

It is straightforward to show that all solutions $(\bar{s}, \bar{i}, \bar{w}, \bar{r})$ of model (5.3) are positive and bounded for all $t > 0$, where $\bar{s} = (s_1(t), s_2(t), \dots, s_n(t))$, $\bar{i} = (i_1(t), i_2(t), \dots, i_n(t))$, $\bar{w} = (w_1(t), w_2(t), \dots, w_m(t))$ and $\bar{r} = (r_1(t), r_2(t), \dots, r_n(t))$. Thus, the feasible region of model (5.3) is given by

$$\Omega = \Omega_H^n \times \Omega_P^m \subset \mathbb{R}_+^{n \times n} \times \mathbb{R}_+^m, \quad (5.5)$$

where

$$\Omega_P^m = \{ \bar{w} \in \mathbb{R}_+^m \quad : \quad 0 \leq w_k \leq 1 \},$$

and

$$\Omega_H^n = \{ (\bar{s}, \bar{i}, \bar{r}) \in \mathbb{R}_+^{3n} \quad : \quad s_j + i_j + r_j = 1 \},$$

are the feasible region of the pathogen and human components respectively of model (5.3). The feasible region Ω is positively-invariant under the flow induced by (5.3), thus it is sufficient to study the dynamics of (5.3) in Ω . Note that the superscript m is use to emphasis on the number of water sources and n is the number of patches. In order to understand the dynamics of model (5.3), we start with a qualitative analysis of the model with special case $n = 2$.

5.3.1 Quantifying heterogeneity

Here, we investigate the heterogeneity in the transmission dynamics of the model (5.3). Since secondary infections are generated in two different ways: within each patch and between the patches, it is expected that heterogeneity could also arise in the same manner.

Heterogeneity within each patch only

Heterogeneity in disease transmission can be measured as the variance in transmission rates or contact rates among patches [76]. For heterogeneity within patch 1, we propose the following measure of heterogeneity:

$$H_1 = \left(\sum_{j=1}^m w_j (\nu_{1j} - \bar{\nu}_1)^2 + \sum_{j=1}^m w_j (\beta_{1j} - \bar{\beta}_1)^2 \right) / \sum_{j=1}^m w_j,$$

where $\bar{\nu}_1 = \sum_{j=1}^m w_j \nu_{1j} / \sum_{j=1}^m w_j$ and $\bar{\beta}_1 = \sum_{j=1}^m w_j \beta_{1j} / \sum_{j=1}^m w_j$. By considering the following transformation

$$w'_k = w_k / \sum_{j=1}^m w_j, \quad k = 1, 2, \dots, m, \quad (5.6)$$

the measure of heterogeneity H_1 can be normalized to

$$H_1 = \sum_{j=1}^m w'_j (\nu_{1j} - \bar{\nu}_1)^2 + \sum_{j=1}^m w'_j (\beta_{1j} - \bar{\beta}_1)^2, \quad (5.7)$$

with $\bar{\nu}_1 = \sum_{j=1}^m w'_j \nu_{1j}$ and $\bar{\beta}_1 = \sum_{j=1}^m w'_j \beta_{1j}$, since $\sum_{j=1}^m w'_j = 1$.

Similarly, the measure of heterogeneity H_2 within patch 2 is given by

$$H_2 = \sum_{j=1}^m w'_j (\nu_{2j} - \bar{\nu}_2)^2 + \sum_{j=1}^m w'_j (\beta_{2j} - \bar{\beta}_2)^2, \quad (5.8)$$

where $\bar{\nu}_2 = \sum_{j=1}^m w'_j \nu_{2j}$ and $\bar{\beta}_2 = \sum_{j=1}^m w'_j \beta_{2j}$.

The total heterogeneity within the two patches can be defined as

$$H = H_1 + H_2. \quad (5.9)$$

Heterogeneity between two patches only

The contact rate and shedding rate of individuals in patch 1 is certainly not the same as that of patch 2. To estimate this variation in transmission dynamics between the patch 1 and 2, we proposed the following measure of heterogeneity:

$$\mathcal{H}_{12} = \sum_{j=1}^m w'_j (\nu_{1j} - \nu_{2j})^2 + \sum_{j=1}^m w'_j (\beta_{1j} - \beta_{2j})^2. \quad (5.10)$$

Noting that $\mathcal{H}_{21} = \mathcal{H}_{12}$, the total variation in transmission between the two patches can be written as

$$\mathcal{H} = \mathcal{H}_{12}. \quad (5.11)$$

If we have a single water source, i.e., $m = 1$, the measure of heterogeneity \mathcal{H} becomes

$$\mathcal{H} = (\nu_{11} - \nu_{21})^2 + (\beta_{11} - \beta_{21})^2. \quad (5.12)$$

Geometrically, equation (5.12) represents a circle with center (ν_{11}, β_{11}) and radius $\sqrt{\mathcal{H}}$ when (ν_{11}, β_{11}) is fixed and (ν_{21}, β_{21}) is allow to vary. Since our interest is in the dynamics of water-borne disease for multiple water sources, to have a geometric view of measure of heterogeneity \mathcal{H} between the two patches, we can also define \mathcal{H} as

$$\mathcal{H} = (\bar{\nu}_1 - \bar{\nu}_2)^2 + (\bar{\beta}_1 - \bar{\beta}_2)^2. \quad (5.13)$$

If we fix $(\bar{\nu}_1, \bar{\beta}_1)$ and \mathcal{H} and allow $(\bar{\nu}_2, \bar{\beta}_2)$ to vary, geometrically, equation (5.13) will represent a circle with center $(\bar{\nu}_1, \bar{\beta}_1)$ and radius $\sqrt{\mathcal{H}}$ while if we fix $(\bar{\nu}_1, \bar{\beta}_1)$ only and allow \mathcal{H} and $(\bar{\nu}_2, \bar{\beta}_2)$ to vary, equation (5.13) becomes a paraboloid. The numerical illustrations of these are given in Figure 5.1. In Figure 5.1(a), $(\nu_1, \beta_1) = (\bar{\nu}_1, \bar{\beta}_1)$ is fixed as the center of the circles while $(\nu_2, \beta_2) = (\bar{\nu}_2, \bar{\beta}_2)$ and \mathcal{H} varies. The radius of each circle represents the magnitude of heterogeneity between the two patches. Thus the bigger the radius of the circle, the greater the heterogeneity between the two patches.

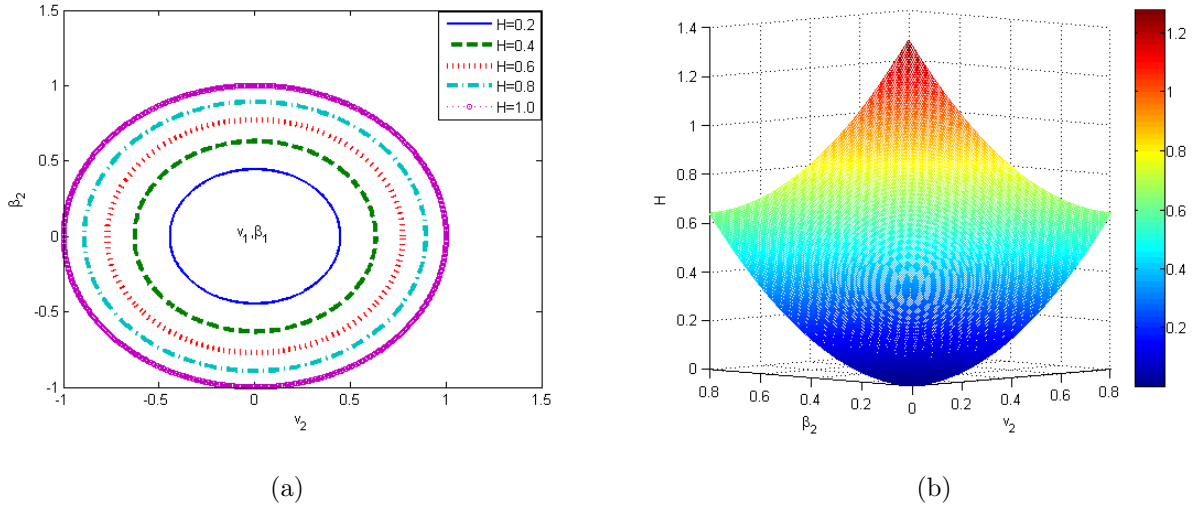


Figure 5.1: Numerical illustration of heterogeneity between patch 1 and 2 assuming heterogeneity within the patches: (a) for $(\bar{\nu}_1, \bar{\beta}_1)$, \mathcal{H} fixed (b) for $(\bar{\nu}_1, \bar{\beta}_1)$ fixed

Total heterogeneity

We have seen that there are two sources of heterogeneity in the system (5.3) namely: heterogeneity due to variation in transmission within a patch and heterogeneity due to variation in transmission between the patches. Therefore, the total heterogeneity \mathbb{H} in the system (5.3) can be defined as the sum of all the heterogeneity H within the patches and heterogeneity \mathcal{H} between the patches and is given by

$$\mathbb{H} = H + \mathcal{H}. \quad (5.14)$$

5.3.2 Homogeneous version of model (5.3)

To determine the effects of heterogeneity, it is necessary to obtain some of the mathematical features of the homogeneous version of model (5.3) and thereafter compare them with that of the heterogeneous model (5.3). The homogeneous version of the model (5.3) is obtained by considering the entire population as a homogeneous mixing population where all the individuals

have access to a single water source. The homogeneous version of model (5.3) is given by

$$\begin{aligned}
\dot{S}(t) &= \mu N(t) - bS(t)W(t) - \mu S(t), \\
\dot{I}(t) &= bS(t)W(t) - (\mu + \gamma)I(t), \\
\dot{W}(t) &= \theta I(t) - \sigma W(t), \\
\dot{R}(t) &= \gamma I(t) - \mu R(t).
\end{aligned} \tag{5.15}$$

Note that (5.15) is simply obtained from the original model (5.2) by taking $n = m = 1$ and ignoring the subscripts. By rescaling (5.15) as follows: $s = S/N$, $i = I/N$, $r = R/N$, $w = \sigma W/\theta N$, $\beta = b\theta N/\sigma$, we obtain a non-dimensional version of it:

$$\begin{aligned}
\dot{s} &= \mu - \beta s w - \mu s, \\
\dot{i} &= \beta s w - (\mu + \gamma)i, \\
\dot{w} &= \sigma(i - w), \\
\dot{r} &= \gamma i - \mu r.
\end{aligned} \tag{5.16}$$

The disease free equilibrium (DFE) and the basic reproduction number of the homogeneous model (5.16) are given by

$$(s^0, i^0, w^0) = (1, 0, 0), \tag{5.17}$$

and

$$\mathcal{R}_0 = \beta/(\mu + \gamma), \tag{5.18}$$

respectively. To establish a relationship between the heterogeneous model (5.3) and the homogeneous model (5.16), we define the contact rate, recovery rate and decay rate as follows:

$$\beta = \sum_{j=1}^2 \beta_j N_j/N = \sum_{j=1}^2 \sum_{k=1}^m \beta_{jk} N_j/N, \quad \sigma = \sum_{k=1}^m w'_k \sigma_k, \quad \gamma = \sum_{j=1}^2 N_j \gamma_j/N.$$

Based on this definition, we will see later that in the absent of heterogeneity (both within and between the patches), most of the mathematical features of the heterogeneous model (5.3) such as the basic reproduction number will reduce to that of the homogeneous model (5.16).

5.3.3 The basic reproduction number

The basic reproduction number is a useful epidemiological quantity that determines whether a disease will persist or not in a population. We determine the basic reproduction number of (5.3) using the next generation matrix approach of van den Driessche and Watmough [90]. The associated next generation matrices are given by

$$\mathcal{F} = \begin{pmatrix} 0 & 0 & \beta_{11} & \beta_{12} & \beta_{13} & \dots & \beta_{1m} \\ 0 & 0 & \beta_{21} & \beta_{22} & \beta_{23} & \dots & \beta_{2m} \\ 0 & 0 & 0 & 0 & 0 & \dots & 0 \\ \vdots & \vdots & & & & \dots & \\ 0 & 0 & 0 & 0 & 0 & \dots & 0 \end{pmatrix}, \quad \mathcal{V} = \begin{pmatrix} \mu + \gamma_1 & 0 & 0 & 0 & 0 & 0 & \dots & 0 \\ 0 & \mu + \gamma_2 & 0 & 0 & 0 & 0 & \dots & 0 \\ -\sigma_1\nu_{11} & -\sigma_1\nu_{21} & \sigma_1 & 0 & 0 & 0 & \dots & 0 \\ -\sigma_2\nu_{12} & -\sigma_2\nu_{22} & 0 & \sigma_2 & 0 & 0 & \dots & 0 \\ \vdots & \vdots & & & & & \dots & \\ -\sigma_m\nu_{1m} & -\sigma_m\nu_{2m} & 0 & 0 & 0 & \dots & 0 & \sigma_m \end{pmatrix},$$

with

$$\mathcal{F}\mathcal{V}^{-1} = \begin{pmatrix} \mathcal{R}_{11}^m & \mathcal{R}_{12}^m & \beta_{11}/\sigma_1 & \beta_{12}/\sigma_2 & \dots & \beta_{1m}/\sigma_m \\ \mathcal{R}_{21}^m & \mathcal{R}_{22}^m & \beta_{21}/\sigma_1 & \beta_{22}/\sigma_2 & \dots & \beta_{2m}/\sigma_m \\ 0 & 0 & 0 & 0 & \dots & 0 \\ \vdots & \vdots & & & \dots & \\ 0 & 0 & 0 & 0 & \dots & 0 \end{pmatrix}, \quad (5.19)$$

where

$$\mathcal{R}_{11}^m = \sum_{j=1}^m \nu_{1j}\beta_{1j}/(\mu + \gamma_1), \quad \mathcal{R}_{12}^m = \sum_{j=1}^m \nu_{2j}\beta_{1j}/(\mu + \gamma_2), \quad (5.20)$$

$$\mathcal{R}_{21}^m = \sum_{j=1}^m \nu_{1j}\beta_{2j}/(\mu + \gamma_1), \quad \mathcal{R}_{22}^m = \sum_{j=1}^m \nu_{2j}\beta_{2j}/(\mu + \gamma_2). \quad (5.21)$$

The basic reproduction number is the dominant eigenvalue of the matrix $\mathcal{F}\mathcal{V}^{-1}$ and is given by

$$\mathcal{R}_0^m = \left(\mathcal{R}_{11}^m + \mathcal{R}_{22}^m + \sqrt{(\mathcal{R}_{11}^m - \mathcal{R}_{22}^m)^2 + 4\mathcal{R}_{12}^m\mathcal{R}_{21}^m} \right) / 2. \quad (5.22)$$

From this equation (5.22), we notice that to have any chance of controlling the spread of infection (i.e., $\mathcal{R}_0^m < 1$), then it is necessary that $\mathcal{R}_{11}^m < 1$ and $\mathcal{R}_{22}^m < 1$ hold.

Suppose the entire population share a common water sources (i.e., $m = 1$), then the basic reproduction number \mathcal{R}_0^m becomes

$$\begin{aligned}\mathcal{R}_0^1 &= \left(\mathcal{R}_{11}^1 + \mathcal{R}_{22}^1 + \sqrt{(\mathcal{R}_{11}^1 - \mathcal{R}_{22}^1)^2 + 4\mathcal{R}_{12}^1\mathcal{R}_{21}^1} \right) / 2, \\ &= \mathcal{R}_{11}^1 + \mathcal{R}_{22}^1,\end{aligned}\tag{5.23}$$

where

$$\mathcal{R}_{11}^1 = \nu_{11}\beta_{11}/(\mu + \gamma_1), \quad \mathcal{R}_{12}^1 = \nu_{21}\beta_{11}/(\mu + \gamma_2), \quad \mathcal{R}_{21}^1 = \nu_{11}\beta_{21}/(\mu + \gamma_1), \quad \mathcal{R}_{22}^1 = \nu_{21}\beta_{21}/(\mu + \gamma_2).$$

Using a global stability result by Castillo-Chavez et al. [13] we establish the following theorem:

Theorem 5.3.1. *The DFE of model (5.3) is globally asymptotically stable if $\mathcal{R}_0^m < 1$.*

Next, we investigate the effects of heterogeneity by comparing the basic reproduction numbers of our models. Noting that the basic reproduction numbers are parameter dependent, we modify the contact rates, shedding rates and recovery rates as follows:

Since individuals do not have equal access to each of the contaminated water sources, we can rewrite ν_{ij} and β_{ij} as

$$\nu_{ij} = \nu_{i1}a^{j-1}, \quad \beta_{ij} = \beta_{i1}b^{j-1},\tag{5.24}$$

where $0 < a, b < 1$. If, in addition, we assume that individuals in patch 1 are more exposed to infections than those in patch 2, those in patch 2 are more exposed than those in patch 3, in this order till patch n , then we have that

$$\nu_{ij} = \nu_{11}q^{i-1}a^{j-1}, \quad \beta_{ij} = \beta_{11}p^{i-1}b^{j-1}, \quad \gamma_i = \gamma_1c^{i-1},\tag{5.25}$$

where $0 < p, q < 1$ and $c > 1$. Note that we also assumed that individuals in patch n recover faster than those in patch $n - 1$ while those in patch $n - 1$ recover faster than those in $n - 2$ in this order till patch 1 which account for having $c > 1$. By considering equation (5.25), \mathcal{R}_0^m simplifies to

$$\mathcal{R}_0^m = \mathcal{R}_{11}^m + \mathcal{R}_{22}^m.\tag{5.26}$$

With these modifications, we can now go ahead and carry out the analysis as follows:

Firstly, we compare the basic reproduction number \mathcal{R}_0^m of model (5.3) with that of \mathcal{R}_0 homogeneous model (5.16). Taking limits of \mathcal{R}_0^m and \mathcal{R}_0 as $a, b, c, p, q \rightarrow 1$ or as $a, b, p, q \rightarrow 0, c \rightarrow \infty$ we obtain that

$$\mathcal{R}_0 < \mathcal{R}_0^m \quad (5.27)$$

for both cases. This suggests that heterogeneity increases the basic reproduction number. Thus considering heterogeneity might lead to an increase in the number of secondary infections in the entire community.

Note that $a, b, c, p, q \rightarrow 1$ means a situation when the difference in transmission between the patches becomes very small, while $a, b, p, q \rightarrow 0, c \rightarrow \infty$ implies that the difference in transmission between the patches becomes very large.

Secondly, we compare the basic reproduction number of our models for the case when there is heterogeneity only within the patches i.e., $H \neq 0$ and $\mathcal{H} = 0$. In this case, $\nu_{1j} = \nu_{2j}, \beta_{1j} = \beta_{2j}$ and the basic reproduction number \mathcal{R}_0^m becomes

$$\mathcal{R}_0^H = \mathcal{R}_{11}^m + \mathcal{R}_{22}^m. \quad (5.28)$$

Taking limits as $a, b, c, p, q \rightarrow 1$ or as $a, b, p, q \rightarrow 0, c \rightarrow \infty$, we obtain that

$$\mathcal{R}_0 < \mathcal{R}_0^H. \quad (5.29)$$

Thirdly, for the case when there is heterogeneity only between the patches i.e., $H = 0$ and $\mathcal{H} \neq 0$. Here we have $\bar{\nu}_1 = \nu_{1j}, \bar{\nu}_2 = \nu_{2j}, \bar{\beta}_1 = \beta_{1j}$ and $\bar{\beta}_2 = \beta_{2j}$ and \mathcal{R}_0^m becomes

$$\mathcal{R}_0^{\mathcal{H}} = \mathcal{R}_{11}^m + \mathcal{R}_{22}^m. \quad (5.30)$$

Taking limits as $a, b, c, p, q \rightarrow 1$ or as $a, b, p, q \rightarrow 0, c \rightarrow \infty$, we obtain that

$$\mathcal{R}_0 < \mathcal{R}_0^{\mathcal{H}}. \quad (5.31)$$

The above results show that an increase in heterogeneity increases the basic reproduction number. These are also consistent with the results of [76] that says that the basic reproduction number is an increasing function of heterogeneity.

Suppose the patches are isolated such that there is no sharing of water sources, then \mathcal{R}_0^m becomes

$$\mathcal{R}_0^s = \max\{\mathcal{R}_{11}^m, \mathcal{R}_{22}^m\}, \quad (5.32)$$

where $\mathcal{R}_{11} = \nu_{11}\beta_{11}/(\mu + \gamma_1)$ and $\mathcal{R}_{22} = \nu_{22}\beta_{22}/(\mu + \gamma_2)$. It is obvious that

$$\mathcal{R}_0^s < \mathcal{R}_0^m. \quad (5.33)$$

This shows that sharing of water sources increases the basic reproduction number compared to when patches are isolated. Notice that if there is no sharing of water sources, heterogeneity within the patches vanishes i.e., $H = 0$. Therefore, sharing of water sources increases heterogeneity in transmission of waterborne diseases.

Furthermore, we have from equation (5.23) that when the entire population share a common water sources, that \mathcal{R}_0^m becomes $\mathcal{R}_0^1 = \mathcal{R}_{11}^1 + \mathcal{R}_{22}^1$. For this case, we also notice that heterogeneity within the patches vanishes i.e., $H = 0$. This implies that reducing the number of water sources that the population shared decreases heterogeneity in transmission. Moreover,

$$\mathcal{R}_0^1 < \mathcal{R}_0^m, \quad (5.34)$$

showing that the greater the number of water sources shared by the population, the greater the basic reproduction number. Therefore, an increase in the number of water sources shared by the population leads to increases heterogeneity in transmission of waterborne diseases. This support our earlier results that say that heterogeneity increases the reproduction number of the disease. Thus, heterogeneity has some influence on the dynamics of waterborne disease. Therefore, to effectively reduce the spread of waterborne disease in a meta-population setting, heterogeneity within the patches should be put into consideration while designing control intervention strategies.

5.3.4 Type reproduction numbers

The type reproduction number \mathcal{T}_i represents the expected number of secondary infections produced by an infected individual in a susceptible patch i over his/her lifetime. To determine the

proper control effort needed to eradicate the spread of the infection while targeting control at one particular patch, and having no control over reducing the spread of the disease in other patches, it is necessary that we consider the type reproduction number rather than the basic reproduction number [75, 37]. We compute \mathcal{T}_1 for patch 1 to be

$$\mathcal{T}_1 = \mathcal{R}_{11}^m + \mathcal{R}_{12}^m \mathcal{R}_{21}^m / (1 - \mathcal{R}_{22}^m), \quad (5.35)$$

provided that $\mathcal{R}_{22}^m \neq 1$. Similarly, the type reproduction number \mathcal{T}_2 for patch 2 is given by

$$\mathcal{T}_2 = \mathcal{R}_{22}^m + \mathcal{R}_{12}^m \mathcal{R}_{21}^m / (1 - \mathcal{R}_{11}^m), \quad (5.36)$$

provided that $\mathcal{R}_{11}^m \neq 1$.

Equations (5.35) can be re-written as

$$(\mathcal{T}_1 - \mathcal{R}_{11}^m)(1 - \mathcal{R}_{22}^m) = \mathcal{R}_{12}^m \mathcal{R}_{21}^m. \quad (5.37)$$

Since $\mathcal{R}_{12}^m > 0$ and $\mathcal{R}_{21}^m > 0$, then we must have that $\mathcal{T}_1 > \mathcal{R}_{11}^m$ and $1 > \mathcal{R}_{22}^m$ or $\mathcal{T}_1 < \mathcal{R}_{11}^m$ and $1 < \mathcal{R}_{22}^m$. Similarly, from (5.36) we obtain $\mathcal{T}_2 > \mathcal{R}_{22}^m$ and $1 > \mathcal{R}_{11}^m$ or $\mathcal{T}_2 < \mathcal{R}_{22}^m$ and $1 < \mathcal{R}_{11}^m$. Given that a necessary condition to control the spread of infection is that $\mathcal{R}_{11}^m < 1$ and $\mathcal{R}_{22}^m < 1$, we must have that

$$\mathcal{R}_{11}^m < \mathcal{T}_1, \quad \mathcal{R}_{22}^m < \mathcal{T}_2. \quad (5.38)$$

On the other hand, if $\mathcal{R}_{11}^m > 1$ and $\mathcal{R}_{22}^m > 1$, then

$$\mathcal{R}_{11}^m > \mathcal{T}_1, \quad \mathcal{R}_{22}^m > \mathcal{T}_2. \quad (5.39)$$

In this case, there is no chance of controlling the spread of infection.

To determine the effect of heterogeneity on the type reproduction numbers of model (5.3), we consider the following cases: Suppose there is heterogeneity only within the patches i.e., $H \neq 0$ and $\mathcal{H} = 0$, then the type reproduction numbers \mathcal{T}_1 and \mathcal{T}_2 becomes

$$\mathcal{T}_1^H = \mathcal{R}_{11}^m / (1 - \mathcal{R}_{22}^m), \quad \mathcal{T}_2^H = \mathcal{R}_{22}^m / (1 - \mathcal{R}_{11}^m). \quad (5.40)$$

Similarly, if there is heterogeneity only between the patches i.e., $H = 0$ and $\mathcal{H} \neq 0$, the type reproduction numbers \mathcal{T}_1 and \mathcal{T}_2 become

$$\mathcal{T}_1^{\mathcal{H}} = \mathcal{R}_{11}^m / (1 - \mathcal{R}_{22}^m), \quad \mathcal{T}_2^{\mathcal{H}} = \mathcal{R}_{22}^m / (1 - \mathcal{R}_{11}^m). \quad (5.41)$$

Suppose there is no sharing of water sources, then the type reproduction numbers \mathcal{T}_1 and \mathcal{T}_2 become

$$\mathcal{T}_1^s = \mathcal{R}_{11}^m, \quad \mathcal{T}_2^s = \mathcal{R}_{22}^m. \quad (5.42)$$

We can easily see

$$\mathcal{T}_1^s < \mathcal{T}_1, \quad \mathcal{T}_2^s < \mathcal{T}_2. \quad (5.43)$$

This implies that sharing of water sources increases the type reproduction numbers. Based on our earlier results, we can say that heterogeneity increases the type reproduction numbers.

5.3.5 Final outbreak size

The basic reproduction number/type reproduction number is very important for determining whether or not an outbreak will occur. To determine the magnitude of an outbreak, it is necessary to compute the final outbreak size. The final outbreak size denoted by z of the *SIR* models together with some other related models is given by the relation [57]

$$z = 1 - \exp(-\mathcal{R}_0 z). \quad (5.44)$$

This relation does not hold for model (5.3). However, when $\mu = 0$, $\mathcal{R}_0^m > 1$ and $w_j(0) = 0$, then the final outbreak size in patch 1 and patch 2 denoted by z_1 and z_2 respectively are given by the following equations:

$$z_1^m = 1 - \exp(-\mathcal{R}_{11}^m z_1^m - \mathcal{R}_{12}^m z_2^m), \quad (5.45)$$

$$z_2^m = 1 - \exp(-\mathcal{R}_{22}^m z_2^m - \mathcal{R}_{21}^m z_1^m). \quad (5.46)$$

Proof. We consider the same approach used in [84, 57]. Let

$$F_1(t) = \log s_1(t) + r_1(t) \sum_{j=1}^m \nu_{1j} \beta_{1j} / \gamma_1 + r_2(t) \sum_{j=1}^m \nu_{2j} \beta_{1j} / \gamma_2 - \sum_{j=1}^m \beta_{1j} w_j(t) / \sigma_j, \quad (5.47)$$

$$F_2(t) = \log s_2(t) + r_2(t) \sum_{j=1}^m \nu_{2j} \beta_{2j} / \gamma_2 + r_1(t) \sum_{j=1}^m \nu_{1j} \beta_{2j} / \gamma_1 - \sum_{j=1}^m \beta_{2j} w_j(t) / \sigma_j. \quad (5.48)$$

Differentiating F_1 with respect to time t gives

$$\begin{aligned}
\dot{F}_1 &= \dot{s}_1/s_1 + \dot{r}_1(t) \sum_{j=1}^m \nu_{1j}\beta_{1j}/\gamma_1 + \dot{r}_2(t) \sum_{j=1}^m \nu_{2j}\beta_{1j}/\gamma_2 - \sum_{j=1}^m \beta_{1j}\dot{w}_j(t)/\sigma_j, \\
&= - \sum_{j=1}^m \beta_{1j}w_j(t) + i_1(t) \sum_{j=1}^m \nu_{1j}\beta_{1j} + i_2(t) \sum_{j=1}^m \nu_{2j}\beta_{1j} - \sum_{j=1}^m \beta_{1j}(\nu_{1j}i_1(t) + \nu_{2j}i_2(t) - w_j(t)), \\
&= 0.
\end{aligned}$$

Hence, F_1 is constant function along solution trajectories of model (5.3). Similarly, F_2 is also constant function along the solution trajectories. Since $\mu = 0$, then susceptible individuals $s_1(t)$ and $s_2(t)$ decrease monotonically to limits \bar{s}_1 and \bar{s}_2 respectively while the recovered individuals $r_1(t)$ and $r_2(t)$ increase monotonically to limits \bar{r}_1 and \bar{r}_2 respectively. By lemma 2 of [84], $(i_1(t), i_2(t)) \rightarrow (0, 0)$ and $w_j(t) \rightarrow 0$. Consequently, $\bar{s}_1 = 1 - \bar{r}_1$ and $\bar{s}_2 = 1 - \bar{r}_2$.

Taking limits of (5.47) and (5.48), we obtain

$$\begin{aligned}
\lim_{t \rightarrow \infty} F_1(t) &= \log(1 - \bar{r}_1) + \bar{r}_1 \sum_{j=1}^m \nu_{1j}\beta_{1j}/\gamma_1 + \bar{r}_2 \sum_{j=1}^m \nu_{2j}\beta_{1j}/\gamma_2, \\
\lim_{t \rightarrow \infty} F_2(t) &= \log(1 - \bar{r}_2) + \bar{r}_2 \sum_{j=1}^m \nu_{2j}\beta_{2j}/\gamma_2 + \bar{r}_1 \sum_{j=1}^m \nu_{1j}\beta_{2j}/\gamma_1.
\end{aligned}$$

At $t = 0$,

$$\begin{aligned}
F_1(0) &= \log s_1(0) + r_1(0) \sum_{j=1}^m \nu_{1j}\beta_{1j}/\gamma_1 + r_2(0) \sum_{j=1}^m \nu_{2j}\beta_{1j}/\gamma_2 - \sum_{j=1}^m \beta_{1j}w_j(0)/\sigma_j, \\
F_2(0) &= \log s_2(0) + r_2(0) \sum_{j=1}^m \nu_{2j}\beta_{2j}/\gamma_2 + r_1(0) \sum_{j=1}^m \nu_{1j}\beta_{2j}/\gamma_1 - \sum_{j=1}^m \beta_{2j}w_j(0)/\sigma_j.
\end{aligned}$$

Letting $s_1(0) \rightarrow 1$, $s_2(0) \rightarrow 1$ then $(r_1(0), r_2(0)) \rightarrow (0, 0)$ and $w_j(0) \rightarrow 0$. Since $F_1(t)$ and $F_2(t)$ are constant along solution trajectories, then $\lim_{t \rightarrow \infty} F_1(t) = F_1(0) = 0$ and $\lim_{t \rightarrow \infty} F_2(t) = F_2(0) = 0$, so

$$\log(1 - \bar{r}_1) + \bar{r}_1 \sum_{j=1}^m \nu_{1j}\beta_{1j}/\gamma_1 + \bar{r}_2 \sum_{j=1}^m \nu_{2j}\beta_{1j}/\gamma_2 = 0, \tag{5.49}$$

$$\log(1 - \bar{r}_2) + \bar{r}_2 \sum_{j=1}^m \nu_{2j}\beta_{2j}/\gamma_2 + \bar{r}_1 \sum_{j=1}^m \nu_{1j}\beta_{2j}/\gamma_1 = 0. \tag{5.50}$$

Letting $\bar{r}_1 \rightarrow z_1^m$, $\bar{r}_2 \rightarrow z_2^m$ and noting that $\mathcal{R}_{11}^m = \sum_{j=1}^m \nu_{1j}\beta_{1j}/\gamma_1$, $\mathcal{R}_{12}^m = \sum_{j=1}^m \nu_{2j}\beta_{1j}/\gamma_2$, $\mathcal{R}_{22}^m = \sum_{j=1}^m \nu_{2j}\beta_{2j}/\gamma_2$ and $\mathcal{R}_{21}^m = \sum_{j=1}^m \nu_{1j}\beta_{2j}/\gamma_1$ when $\mu = 0$, gives the desired result. \square

The final outbreak size z^m in the entire population is therefore given by [57]

$$z^m = \sum_{i=1}^2 z_i^m N_i / N. \quad (5.51)$$

Taking limits as $a, b, c, p, q \rightarrow 1$ or as $a, b, p, q \rightarrow 0, c \rightarrow \infty$, we obtain that

$$z \leq z^m, \quad (5.52)$$

where z is the final outbreak size of the homogeneous model (5.16).

We observe that the final outbreak size z_1^m in patch 1 is affected by the shedding from patch 2 and vice versa. This could be due to heterogeneity in transmission between the two patches. Hence, it is necessary to determine the effects of heterogeneity in the final outbreak size. Suppose there is heterogeneity only within the patches i.e., $H \neq 0$ and $\mathcal{H} = 0$, the final outbreak size z_1^m in patch 1 and z_2^m in patch 2 become

$$z_1^H = 1 - \exp(-\mathcal{R}_{11}^m z_1^H - \mathcal{R}_{12}^m z_2^H), \quad (5.53)$$

$$z_2^H = 1 - \exp(-\mathcal{R}_{22}^m z_2^H - \mathcal{R}_{21}^m z_1^H), \quad (5.54)$$

and final outbreak size z^m in the entire population is

$$z^H = \sum_{i=1}^2 z_i^H N_i / N. \quad (5.55)$$

Taking limits as $a, b, c, p, q \rightarrow 1$ or as $a, b, p, q \rightarrow 0, c \rightarrow \infty$, we obtain that

$$z \leq z^H. \quad (5.56)$$

On the other hand, if there is heterogeneity only between the patches i.e., $H = 0$ and $\mathcal{H} \neq 0$, the final outbreak size z_1^m in patch 1 and z_2^m in patch 2 become

$$z_1^{\mathcal{H}} = 1 - \exp(-\mathcal{R}_{11}^m z_1^{\mathcal{H}} - \mathcal{R}_{12}^m z_2^{\mathcal{H}}), \quad (5.57)$$

$$z_2^{\mathcal{H}} = 1 - \exp(-\mathcal{R}_{22}^m z_2^{\mathcal{H}} - \mathcal{R}_{21}^m z_1^{\mathcal{H}}), \quad (5.58)$$

and final outbreak size z^m in the entire population is

$$z^{\mathcal{H}} = \sum_{i=1}^2 N_i z_i^{\mathcal{H}} / N. \quad (5.59)$$

Taking limits as $a, b, c, p, q \rightarrow 1$ or as $a, b, p, q \rightarrow 0, c \rightarrow \infty$, we obtain that

$$z \leq z^{\mathcal{H}}. \quad (5.60)$$

These results suggest that an increase in heterogeneity increases the final outbreak size.

In addition to this, if the patches are isolated such that there is no sharing of water sources, then the final outbreak size relation in patch 1 and patch 2 becomes

$$z_1^s = 1 - \exp(-\mathcal{R}_{11}z_1^s), \quad (5.61)$$

$$z_2^s = 1 - \exp(-\mathcal{R}_{22}z_2^s), \quad (5.62)$$

respectively, where $\mathcal{R}_{11} = \nu_{11}\beta_{11}/\gamma_1$ and $\mathcal{R}_{22} = \nu_{22}\beta_{22}/\gamma_2$. Clearly

$$z_1^s < z_1^m, \quad z_2^s < z_2^m. \quad (5.63)$$

This shows that sharing of water sources increases the final outbreak size compared to when patches are isolated.

5.3.6 The general n -patch model with shared multiple water sources

In this section, we extend some of the results obtained in the 2-patch model to the general n -patch model (5.3). The next generation matrix \mathcal{FV}^{-1} of the general n -patch model is given by

$$\mathcal{FV}^{-1} = \begin{pmatrix} \mathcal{R}_{11}^m & \mathcal{R}_{12}^m & \dots & \mathcal{R}_{1n}^m & \beta_{11}/\sigma_1 & \beta_{12}/\sigma_2 & \dots & \beta_{1m}/\sigma_m \\ \mathcal{R}_{21}^m & \mathcal{R}_{22}^m & \dots & \mathcal{R}_{2n}^m & \beta_{21}/\sigma_1 & \beta_{22}/\sigma_2 & \dots & \beta_{2m}/\sigma_m \\ \vdots & \vdots & \dots & & & & & \\ \mathcal{R}_{n1}^m & \mathcal{R}_{n2}^m & \dots & \mathcal{R}_{nn}^m & \beta_{n1}/\sigma_1 & \beta_{n2}/\sigma_2 & \dots & \beta_{nm}/\sigma_m \\ 0 & 0 & \dots & 0 & 0 & 0 & \dots & 0 \\ \vdots & \vdots & & & & & & \\ 0 & 0 & \dots & 0 & 0 & 0 & \dots & 0 \end{pmatrix}, \quad (5.64)$$

where $\mathcal{R}_{jk}^m = \sum_{p=1}^m \nu_{kp}\beta_{jp}/(\mu + \gamma_k)$. Similar to the case of two patches, the basic reproduction number \mathcal{R}_0^m is the dominant eigenvalue of the matrix \mathcal{FV}^{-1} . In this case, \mathcal{R}_0^m is the largest

positive root of the polynomial

$$a_{n+m}\lambda^{n+m} + a_{n+m-1}\lambda^{n+m-1} + a_{n+m-2}\lambda^{n+m-2} + \cdots + a_1\lambda + a_0 = 0, \quad (5.65)$$

where a_0, a_1, \dots, a_{n+m} are constants functions of \mathcal{R}_{jk}^m and $N_j\beta_{jk}/\sigma_k$.

If the patches are isolated such that there is no sharing of water sources, then \mathcal{R}_0^m for the general case becomes

$$\mathcal{R}_0^s = \max\{\mathcal{R}_{jj}^m\}, \quad j = 1, 2, \dots, n, \quad (5.66)$$

where $\mathcal{R}_{jj} = \nu_{jj}\beta_{jj}/(\mu + \gamma_j)$.

For heterogeneity within any patch i of the general n -patch model (5.3), we propose the following measure of heterogeneity:

$$H_i = \sum_{j=1}^m w'_j(\nu_{ij} - \bar{\nu}_i)^2 + \sum_{j=1}^m w'_j(\beta_{ij} - \bar{\beta}_i)^2, \quad (5.67)$$

where $\bar{\nu}_i = \sum_{j=1}^m w'_j\nu_{ij}$ and $\bar{\beta}_i = \sum_{j=1}^m w'_j\beta_{ij}$.

The total heterogeneity within all the patches can be defined as

$$H = \sum_{i=1}^n H_i. \quad (5.68)$$

The variation in transmission dynamics between any two patches p and q , can be estimated by the following measure of heterogeneity:

$$\mathcal{H}_{pq} = \sum_{j=1}^m w'_j(\nu_{pj} - \nu_{qj})^2 + \sum_{j=1}^m w'_j(\beta_{pj} - \beta_{qj})^2. \quad (5.69)$$

Note that $\mathcal{H}_{pq} = \mathcal{H}_{qp}$ and $\mathcal{H}_{pp} = \mathcal{H}_{qq} = 0$. The total heterogeneity between all the patches in the system can be estimated as follows: the heterogeneity between patch 1 and each of the remaining $n - 1$ patches starting from patch 2 to patch n are $\mathcal{H}_{12}, \mathcal{H}_{13}, \mathcal{H}_{14}, \dots, \mathcal{H}_{1n}$. Similarly, the heterogeneity between patch 2 and each of the remaining $n - 2$ patches starting from patch 3 to patch n are $\mathcal{H}_{23}, \mathcal{H}_{24}, \mathcal{H}_{25}, \dots, \mathcal{H}_{2n}$. Notice that at each stage the number of measures of heterogeneity decreases by 1. We can continue in this order to the last term which is $\mathcal{H}_{n-1 n}$. There are a total of $n(n - 1)/2$ distinct measure of heterogeneities \mathcal{H}_{pq} between any

two patches. Hence the total heterogeneity between each of the patches in the system can be calculated explicitly as

$$\mathcal{H} = \sum_{i=2}^n \mathcal{H}_{1i} + \sum_{i=3}^n \mathcal{H}_{2i} + \sum_{i=4}^n \mathcal{H}_{3i} + \cdots + \sum_{i=n-1}^n \mathcal{H}_{n-2 i} + \sum_{i=n}^n \mathcal{H}_{n-1 i}, \quad (5.70)$$

where $\sum_{i=n}^n \mathcal{H}_{n-1 i} = \mathcal{H}_{n-1 n}$.

The total heterogeneity \mathbb{H} in the general n -patch system (5.3) can be defined as the sum of all the heterogeneity H within the patches and heterogeneity \mathcal{H} between the patches and is given by

$$\mathbb{H} = H + \mathcal{H}. \quad (5.71)$$

The final outbreak size relation can also be derived for each of the patches of the general model (5.3). Consider the function

$$\begin{aligned} F_j(t) &= \log s_j(t) + r_1(t) \sum_{k=1}^m \nu_{1k} \beta_{jk} / \gamma_1 + r_2(t) \sum_{k=1}^m \nu_{2k} \beta_{jk} / \gamma_2 + \cdots + r_n(t) \sum_{k=1}^m \nu_{nk} \beta_{jk} / \gamma_n \\ &\quad - \sum_{k=1}^m \beta_{jk} w_k(t) / \sigma_k. \end{aligned}$$

Derivative of F_j with respect to time gives

$$\begin{aligned} \dot{F}_j &= \dot{s}_j / s_j + \dot{r}_1 \sum_{k=1}^m \nu_{1k} \beta_{jk} / \gamma_1 + \dot{r}_2 \sum_{k=1}^m \nu_{2k} \beta_{jk} / \gamma_2 + \cdots + \dot{r}_n \sum_{k=1}^m \nu_{nk} \beta_{jk} / \gamma_n - \sum_{k=1}^m \beta_{jk} \dot{w}_k / \sigma_k, \\ &= - \sum_{k=1}^m \beta_{jk} w_k + i_1 \sum_{k=1}^m \nu_{1k} \beta_{jk} + i_2 \sum_{k=1}^m \nu_{2k} \beta_{jk} + \cdots + i_n \sum_{k=1}^m \nu_{nk} \beta_{jk} - \sum_{k=1}^m \beta_{jk} \left(\sum_{j=1}^n \nu_{jk} i_j - w_k \right), \\ &= 0. \end{aligned}$$

Thus F_j is a constant function along solution trajectories of model (5.3). Since $\mu = 0$, then susceptible individuals $s_j(t)$ decreases monotonically to limits \bar{s}_j while the recovered individuals $r_j(t)$ increases monotonically to limits \bar{r}_j for each $j = 1, 2, \dots, n$. By lemma 2 of [84], $i_j(t) \rightarrow 0$ and $w_k(t) \rightarrow 0$ for each $k = 1, 2, \dots, m$. This implies that, $\bar{s}_j = 1 - \bar{r}_j$. Since F_j is constant, setting $F_j(0) = \lim_{t \rightarrow \infty} F_j(t)$ gives

$$\begin{aligned} &\log s_j(0) + r_1(0) \sum_{k=1}^m \nu_{1k} \beta_{jk} / \gamma_1 + r_2(0) \sum_{k=1}^m \nu_{2k} \beta_{jk} / \gamma_2 + \cdots + r_n(0) \sum_{k=1}^m \nu_{nk} \beta_{jk} / \gamma_n - \sum_{k=1}^m \beta_{jk} w_k(0) / \sigma_k \\ &= \log(1 - \bar{r}_j) + \bar{r}_1 \sum_{k=1}^m \nu_{1k} \beta_{jk} / \gamma_1 + \bar{r}_2 \sum_{k=1}^m \nu_{2k} \beta_{jk} / \gamma_2 + \cdots + \bar{r}_n \sum_{k=1}^m \nu_{nk} \beta_{jk} / \gamma_n. \end{aligned} \quad (5.72)$$

Let $s_j(0) \rightarrow 1$ and $w_k(0) \rightarrow 0$ in (5.72) and note that $s_j(0) \rightarrow 1$ will force $r_j(0) \rightarrow 0$, we have

$$\log(1 - \bar{r}_j) = - \left(\bar{r}_1 \sum_{k=1}^m \nu_{1k} \beta_{jk} / \gamma_1 + \bar{r}_2 \sum_{k=1}^m \nu_{2k} \beta_{jk} / \gamma_2 + \dots + \bar{r}_n \sum_{k=1}^m \nu_{nk} \beta_{jk} / \gamma_n \right). \quad (5.73)$$

By letting $\bar{r}_j = z_j^m$ and simplifying (5.73) gives the final outbreak size relation

$$z_j^m = 1 - \exp \left(- \sum_{k=1}^m \mathcal{R}_{jk}^m z_k^m \right), \quad (5.74)$$

which is the desired result with $\mathcal{R}_{jk}^m = \sum_{p=1}^m \nu_{kp} \beta_{jp} / \gamma_k$. Therefore, the final outbreak size in patch j of the general model (5.3) is given by z_j^m . Thus, the final outbreak size z^m in the entire population is

$$z^m = \sum_{j=1}^n z_j^m N_j / N. \quad (5.75)$$

If there is no sharing of water sources, then the final outbreak size relation in patch j becomes

$$z_j^s = 1 - \exp \left(- \mathcal{R}_{jj} z_j^s \right), \quad (5.76)$$

where $\mathcal{R}_{jj} = \nu_{jj} \beta_{jj} / \gamma_j$. Moreover,

$$z^s = \sum_{j=1}^n z_j^s N_j / N. \quad (5.77)$$

By a similar reasoning as in the case of 2-patches, we can show that

$$z_j^s < z_j^m. \quad (5.78)$$

This implies that sharing of water sources increases the final outbreak size compared to when patches are isolated for the general case.

5.4 Application of model (5.1) to cholera outbreak in Haiti

In order to deepen our understanding on the dynamics of this serious cholera outbreak, as well as to control and possibly predict future epidemics, we apply our model (5.3) to investigate the

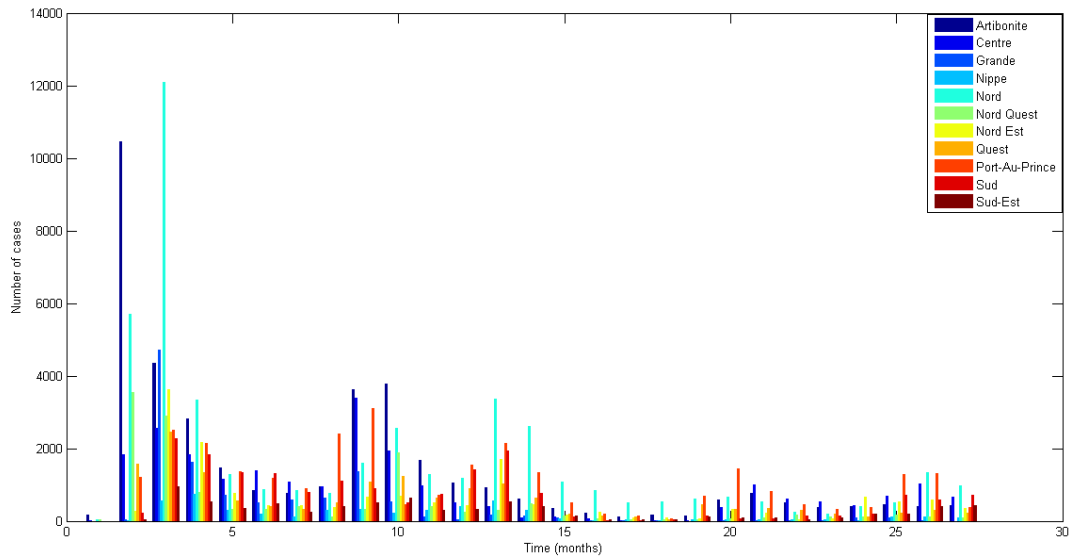


Figure 5.2: Bar chart representing the number of reported hospitalized cholera cases in each Department in Haiti from October 30, 2010, to December 24, 2012, [60].

Haiti cholera outbreak [52]. The cholera outbreak in Haiti was confirmed on October 21, 2010 by the National Laboratory of Public Health of the Ministry of Public Health and Population (MSPP) [63]. By August 4, 2013, 669,396 cases and 8,217 deaths have been reported since the beginning of the epidemic [15]. The outbreak started in Artibonite region, a rural area north of Port-au-Prince, but spread to all the administrative Departments in the country. This shows that there are connections between all the water sources or individuals across the Departments in Haiti. This is taken care of in our model since we assume that an infected individual from any patch can shed pathogen into any of the water sources across the patches and consequently susceptible individuals can contact the disease through drinking from any of the contaminated water sources.

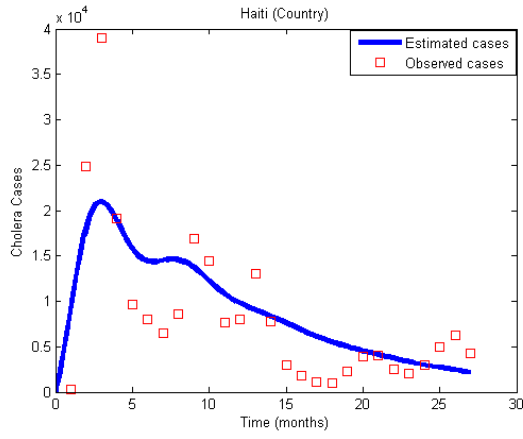
In order to validate model, we fit it to data from Haiti. To get reasonable results, we modify the parameters as follows: First, we take $n = 11$ such that each patch N_i in our model represents a Department in Haiti while the total population N becomes the total population in Haiti. According to the CIA [16], 49% and 90% of Haiti population in rural areas do not have access to improved drinking water sources and sanitation facilities respectively. Furthermore, 15%

and 76% of Haiti population living in urban areas also do not have access to improved drinking water source and sanitation facilities respectively. We take $m = 2$ and assume that W_1 measures the pathogen concentration of unimproved water source in the rural area while W_2 measures the pathogen concentration of unimproved water source in the urban area. The population of each Department in Haiti is taken from 2009 Haiti population data before the outbreak started [14] while the birth rate is estimated from [16].

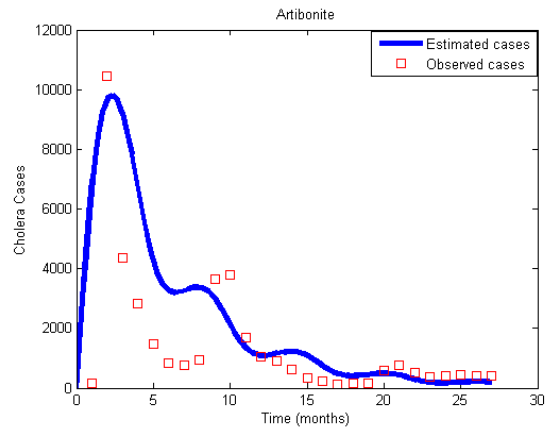
We notice from Figure 5.2 that, following the initial epidemic wave, the number of reported hospitalized cholera cases seems to increase during the rainy season. Recurrent seasonal epidemics is one of the characteristics of the disease [80]. To take the seasonal variations of the outbreak into account, we replace the contact rate β_{ij} in our model by the sine function

$$\beta_{ij}(t) = \beta_{ij} (1 + \delta_i \sin(2\pi t/(365\rho))), \quad (5.79)$$

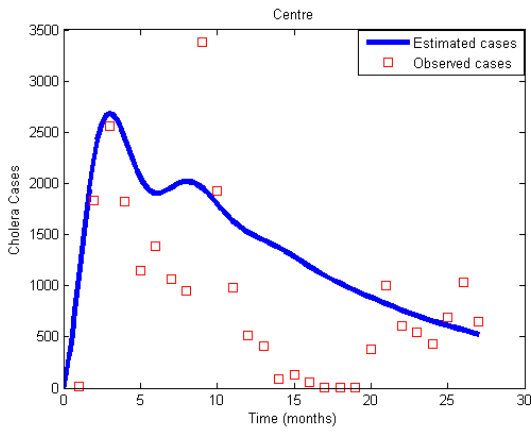
where β_{ij} is the mean contact rate, δ_i describes the relative amplitude of seasonal variations in patch i and ρ is a scaling factor. We also take $\sigma = 0.333$ [19, 84]. The mean contact rates, shedding rates and recovery rates are chosen from a realistic range. The comparison of the results of incorporating these parameter values for our model and the data for Haiti are shown in Figures 5.3 (a)–(f) and Figures 5.4 (a)–(f). The Figures reveal that our model is applicable to the Haiti cholera outbreak at both departmental level and national level to some extent. However, we should notice from the Figures that the outbreak does not have a predictable recurrent seasonal epidemic waves in some departments like Nippe and Centre, as a result, our assumption of seasonality could not determine the best fit for these departments.



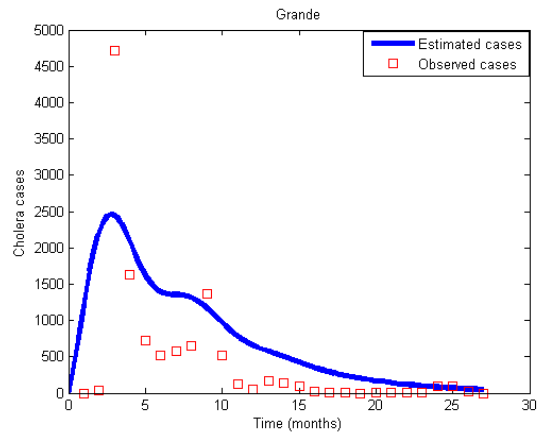
(a)



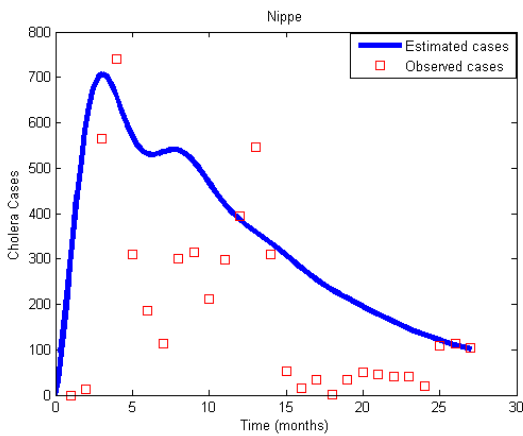
(b)



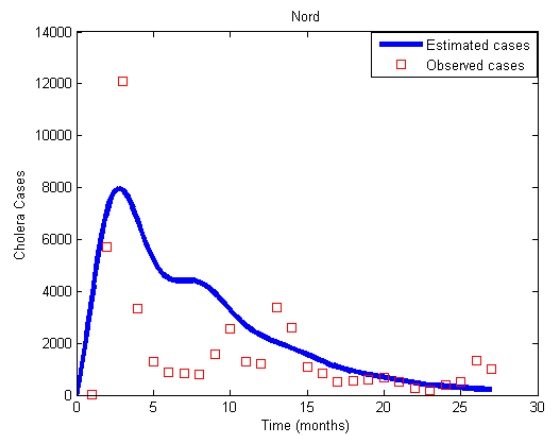
(c)



(d)

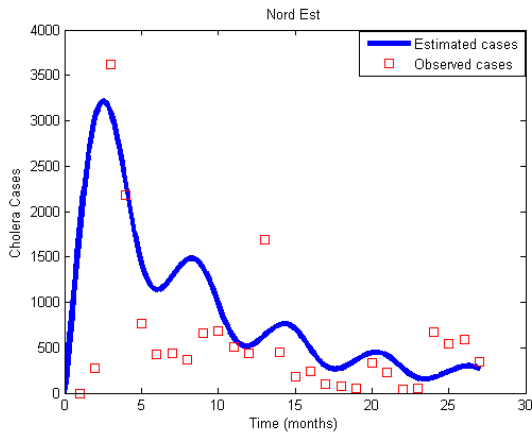


(e)

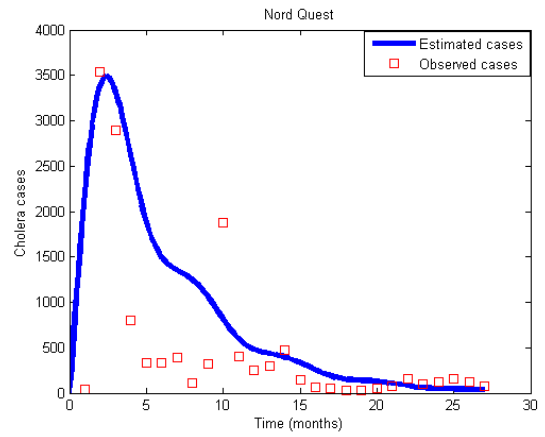


(f)

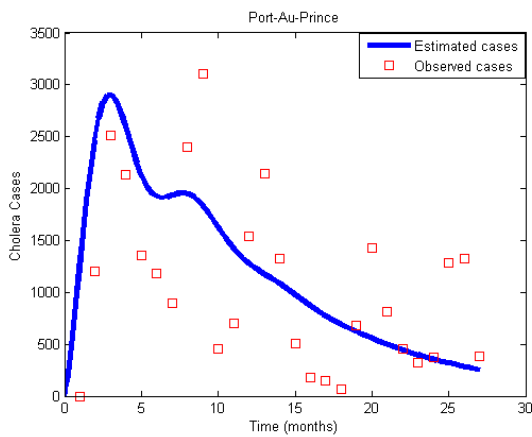
Figure 5.3: Model fitting for the number of reported hospitalized cholera cases in Haiti.



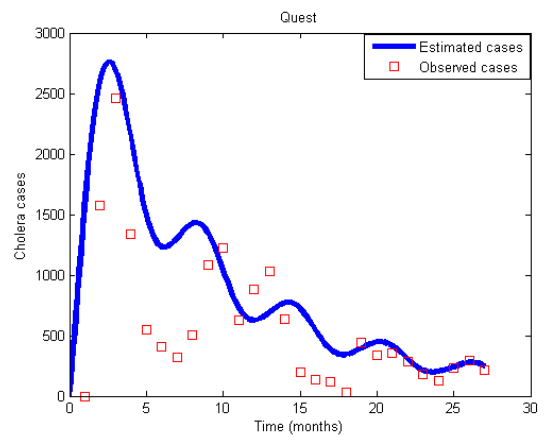
(a)



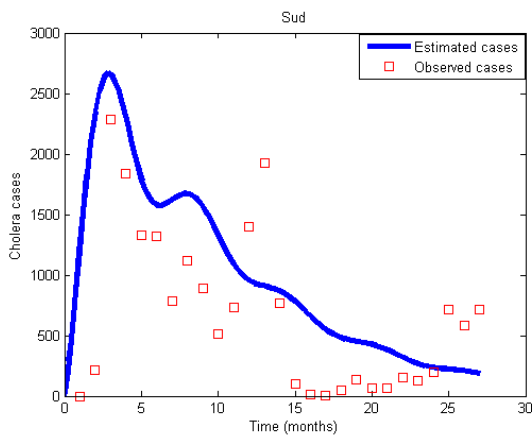
(b)



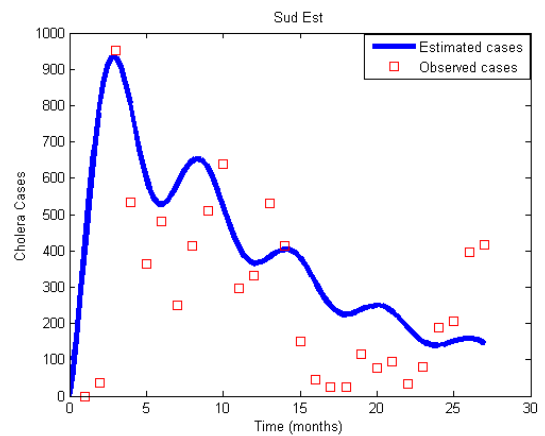
(c)



(d)



(e)



(f)

Figure 5.4: Model fitting for the number of reported hospitalized cholera cases in Haiti.

5.5 The multiple control strategy model

In this section, we extend model (5.3) by considering three types of control intervention strategies: vaccination, treatment and water purification. We assume that individuals in patch j are vaccinated at rate ϕ_j with a vaccine whose efficacy is ε_j and wane rate ω_j . Individuals in this patch receive treatment at rate τ_j . Treated individual $T_j(t)$ recover at rate η_j . Individuals in this patch can also be provided with clean water by purifying contaminated water sources. This water purification reduces pathogen concentration by a rate d_k . Both the vaccinated individuals $V_j(t)$ and the treated individuals in patch j die a natural death at rate μ . The new model is given by

$$\begin{aligned}
\dot{s}_j &= \mu + \omega_j v_j - s_j \sum_{k=1}^m \beta_{jk} w_k - (\mu + \phi_j) s_j, \\
\dot{v}_j &= \phi_j s_j - (1 - \varepsilon_j) v_j \sum_{k=1}^m \beta_{jk} w_k - (\mu + \omega_j) v_j, \\
\dot{i}_j &= (s_j + (1 - \varepsilon_j) v_j) \sum_{k=1}^m \beta_{jk} w_k - (\mu + \gamma_j + \tau_j) i_j, \\
\dot{\Gamma}_j &= \tau_j i_j - (\mu + \eta_j) \Gamma_j, \\
\dot{w}_k &= \sigma_k \left(\sum_{j=1}^n \nu_{jk} i_j - (1 + d_k / \sigma_k) w_k \right), \\
\dot{r}_j &= \gamma_j i_j + \eta_j \Gamma_j - \mu r_j,
\end{aligned} \tag{5.80}$$

where $v_j = V_j/N_j$, $\Gamma_j = T_j/N_j$. The initial conditions are assumed as follows:

$$s_j(0) > 0, \quad v_j(0) \geq 0, \quad i_j(0) \geq 0, \quad \Gamma_j(0) \geq 0, \quad w_k(0) \geq 0, \quad r_j(0) \geq 0. \tag{5.81}$$

5.5.1 Analysis of the multiple control strategy model

A unique DFE exists in model (5.80) and is given by

$$(s_j^0, v_j^0, i_j^0, \Gamma_j^0, w_k^0, r_j^0) = ((\mu + \omega_j) / (\mu + \omega_j + \phi_j), \phi_j / (\mu + \omega_j + \phi_j), 0, 0, 0, 0). \tag{5.82}$$

The basic reproduction number of multiple control strategy model (5.80) is given by

$$\mathcal{R}_0^c = \left(\mathcal{R}_{11}^c + \mathcal{R}_{22}^c + \sqrt{(\mathcal{R}_{11}^c - \mathcal{R}_{22}^c)^2 + 4\mathcal{R}_{12}^c \mathcal{R}_{21}^c} \right) / 2, \tag{5.83}$$

where

$$\begin{aligned}
\mathcal{R}_{11}^c &= \frac{\mu + \omega_1 + (1 - \varepsilon_1)\phi_1}{(\mu + \gamma_1 + \tau_1)(\mu + \omega_1 + \phi_1)} \sum_{j=1}^m \nu_{1j}\beta_{1j}\sigma_j/(\sigma_j + d_j), \\
\mathcal{R}_{12}^c &= \frac{\mu + \omega_1 + (1 - \varepsilon_1)\phi_1}{(\mu + \gamma_2 + \tau_2)(\mu + \omega_1 + \phi_1)} \sum_{j=1}^m \nu_{2j}\beta_{1j}\sigma_j/(\sigma_j + d_j), \\
\mathcal{R}_{21}^c &= \frac{\mu + \omega_2 + (1 - \varepsilon_2)\phi_2}{(\mu + \gamma_1 + \tau_1)(\mu + \omega_2 + \phi_2)} \sum_{j=1}^m \nu_{1j}\beta_{2j}\sigma_j/(\sigma_j + d_j), \\
\mathcal{R}_{22}^c &= \frac{\mu + \omega_2 + (1 - \varepsilon_2)\phi_2}{(\mu + \gamma_2 + \tau_2)(\mu + \omega_2 + \phi_2)} \sum_{j=1}^m \nu_{2j}\beta_{2j}\sigma_j/(\sigma_j + d_j).
\end{aligned}$$

Clearly,

$$\mathcal{R}_{11}^c < \mathcal{R}_{11}^m, \quad \mathcal{R}_{12}^c < \mathcal{R}_{12}^m, \quad \mathcal{R}_{21}^c < \mathcal{R}_{21}^m, \quad \mathcal{R}_{22}^c < \mathcal{R}_{22}^m. \quad (5.84)$$

The threshold quantity \mathcal{R}_0^c above represents the expected number of secondary infections that result from introducing a single infected individual into an otherwise susceptible population in the presence of vaccination, treatment and water purification.

The type reproduction number \mathcal{T}_1^c for patch 1 of the multiple control model is given by

$$\mathcal{T}_1^c = \mathcal{R}_{11}^c + \mathcal{R}_{12}^c \mathcal{R}_{21}^c / (1 - \mathcal{R}_{22}^c), \quad (5.85)$$

provided that $\mathcal{R}_{22}^c \neq 1$. Similarly, the type reproduction number \mathcal{T}_2^c for patch 2 is given by

$$\mathcal{T}_2^c = \mathcal{R}_{22}^c + \mathcal{R}_{12}^c \mathcal{R}_{21}^c / (1 - \mathcal{R}_{11}^c), \quad (5.86)$$

provided that $\mathcal{R}_{11}^c \neq 1$. Obviously

$$\mathcal{T}_1^c < \mathcal{T}_1, \quad \mathcal{T}_2^c < \mathcal{T}_2. \quad (5.87)$$

This shows that the multiple control intervention strategy has the capacity of reducing the number of secondary infections in each of the subpopulations in the community to a certain level. Due to limited resources, only some of the communities can afford the multiple control strategy. As a result, it is necessary to investigate the effect of considering single control intervention strategies to reduce the spread of the disease.

5.6 The single control intervention strategy

In this section, we shall focus on the effects of each of the controls individually.

5.6.1 Effects of vaccination

In the absence of treatment, $\tau_i = 0$, $\eta_i = 0$, and water purification, $d_i = 0$, we have that the vaccination-induced basic reproduction number is given by

$$\mathcal{R}_0^v = \left(\mathcal{R}_{11}^v + \mathcal{R}_{22}^v + \sqrt{(\mathcal{R}_{11}^v - \mathcal{R}_{22}^v)^2 + 4\mathcal{R}_{12}^v \mathcal{R}_{21}^v} \right) / 2, \quad (5.88)$$

where

$$\begin{aligned} \mathcal{R}_{11}^v &= \mathcal{R}_{11}^m (\mu + \omega_1 + (1 - \varepsilon_1)\phi_1) / (\mu + \omega_1 + \phi_1), \\ \mathcal{R}_{12}^v &= \mathcal{R}_{12}^m (\mu + \omega_1 + (1 - \varepsilon_1)\phi_1) / (\mu + \omega_1 + \phi_1), \\ \mathcal{R}_{21}^v &= \mathcal{R}_{21}^m (\mu + \omega_2 + (1 - \varepsilon_2)\phi_2) / (\mu + \omega_2 + \phi_2), \\ \mathcal{R}_{22}^v &= \mathcal{R}_{22}^m (\mu + \omega_2 + (1 - \varepsilon_2)\phi_2) / (\mu + \omega_2 + \phi_2). \end{aligned}$$

We observe that

$$\mathcal{R}_{11}^v < \mathcal{R}_{11}^m, \quad \mathcal{R}_{12}^v < \mathcal{R}_{12}^m, \quad \mathcal{R}_{21}^v < \mathcal{R}_{21}^m, \quad \mathcal{R}_{22}^v < \mathcal{R}_{22}^m, \quad (5.89)$$

provided $0 < \phi_1, \phi_2 < 1$ and $0 < \varepsilon_1, \varepsilon_2 < 1$.

Furthermore, the vaccination-induced type reproduction numbers for patch 1 and patch 2 are given by

$$\mathcal{T}_1^v = \mathcal{R}_{11}^v + \mathcal{R}_{12}^v \mathcal{R}_{21}^v / (1 - \mathcal{R}_{22}^v), \quad \mathcal{T}_2^v = \mathcal{R}_{22}^v + \mathcal{R}_{12}^v \mathcal{R}_{21}^v / (1 - \mathcal{R}_{11}^v), \quad (5.90)$$

respectively, provided that $\mathcal{R}_{11}^v \neq 1$ and $\mathcal{R}_{22}^v \neq 1$. Truly

$$\mathcal{T}_1^v < \mathcal{T}_1, \quad \mathcal{T}_2^v < \mathcal{T}_2. \quad (5.91)$$

This reveals that effective vaccination only can reduce the number of secondary infections in each the subpopulations in the community. Next, comparing this with that of the multiple control model, we obtain

$$\mathcal{R}_{11}^c < \mathcal{R}_{11}^v, \quad \mathcal{R}_{12}^c < \mathcal{R}_{12}^v, \quad \mathcal{R}_{21}^c < \mathcal{R}_{21}^v, \quad \mathcal{R}_{22}^c < \mathcal{R}_{22}^v, \quad (5.92)$$

and

$$\mathcal{T}_1^c < \mathcal{T}_1^v, \quad \mathcal{T}_2^c < \mathcal{T}_2^v, \quad (5.93)$$

showing that even though vaccination can reduce the spread of infections, the multiple control intervention strategy will yield a better result. This result agrees with intuitive expectations.

5.6.2 Effects of treatment

In the absence of vaccination, $\phi_i = 0$, $\omega_i = 1$, $\varepsilon_i = 0$, and water purification, $d_i = 0$, we have the treatment-induced basic reproduction number as

$$\mathcal{R}_0^\tau = \left(\mathcal{R}_{11}^\tau + \mathcal{R}_{22}^\tau + \sqrt{(\mathcal{R}_{11}^\tau - \mathcal{R}_{22}^\tau)^2 + 4\mathcal{R}_{12}^\tau \mathcal{R}_{21}^\tau} \right) / 2, \quad (5.94)$$

respectively, where

$$\begin{aligned} \mathcal{R}_{11}^\tau &= \mathcal{R}_{11}^m(\mu + \gamma_1)/(\mu + \gamma_1 + \tau_1), & \mathcal{R}_{12}^\tau &= \mathcal{R}_{12}^m(\mu + \gamma_2)/(\mu + \gamma_2 + \tau_2), \\ \mathcal{R}_{21}^\tau &= \mathcal{R}_{21}^m(\mu + \gamma_1)/(\mu + \gamma_1 + \tau_1), & \mathcal{R}_{22}^\tau &= \mathcal{R}_{22}^m(\mu + \gamma_2)/(\mu + \gamma_2 + \tau_2). \end{aligned}$$

Similar to the case of vaccination, we can show that

$$\mathcal{R}_{11}^c < \mathcal{R}_{11}^\tau < \mathcal{R}_{11}^m, \quad \mathcal{R}_{12}^c < \mathcal{R}_{12}^\tau < \mathcal{R}_{12}^m, \quad \mathcal{R}_{21}^c < \mathcal{R}_{21}^\tau < \mathcal{R}_{21}^m, \quad \mathcal{R}_{22}^c < \mathcal{R}_{22}^\tau < \mathcal{R}_{22}^m. \quad (5.95)$$

Furthermore, the treatment-induced type-reproduction numbers for patch 1 and patch 2 are given by

$$\mathcal{T}_1^\tau = \mathcal{R}_{11}^\tau + \mathcal{R}_{12}^\tau \mathcal{R}_{21}^\tau / (1 - \mathcal{R}_{22}^\tau), \quad \mathcal{T}_2^\tau = \mathcal{R}_{22}^\tau + \mathcal{R}_{12}^\tau \mathcal{R}_{21}^\tau / (1 - \mathcal{R}_{11}^\tau), \quad (5.96)$$

respectively, provided that $\mathcal{R}_{11}^\tau \neq 1$ and $\mathcal{R}_{22}^\tau \neq 1$.

$$\mathcal{T}_1^c < \mathcal{T}_1^\tau < \mathcal{T}_1, \quad \mathcal{T}_2^c < \mathcal{T}_2^\tau < \mathcal{T}_2. \quad (5.97)$$

This result demonstrates that proper treatment of infected individuals only can reduce the number of secondary infections in each of the subpopulations in the community. In addition, we discover that the multiple control will be more effective in reducing the spread of disease if applied concurrently.

5.6.3 Effects of water purification

In the absence of treatment, $\tau_i = 0$, $\eta_i = 0$, and vaccination, $\phi_i = 0$, the water purification-induced basic reproduction number is given by

$$\mathcal{R}_0^w = \left(\mathcal{R}_{11}^w + \mathcal{R}_{22}^w + \sqrt{(\mathcal{R}_{11}^w - \mathcal{R}_{22}^w)^2 + 4\mathcal{R}_{12}^w \mathcal{R}_{21}^w} \right) / 2, \quad (5.98)$$

respectively, where

$$\begin{aligned} \mathcal{R}_{11}^w &= \frac{1}{\mu + \gamma_2} \sum_{j=1}^m \nu_{2j} \beta_{1j} \sigma_j / (\sigma_j + d_j), \\ \mathcal{R}_{12}^w &= \frac{1}{\mu + \gamma_1} \sum_{j=1}^m \nu_{1j} \beta_{1j} \sigma_j / (\sigma_j + d_j), \\ \mathcal{R}_{21}^w &= \frac{1}{\mu + \gamma_1} \sum_{j=1}^m \nu_{1j} \beta_{2j} \sigma_j / (\sigma_j + d_j), \\ \mathcal{R}_{22}^w &= \frac{1}{\mu + \gamma_2} \sum_{j=1}^m \nu_{2j} \beta_{2j} \sigma_j / (\sigma_j + d_j). \end{aligned}$$

We can see that

$$\mathcal{R}_{11}^c < \mathcal{R}_{11}^w < \mathcal{R}_{11}^m, \quad \mathcal{R}_{12}^c < \mathcal{R}_{12}^w < \mathcal{R}_{12}^m, \quad \mathcal{R}_{21}^c < \mathcal{R}_{21}^w < \mathcal{R}_{21}^m, \quad \mathcal{R}_{22}^c < \mathcal{R}_{22}^w < \mathcal{R}_{22}^m. \quad (5.99)$$

The water purification-induced type reproduction numbers for patch 1 and patch 2 are given by

$$\mathcal{T}_1^w = \mathcal{R}_{11}^w + \mathcal{R}_{12}^w \mathcal{R}_{21}^w / (1 - \mathcal{R}_{22}^w), \quad \mathcal{T}_2^w = \mathcal{R}_{22}^w + \mathcal{R}_{12}^w \mathcal{R}_{21}^w / (1 - \mathcal{R}_{11}^w), \quad (5.100)$$

respectively, provided that $\mathcal{R}_{11}^w \neq 1$ and $\mathcal{R}_{22}^w \neq 1$. Obviously,

$$\mathcal{T}_1^c < \mathcal{T}_1^w < \mathcal{T}_1, \quad \mathcal{T}_2^c < \mathcal{T}_2^w < \mathcal{T}_2. \quad (5.101)$$

This result also shows that provision of clean water to the same number of individuals who would have been vaccinated will also reduce the number of secondary infections. However, the multiple control is still more effective in reducing the spread of the disease.

5.7 Discussion

Most of the factors affecting waterborne disease transmission are not constant, hence leading to heterogeneity in disease transmission. To improve our understanding of the effects of heterogeneity on the dynamics of waterborne disease, we formulated an n -patch model where disease can spread both within a patch and between patches and noted that heterogeneity can arise both within a patch and between patches. To understand the magnitude of differences in transmission within a patch, we define a measure of heterogeneity within a patch. Similarly, the magnitude of differences in transmission between any two patches is also determined by defining a measure of heterogeneity between patches. The total variation in transmission existing in the whole meta-population automatically becomes the total sum of measures of heterogeneity. A homogeneous version of the n -patch model was formulated to help understand whether heterogeneity has a positive or negative impact on dynamics of the disease.

By carrying out qualitative analyses of these models, we discovered that considering heterogeneity leads to an increase in the number of secondary infections in each of the subpopulations as well as the entire community. We also showed that heterogeneity within the patches has a tendency to generate greater number of secondary infections and severe outbreak than heterogeneity between the patches. Based on this, we suggested that to effectively reduce the spread of waterborne disease in a heterogeneous population setting, heterogeneity within the patches should be put into consideration while defining control intervention strategies. Since heterogeneity is more realistic, it means that not considering heterogeneity implies an underestimation of an outbreak and this is very hazardous to the population. Furthermore, we discovered that considering heterogeneity leads to a greater outbreak in each of the subpopulations as well as the entire community at the endemic stage of the outbreak. More so, we discovered that sharing of water sources increases the final outbreak size compared to when patches are isolated.

We verified the analytical predictions by considering the most recent Haiti cholera outbreak as a realistic case study. Our results are consistent with the analytical predictions, thus the model (5.3) is applicable to the cholera dynamics in Haiti. It should be noted that our model

(5.3), accurately describes the evolution of the disease in Haiti and thus can provide insight into the future evolution of cholera dynamics in the place. Since our model is a more general heterogeneous model, we expect that it can be used to carry out similar studies to other cholera-endemic countries (with different parameter values).

Having shown that model (5.3) is applicable to a real-world situation, we extended the n -patch model by introducing three different types of control intervention strategies: vaccination, treatment and water purification separately. Our analysis revealed that each of the control strategies has some influence in reducing the spread of the disease to a certain level such that an outbreak do not occur when the control is implemented appropriately. The case whereby the three controls are introduced simultaneously was shown to be more effective in reducing the spread of infection across the meta-population.

Chapter 6

Summary

In this thesis, mathematical epidemiological models which comprise of systems of non-linear ordinary differential equations were used to investigate the dynamics of waterborne diseases under various conditions. By extending the models, the possible benefits of control intervention strategies such as vaccination, treatment and provision of clean water were also determined. Furthermore, the optimal control theory (i.e., Pontryagin's Maximum principle) was used to determine the optimal intervention strategies that mitigate the spread of waterborne diseases.

We began by discussing a very simple SIWR waterborne disease model and showed that both the short-term and long-term dynamics of the model can be described using stability arguments. Elaborating on this model we considered the effects of seasonal variations on the dynamics of the disease. Extensions of the model were used to investigate the possible benefits of control intervention strategies such as vaccination, provision of clean water and treatment. We discovered that the multiple control strategy is the best intervention strategy, followed by vaccination, provision of clean water and then treatment, in this order. We also showed that it is optimal to treat individuals immediately as they get infected and begin to vaccinate and provide clean water as soon as the outbreak starts and continue with maximal effort until the outbreak ends.

In Chapter 3 we discussed the impact of socioeconomic classes on the dynamics of waterborne disease in a community by formulating an n -patch waterborne disease model where each patch represents a socioeconomic class. The conditions under which the disease can either terminate or persist in the community were determined. We discovered that under the assumption of

uniform migration rates due to socioeconomic reasons, the outbreak growth rates and the number of secondary infections generated by an infected individual in the lower socioeconomic classes always dominate that of higher socioeconomic classes. However, if the migration rates are not uniform, we proved that outbreaks/secondary infections dominate in either the lower socioeconomic class or higher socioeconomic class depending on the rate at which individuals migrate due to socioeconomic reasons. The important parameters relative to initial disease transmission and prevalence of the disease in the community were also identified.

In Chapter 4 we addressed the issue of minimizing outbreak in a community where there are multiple contaminated water sources. By considering a waterborne disease model under the assumption that individuals are exposed to multiple contaminated water sources, we investigated the long-term dynamics of the disease across the community. Using the model, we showed that outbreaks are under estimated whenever a single water source is considered for the study of the dynamics of waterborne disease for a community where individuals are exposed to more than one contaminated water source. Particularly, we examined outbreak growth rates, the expected final size of the outbreak and the rate at which secondary infections are generated. We proved that this model is realistic by showing that it is applicable to the recent cholera outbreak in Haiti. We further investigated the effects of introducing vaccination in such an area by introducing vaccination in the model. For the vaccination model, we showed that it is optimal to start vaccinating as soon as possible and to continue vaccinating with maximal effort until the outbreak ends and also to maximally control vaccine wane if wane rate is large and minimally control vaccine wane if wane rate is small.

In Chapter 5 we addressed the problem of mitigating the spread of waterborne disease under the assumption of heterogeneous mixing population. We started by considering a more general n -patch waterborne disease model that takes heterogeneity in transmission into account. We proved that heterogeneity in transmission increases the number of secondary infections and leads to a greater outbreak in each of the subpopulations as well as the entire community. Furthermore, we showed that heterogeneity within the patches leads to a more severe outbreak than heterogeneity between the patches at both the epidemic and endemic stage of the outbreak. Based on this, we concluded that heterogeneity within the patches should be put into account

while designing control intervention strategies to effectively reduce the spread of waterborne disease in a heterogeneous population setting. Extensions of the model by introducing control intervention strategies such as vaccination, treatment and provision of clean water were used to determine the possible benefits of the control intervention strategies in reducing the spread of the infections in a heterogeneous population setting. Finally, we discovered that the model is applicable to the recent cholera outbreak in Haiti up to the State/Departmental level.

Bibliography

- [1] Z. Agur, L. Cojocar, G. Mazar, R.M. Anderson and Y.L. Danon. Pulse mass measles vaccination across age cohorts. *Proc. Natl. Acad. Sci. USA* **90** (1993), 11698–11702.
- [2] F.B. Augusto. Optimal chemoprophylaxis and treatment control strategies of a tuberculosis transmission model. *World J. Model. Simul.* **5** (2009), 163–173.
- [3] A. Alam, R.C. Larocque, J.B. Harris, C. Vanderspurt, E.T. Ryan, F. Qadri, S.B. Calderwood. Hyperinfectivity of human-passaged *Vibrio cholerae* can be modeled by growth in the infant mouse. *Infect. Immun.* **73** (2005), 6674–6679.
- [4] A. Alexanderian, M.K. Gobbert, K.R. Fister, H. Gaff, S. Lenhart and E. Schaefer. An age-structured model for the spread of epidemic cholera: Analysis and simulation. *Nonlinear Anal Real World Appl.* **12** (2011), 3483–3498.
- [5] R.M. Anderson and R.M. May. *Infectious Diseases of Humans: Dynamics and Control*. Oxford University Press, Oxford (1991).
- [6] N. Ashbolt. Microbial contamination of drinking water and disease outcomes in developing regions. *Toxicology* **198** (2004), 229–238.
- [7] H. Auld, D. MacIver and J. Klaassen. Heavy rainfall and waterborne disease outbreaks: the Walkerton example. *J. Toxicol. Environ. Health A* **67** (2004), 1879–1887.
- [8] L.D. Berkovitz. *Optimal control theory*. Applied Mathematical Sciences vol.12. Springer-Verlag, New York-Heidelberg-Berlin, 1974.

- [9] F. Brauer. Backward bifurcations in simple vaccination models. *J. Math. Anal. Appl.* **298** (2004), 418–431.
- [10] F. Brauer. Epidemic models with heterogeneous mixing and treatment. *Bull. Math. Biol.* **70** (2008), 1869–1885.
- [11] M. Cannon. Lecture note on nonlinear systems. http://www.eng.ox.ac.uk/~comsrc/nlc/nlc_lec3.pdf, (2014).
- [12] V. Capasso and S.L. Paveri-Fontana. A mathematical model for the 1973 cholera epidemic in the European Mediterranean region. *Rev. Epidemiol. Sante* **27** (1979), 121–132.
- [13] C. Castillo-Chavez, Z. Feng and W. Huang. On the computation of R_0 and its role on global stability. *Mathematical approaches for emerging and reemerging infectious diseases: an introduction*, IMA Vol. **125**, Springer-Verlag, 2002.
- [14] Centers for Disease Control and Prevention (CDC). <http://emergency.cdc.gov/situationawareness/haiticholera/data.asp>, (September 2013).
- [15] Centers for Disease Control and Prevention. <http://wwwnc.cdc.gov/travel/notices/watch/haiti-cholera>, (September 2013).
- [16] Central Intelligence Agency (CIA), World Factbook, Haiti. <https://www.cia.gov/library/publications/the-world-factbook/geos/ha.html>, (September 2013).
- [17] N. Chitnis, J.M. Hyman and J.M. Cushing. Determining Important Parameters in the Spread of Malaria Through the Sensitivity Analysis of a Mathematical Model. *Bull. Math. Biol.* **70** (2008), 1272–1296.
- [18] Cholera: Scourge of the Poor. <http://www.infoplease.com/cig/dangerous-diseases-epidemics/cholera-scourge-poor.html>, (November 2013).
- [19] C.T. Codeco. Endemic and epidemic of cholera: the role of the aquatic reservoir. *BMC Infect. Dis.* **1** (2001) doi:10.1186/1471-2334-1-1.

- [20] O.C. Collins and K.S. Govinder. Analysis and control intervention strategies of a waterborne disease model. *Commun. Nonlinear Sci. Numer. Simul.* (2013), Submitted.
- [21] O.C. Collins, S. L. Robertson and K.S. Govinder. Analysis of a waterborne disease model with socioeconomic classes. *Preprint: University of KwaZulu-Natal*, (2013).
- [22] O.C. Collins and K.S. Govinder. On the mathematical analysis and application of a waterborne disease model with multiple water sources. *Nonlinear Anal. Real World Appl.* (2013), Submitted.
- [23] O.C. Collins and K.S. Govinder. Heterogeneity and control intervention strategies of an n -patch waterborne disease model. *J. Theor. Biol.* (2013), Submitted.
- [24] R.R. Colwell and A. Huq. Environmental reservoir of *Vibrio cholerae*, the causative agent of cholera. *Ann. New York Acad. Sci.* **740** (1994), 44–53.
- [25] F. Curriero, J. Patz, J. Rose and S. Lele. The association between extreme precipitation and waterborne disease outbreaks in the United States, 1948-1994. *Am. J. Public Health* **91** (2001), 1194–1199.
- [26] E. Devane. Stability theory for systems of differential equations with application to power control in wireless network. PhD thesis, University of Cambridge, 2013.
- [27] J.N. Eisenberg, M. Brookhart, G. Rice, M. Brown and J. Colford. Disease transmission models for public health decision making: analysis of epidemic and endemic conditions caused by waterborne pathogens. *Environ. Health Perspect.* **110** (2002), 783-790.
- [28] M.C. Eisenberg, S.L. Robertson and J.H. Tien. Identifiability and estimation of multiple transmission pathways in cholera and waterborne disease. *J. Theor. Biol.* (2013), <http://dx.doi.org/10.1016/j.jtbi.2012.12.021i>.
- [29] J.N. Eisenberg, B.L. Lewis, T.C. Porco, A.H. Hubbard and J.M. Colford Jr. Bias due to secondary transmission in estimation of attributable risk from intervention trials. *Epidemiology* **14** (2003), 442–450.

- [30] C. Fang. Migration and socio-economic insecurity: patterns, processes and policies. *International Labour Office, Geneva*. <http://www.ilo.org/ses>, (2003).
- [31] S. Faruque, M. Islam, Q. Ahmad, A.S.G. Faruque, D. Sack, G. Nair and J. Mekalanos. Self-limiting nature of seasonal cholera epidemics: role of host-mediated amplification of phage. *Proc. Natl. Acad. Sci. USA* **102** (2005), 6119–6124.
- [32] W.H. Fleming and R.W. Rishel. Deterministic and stochastic optimal control. Springer-Verlag, New York, 1975.
- [33] M. Ghosh, P. Chandra, P. Sinha and J.B. Shukla. Modeling the spread of carrier-dependent infectious diseases with environmental effect. *Appl. Math. Comput.* **154** (2004), 385–402.
- [34] H. Guo. Impacts of migration and Immigration on disease transmission dynamics in heterogeneous populations. *Disc. Cont. Dyn. Syst. B* **17** (2012), 2413–2430.
- [35] E. Hansen. Applications of optimal control theory to infectious disease modeling. PhD thesis, Queen’s University Kingston, Ontario, Canada (2011).
- [36] D.M. Hartley, J.G. Morris and D.L. Smith. Hyperinfectivity: a critical element in the ability of *V. cholerae* to cause epidemics? *PLoS Med.* **3** (2006), 63–69.
- [37] J.A.P. Heesterbeek and M.G. Roberts. The type-reproduction number \mathcal{T} in models for infectious disease control. *Math. Biosci.* **206** (2007), 3–10.
- [38] T.R. Hendrix. The pathophysiology of cholera. *Bull. New York Acad. Med.* **47** (1971), 1169–1180.
- [39] S.D. Hove-Musekwa, F. Nyabadza, C. Chiyaka, P. Das, A. Tripathi and Z. Mukandavire. Modelling and analysis of the effects of malnutrition in the spread of cholera. *Math. Comput. Modell.* **53** (2011), 1583–1595.
- [40] P. Hunter, M. Waite and E. Ronchi. Drinking water and infectious disease: establishing the links. CRC Press, Boca Raton (Eds.), 2003.
- [41] J.B. Kaper, J.G. Morris and M.M. Levine. Cholera. *Clin. Microbiol. Rev.* **8** (1995), 48–86.

- [42] A.A. King, E.L. Lonides, M. Pascual and M.J. Bouma. Inapparent infections and cholera dynamics. *Nature* **454** (2008), 877–881.
- [43] A. Korobeinikov and G.C. Wake. Lyapunov functions and global stability for SIR, SIRS, and SIS epidemiological models. *Appl. Math. Lett.* **15** (2002), 955–960.
- [44] A. Korobeinikov. Lyapunov functions and global properties for SEIR and SEIS epidemic models. *Math. Med. Biol.* **21** (2004), 75–83.
- [45] V. Lakshmikantham, S. Leela and A.A. Martynyuk. Stability analysis of nonlinear systems. Marcel Dekker Inc., New York, 1989.
- [46] W. Lamb. Analytical techniques in mathematical biology. Biomaths lecture note, 2011.
- [47] J. LaSalle and S. Lefschetz. Stability by Liapunovs Direct Method. Academic Press, New York, 1961.
- [48] J. LaSalle. Stability of dynamical systems. Hamilton press, Berlin, New Jersey, USA, 1976.
- [49] S. Lenhart and J.T. Workman. Optimal control applied to biological models. Chapman & Hall, London (2007).
- [50] M.M. Levine, J.B. Kaper, D. Herrington, G. Losonsky, J.G. Morris, M.L. Clements, R.E. Black, B. Tall and R. Hall. Volunteer studies of deletion mutants of vibrio cholerae 01 prepared by recombinant techniques. *Infect. Immun.* **56** (1988), 161–167.
- [51] M.Y. LI and J.S. Muldowney. Global stability for the SEIR model in epidemiology. *Math. Biosci.* **125** (1995), 155-164.
- [52] S. Liao and J. Wang. Stability analysis and application of a mathematical cholera model. *Math. Biosci. Eng.* **8** (2011), 733–752.
- [53] X. Liao, L.Q. Wang and P. Yu. Stability of dynamical systems. Elsevier, The Netherlands, 2007.
- [54] A.L. Lloyd and R.M. May. Spatial heterogeneity in epidemic models. *J. Theor. Biol.* **197** (1996), 1–11.

- [55] I.M. Longini, Jr., A. Nizam, M. Ali, M. Yunus, N. Shenvi and J.D. Clemens. Controlling endemic cholera with oral vaccines. *PLoS Med.* **4** (2007), 1776–1783. doi:10.1371/journal.pmed.0040336.
- [56] D.L. Lukes. Differential equations: classical to controlled, mathematics in science and engineering. Academic Press, New York, (1982).
- [57] J. Ma and D.J.D. Earn. Generality of the final size formula for an epidemic of a newly invading infectious disease. *Bull. Math. Biol.* **68** (2006), 679–702.
- [58] D.S. Merrell and S.M. Butler. Host-induced epidemic spread of the cholera bacterium. *Nature* **417** (2002), 642–645.
- [59] R.L. Miller Neilan, E.Schaefer, H.Gaff, K.Renee Fisher and S. Lenhart. Modelling optimal intervention strategies for cholera. *Bull. Math. Biol.* **72** (2010), 2004–2018.
- [60] Ministry of Public Health and Population (MSPP) Haiti. <http://mspp.gouv.ht/newsite/>, (September 2013).
- [61] S.M. Moghadas. Modelling the effect of imperfect vaccines on disease epidemiology. *Discrete Cont. Dyn-B* **4** (2004), 999–1012.
- [62] Z. Mukandavire, S. Liao, J. Wang, H. Gaff, D.L. Smith and J.G. Morris, Jr.. Estimating the reproduction numbers for the 2008-2009 cholera outbreak in Zimbabwe. *Proc. Natl. Acad. Sci. USA* **108** (2011), 8767–8772.
- [63] Z. Mukandavire, D.L. Smith and J.G. Jr. Morris. Cholera in Haiti: Reproductive numbers and vaccination coverage estimates. *Sci. Rep.* **3** (2013), 997: DOI:10.1038/srep00997.
- [64] Z. Mukandavire, A. Tripathi, C. Chiyaka, G. Musuka, F. Nyabadza and H.G. Mwambi. Modelling and analysis of the intrinsic dynamics of cholera. *Differ. Equ. Dyn. Syst.* **19** (2011), 253–265.
- [65] A. Mwasa and J.M. Tchuente. Mathematical analysis of a cholera model with public health interventions. *BioSystems* **105** (2011), 190–200.

- [66] R. Naresh, A. Tripathi and S. Omar. Modelling the spread of AIDS epidemic with vertical transmission. *Appl. Math. Comput.* **178** (2006), 262–272.
- [67] R.M. Nisbet and W.S.C. Gurney, Modelling fluctuating populations, John Wiley & Sons; New York, 1982.
- [68] A. d’Onofrio. On pulse vaccination strategy in the SIR epidemic model with vertical transmission. *Appl. Math. Lett.* **18** (2005), 729–732.
- [69] M. Pascual, X. Rodo, S.P. Ellner, R. Colwell and M.J. Bouma. Cholera dynamics and El Niño-Southern oscillation. *Science* **289** (2000), 1766–1769.
- [70] N.F. Pierce, J.G. Banwell, R.C. Mitra, G.J. Caranasos, R.I. Keimowitz, R.I. Keimowitz, J. Thomas and A. Mondal. Controlled comparison of tetracycline and furazolidone in cholera. *Br. Med. J.* **3** (1968), 277–280, doi:10.1136/bmj.3.5613.277.
- [71] L.S. Pontryagin, V.G. Boltyanskii, R.V. Gamkrelidze and E.F. Mishchenko. The mathematical theory of optimal control process, vol 4. Gordon and Breach Science Publishers, New York, 1986.
- [72] E. Pourabbas, A. d’Onofrio and M. Rafanelli. A method to estimate the incidence of communicable diseases under seasonal fluctuations with application to cholera. *Appl. Math. Comput.* **118** (2001), 161–174.
- [73] L. Righetto, R. Casagrandi, E. Bertuzzo, L. Mari, M. Gatto, I. Rodriguez-Iturbe and A. Rinaldo. The role of aquatic reservoir fluctuations in long-term cholera patterns. *Epidemics* **4** (2012), 33–42.
- [74] A. Rinaldo et al. Reassessment of the 2010-2011 Haiti cholera outbreak and rainfall-driven multiseason projections. *Proc. Natl. Acad. Sci. USA* **109** (2012), 6602–6607.
- [75] M.G. Roberts and J.A.P. Heesterbeek. A new method for estimating the effort required to control an infectious disease. *Proc. R. Soc. Lond. B* **270** (2003), 1359–1364.

- [76] S.L. Robertson, M.C. Eisenberg and J.H. Tien. Heterogeneity in multiple transmission pathways: modelling the spread of cholera and other waterborne disease in networks with a common water source. *J. Biol. Dynam* **7** (2013), 254–275.
- [77] J. Rose. Environmental ecology of *Cryptosporidium* and public health implications. *Annu. Rev. Public Health* **18** (1997), 135–161.
- [78] D.A. Sack, R.B. Sack, G.B. Nair and A.K. Saddique. Cholera. *Lancet* **363** (2004), 223–233.
- [79] M.D. Said. Epidemic cholera in KwaZulu-Natal: the role of natural and social environment. PhD thesis, University of Pretoria, 2006.
- [80] R.P. Sanches, P.F. Ferreira and R.A. Kraenkel. The role of immunity and seasonality in cholera epidemics. *Bull. Math. Biol.* **73** (2011), 2916–2931.
- [81] The American Heritage @ New Dictionary of Cultural Literacy, Third Edition <http://dictionary.reference.com/browse/socioeconomicstatus>, (2013).
- [82] B. Shulgin, L. Stone and Z. Agur. Pulse vaccination strategy in the SIR epidemic model. *Bull. Math. Biol.* **60** (1998), 1123–1148.
- [83] J.P. Tian and J. Wang. Global stability for cholera epidemic models. *Math. Biosci.* **232** (2011), 31–41.
- [84] J.H. Tien and D.J.D. Earn. Multiple transmission pathways and disease dynamics in a waterborne pathogen model. *Bull. Math. Biol.* **72** (2010), 1506–1533.
- [85] J.M. Tchuente, S.A. Khamis, F.B. Augusto and S.C. Mpeshe. Optimal control and sensitivity analysis of an influenza model with treatment and vaccination. *Acta Biotheor.* **59** (2011), 1–28.
- [86] The MathWorks, Inc., Version 08:37:39, R2012b.
- [87] K. Todar. Todar’s online textbooks of bacteriology. <http://textbookofbacteriology.net/cholera.html>, (November, 2013).

- [88] A.R. Tuite, J. Tien, M. Eisenberg, D.J.D. Earn, J. Ma, and D.N. Fisman. Cholera epidemic in Haiti, 2010: Using a transmission model to explain spatial spread of disease and identify optimal control interventions. *Ann. Intern. Med.* **154** (2011), 593–601.
- [89] UNICEF Child Mortality Report, 2012, http://www.unicef.org/videoaudio/PDFs/UNICEF_2012_child_mortality_for_web_0904.pdf, (February, 2014).
- [90] P. van den driessche and J. watmough. Reproduction numbers and sub-threshold endemic equilibria for compartmental models of disease transmission. *Math. Biosci.* **180** (2002), 29–48.
- [91] J. Wang and S. Liao. A generalized cholera model and epidemic-endemic analysis. *J. Biol. Dyn.* **6** (2012), 568–589.
- [92] World Health Organization (WHO). http://www.who.int/water_sanitation_health/hygiene/en/, (November, 2013).
- [93] World Health Organization. http://www.who.int/water_sanitation_health/diseases/burden/en/index.html, (November, 2013).
- [94] WHO. http://www.who.int/gho/mdg/environmental_sustainability/en/index.html. (2013).
- [95] WHO. Global costs and benefits of drinking water supply and sanitation interventions to reach the MDG target and universal coverage, http://apps.who.int/iris/bitstream/10665/75140/1/WHO_HSE_WSH_12.01_eng.pdf. (2012).
- [96] WHO http://www.who.int/gho/epidemic_diseases/cholera/en/index.html, (August 2013).
- [97] WHO <http://apps.who.int/gho/data/node.main.176?lang=en>, (November 2013).
- [98] WHO http://www.who.int/gho/epidemic_diseases/cholera/cases/en/index.html, (October 2013).
- [99] WHO <http://www.who.int/mediacentre/factsheets/fs107/en/>, (February 2014).

- [100] X. Yan, Y. Zou and J. Li. Optimal quarantine and isolation strategies in epidemics control. *World J. Model. Simul.* **3** (2007), 202–211.
- [101] X. Zhou, J. Cui and Z. Zhang. Global results for a cholera model with imperfect vaccination. *J. Franklin Inst.* **349** (2012), 770–791.